Universidade de Aveiro
2021

Bruna Silva Pedrosa

Lipidomics of plant and human opportunistic fungal pathogens of the genus *Lasiodiplodia*

Lipidómica de fungos patogénicos em plantas e oportunistas em humanos do género *Lasiodiplodia*

Universidade de Aveiro
2021

Bruna Silva Pedrosa

Lipidomics of plant and human opportunistic fungal pathogens of the genus *Lasiodiplodia*

Lipidómica de fungos patogénicos em plantas e oportunistas em humanos do género *Lasiodiplodia*

Dissertação apresentada à Universidade de Aveiro para cumprimento dos requisitos necessários à obtenção do grau de Mestre em Biotecnologia, realizada sob a orientação científica da Doutora Maria do Rosário Gonçalves dos Reis Marques Domingues, Professora Associada com agregação do Departamento de Química da Universidade de Aveiro e do Doutor Artur Jorge da Costa Peixoto Alves, Professor Auxiliar com agregação do Departamento de Biologia da Universidade de Aveiro

Apoio financeiro da FCT/MCTES (Portugal) ao CESAM e LAQV-REQUIMTE.

“O homem primeiro tropeça, depois anda, depois corre, um dia voará.”

José Saramago

o júri

presidente	Prof. Doutor Manuel António Coimbra Rodrigues da Silva professor associado com agregação do Departamento de Química da Universidade de Aveiro
orientador	Prof. Doutor Artur Jorge da Costa Peixoto Alves professor auxiliar com agregação do Departamento de Biologia da Universidade de Aveiro
arguente	Doutora Carina Rafaela Faria da Costa Félix investigadora em pós-doutoramento no Instituto Politécnico de Leiria

agradecimentos

Aos meus orientadores, Dra. Maria do Rosário Domingues e Dr. Artur Alves, pela orientação científica, disponibilidade e acompanhamento constantes. Agradeço a atenção, a partilha de ideias e o entusiamo pelo meu trabalho, que me deram motivação até ao final.

À Dra. Ana Cristina Esteves, pela confiança depositada em mim desde que me introduziu ao fantástico universo dos fungos. Agradeço a orientação científica, as palavras honestas, o apoio e a amizade.

À Dra. Tânia Melo, por toda a ajuda que me deu neste trabalho, pela paciência constante e pelos ensinamentos que levarei comigo.

A toda a equipa do laboratório de lipidómica, pela simpatia e disponibilidade, mas em especial à Bruna Neves, Daniela Couto e Tiago Conde, que em conjunto com a Dra. Tânia, me acompanharam nas alturas mais árduas do trabalho prático e cuja ajuda não posso deixar de agradecer. Pela cooperação e ensinamentos, mas também pelos bons momentos.

Ao Micael Gonçalves e à Sandra Hilário, por toda a ajuda e disponibilidade. Agradeço a motivação, as gargalhadas e a partilha de ideias. A toda a equipa do Microlab, pela companhia e apoio. Este laboratório será sempre uma casa para mim.

Ao meu pai, que é sempre tão interessado no meu trabalho, que reconhece sempre o meu esforço. À minha mãe, por acreditar sempre em mim e me dar força nas horas mais difíceis. Agradeço aos dois, pelo apoio incondicional.

À minha irmã Beatriz, que me acompanhou nas semanas de escrita e que me obrigou a fazer as pausas mais divertidas. À minha irmã Carole, por ter sempre palavras sensatas a dizer, pelo apoio mesmo à distância. E à minha irmã Letícia, que espero inspirar a chegar aqui um dia.

Aos meus amigos, que perto ou longe, e cada um à sua maneira, nunca deixaram de me apoiar.

Ao Gonçalo, por ser o meu maior apoio, por me ajudar com as dúvidas mais pertinentes, por acreditar sempre no meu valor. Por estar lá nos bons e nos maus momentos. Obrigada por tudo, o teu valor para mim é imensurável.

palavras-chave

fungos filamentosos, lipidoma, espectrometria de massa, fosfolípido, triacilglicerol, ácido gordo

resumo

O reino dos fungos inclui várias espécies complexas e perigosas, apesar de pouco entendidas. Os fungos patogénicos são conhecidos por causarem inúmeros efeitos nefastos em plantas, animais e humanos. O género *Lasiodiplodia* pertence à família Botryosphaeriaceae e inclui fungos que causam doenças em vários hospedeiros vegetais, mas que também têm sido reportados como causadores de infeção em humanos. *Lasiodiplodia theobromae* e *Lasiodiplodia hormozganensis* são duas espécies conhecidas pela sua capacidade de "cross-kingdom host jump", isto é, por conseguirem infetar repetidamente organismos de diferentes reinos. Sabe-se que lípidos produzidos por fungos patogénicos têm papéis importantes na sua relação com os hospedeiros. De maneira a compreender melhor o comportamento patogénico de espécies do género *Lasiodiplodia*, o objetivo deste estudo foi caracterizar em detalhe o lipidoma de *L. theobromae* e *L. hormozganensis*. Para este propósito, foi utilizada a cromatografia líquida e gasosa associada à espectrometria de massa para identificar fosfolípidos, esfingolípidos, triacilgliceróis e ácidos gordos. Os diferentes lípidos presentes no lipidoma das espécies em estudo corresponderam a 255 espécies moleculares identificadas por LC-MS. Como a maioria dos lípidos identificados estão presentes em ambas as espécies, o total de identificações feito equivaleu a 423. Relativamente a fosfolípidos, foram identificadas 147 espécies moleculares das classes fosfatidilcolina, fosfatidiletanolamina, esfingomielina, ácido fosfatídico, cardiolipina, fosfatidilinositol, fofatidilglicerol e fosfatidilserina. Relativamente a esfingolípidos, foram identificadas duas ceramidas. No perfil de triacilgliceróis foram identificados 83 iões moleculares, que variaram entre TG C47 e TG C61. No perfil de ácidos gordos foram identificados 23 ácidos, que variaram entre FA C14 e C24. Os ácidos gordos mais abundantes foram C16:0, C16:1, C16:2, C18:0, C18:1, C18:2 e C18:3. Ácidos gordos ímpares como C15, C17 e C19 também foram observados no lipidoma de ambas as espécies. Em geral, o perfil lipídico das duas espécies é bastante semelhante. Este é o estudo mais completo do lipidoma de espécies de *Lasiodiplodia* realizado até à data. Esperamos que este trabalho possa ajudar a entender a lipidómica de fungos e fornecer informação acerca dos lípidos que constituem os fungos filamentosos, particularmente espécies patogénicas em plantas e oportunistas em humanos.

keywords filamentous fungi, lipidome, mass spectrometry, phospholipid, triacylglycerol, fatty acid

abstract

The fungal kingdom comprises many complex and dangerous, yet misunderstood species. Pathogenic fungi are known to cause several detrimental effects to plants, animals, and humans. *Lasiodiplodia* genus belongs to the Botryosphaeriaceae family and causes disease on a variety of plant hosts but has also been reported to cause infections in humans. *Lasiodiplodia theobromae* and *Lasiodiplodia hormozganensis* are fungal cross-kingdom pathogens, meaning that they can repeatedly infect organisms from different kingdoms of life. It is known that lipids produced by pathogenic fungi have important roles in the host-pathogen relationship. In order to further understand the pathogenic behaviour of species of the genus *Lasiodiplodia*, the aim of this study was to fully characterize the lipidome of *L. theobromae* and *L. hormozganensis*. For this purpose, liquid and gas chromatography coupled to mass spectrometry technology were used to identify phospholipids, sphingolipids, triacylglycerols and fatty acids. The different lipids present in the lipidome of both fungal species amounted to 255 molecular species. Because most lipids identified are present in both fungi, the total of identifications made was of 423. Regarding phospholipids, 147 molecular species of the classes phosphatidylcholine, phosphatidylethanolamine, sphingomyelin, phosphatidic acid, cardiolipin, phosphatidylinositol, phosphatidylglycerol and phosphatidylserine were identified. Regarding sphingolipids, two ceramides were identified. In the triacylglycerol profile 83 molecular ions were identified, varying between TG C47 to C61. In the fatty acid profile 23 acids were identified, varying between FA C14 to C24. The most abundant fatty acids were C16:0, C16:1, C16:2, C18:0, C18:1, C18:2 and C18:3. Odd numbered fatty acids such as C15:0, C17:0 and C19:0 have also been observed in the lipidome of both species. In general, the lipidomic profiles of both species is very similar. This is the most complete study of the lipidome of *Lasiodiplodia* species until date. We hope this work can help to better understand fungal lipidomics and provide information on the lipids that constitute filamentous fungi, particularly plant pathogenic and human opportunistic species.

Index

Index of figures

Index of tables

List of abbreviations

AGC – automatic gain control

ATP – adenosine triphosphate

CBS – Centraalbureau voor Schimmelcultures

CE – collision energy

Cer – ceramide

CL – cardiolipin

CWDE – cell wall degrading enzyme

DAG – diacylglycerol

DCW – dry cell weight

DPG - diphosphatidylglycerol

ESI – electrospray ionization

FA – fatty acid

FAME – fatty acid methyl ester

GalCer – galactosylceramide

GC – gas chromatography

GlcCer – glucosylceramides

HILIC – hydrophilic interaction liquid chromatography

HPLC – high-performance liquid chromatography

IPC – inositolphosphoryl ceramide

ITS – internal transcribed spacer

LAEE – linoleate ethyl ester

LC – liquid chromatography

LPA – lyso-phosphatidic acid

LPC – lyso-phosphatidylcholine

LPE – lyso-phosphatidylethanolamine

LPI – lyso-phosphatidylinositol

m/z – mass to charge ratio

MS – mass spectrometry

MS/MS – mass spectrometry tandem

NL – neutral lipid

NMR – nuclear magnetic resonance

OAEE – oleate ethyl ester

OCFA – odd-chain fatty acid

PA – phosphatidic acid

PAEE – palmitate ethyl ester

PAMP – pathogen-associated molecular pattern

PC – phosphatidylcholine

PE – phosphatidylethanolamine

PG – phosphatidylglycerol

PI – phosphatidylinositol

PL – phospholipid

PRR – pattern recognition receptors

PS – phosphatidylserine

RAPD – random amplified polymorphic DNA

RIC – reconstructed-ion chromatogram

SAEE – stearate ethyl ester

SM – sphingomyelin

STE – sterol ester

tef1-α – translation elongation factor 1-α

TG, TAG – triacylglycerol

TIC – total ion chromatogram

TLC – thin-layer chromatography

UV – ultraviolet

1. Introduction

1.1. Fungi

Fungi comprise a unique kingdom of life of heterotrophic eukaryotes with a carbohydrate cell wall (1).

The cell wall of fungi is an exceptional feature that distinguishes them from the animals, their closest relatives (2). Besides providing a structural barrier, the cell wall is an essential component of fungi, involved in cell growth, morphogenesis and pathogenicity (3,4). In fungal infections, pathogens establish contact with the host through the cell wall, which by itself can justify the importance of this structure (4).

Regarding its composition, the fungal cell wall has an inner layer of cross-linked fibers, such as (1-3)β-D-glucan, (1-6)β-D-glucan and chitin, which confer rigidity to its structure. The composition of the outer layer can differ considerably depending on the fungal species. It is usually non-fibrous and composed by glycoproteins, in a gel-like matrix where proteins, glucans and mannans aggregate in a strong network of variable permeability (3,4). Some species can include a layer of melanin in the cell wall, increasing cell wall rigidity and enhancing pathogenicity (3). For representation purposes, see **Figure 1**.

Though the composition of the fungal cell wall is well known today, it is important to note that environmental cues, stages of the life cycle and other factors might influence cell wall characteristics, making it a dynamic structure whose composition is not unequivocally fixed (3). Pathogenic dimorphic fungi are even able to change the cell wall composition when developing inside the host, making them less susceptible to its immune responses (5).

The fungal cell wall works mainly to maintain the integrity of the cell and its intracellular osmotic pressure (2), but has other important roles such as determining hyphal growth, establishing interactions with the environment (passage of substances), protection against UV radiation and providing binding sites for wall-bound enzymes (6).

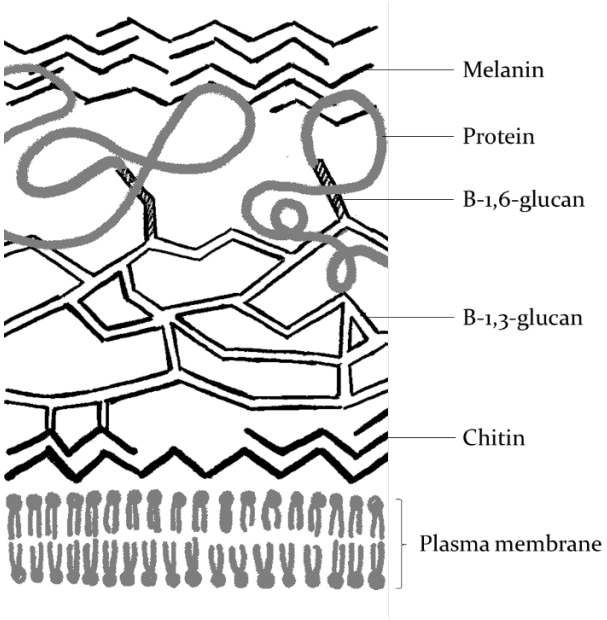

Figure 1 – Schematic representation of the fungal cell wall, adapted from Gow et al. (2017).

The fungal plasma membrane differs from that of other eukaryotes by having ergosterol as the main membrane sterol (opposite to cholesterol in animals and β-sitosterol in plants). For this reason, ergosterol is one of the primary targets of antifungal drugs (2). Sterylglycosides are glycolipids usually found bound to the cell membrane sterols. In fungi, the most common structure of an ergosterol binding sugar is ergosterol-3β-glucoside, and this sterylglycoside is involved in the regulation of host immune responses (7). Glucosylceramides (GlcCer) are also found in the fungal plasma membrane, usually with a β-linked glucose and ceramide backbone. The ceramide is characterized by having a sphingoid base with a C9-methyl group that distinguishes the fungal GlcCer from the mammalian and plant kind. GlcCer promotes tolerance to alkaline to neutral environments and is also involved in virulent behaviour (7).

Fungal cells also comprise microtubules and actin filaments that constitute the cytoskeleton, enabling the extension of hypha but only when a threshold turgor pressure is exceeded (8). Motility structures are not common in fungi but some species are able to produce flagellated spores or zoospores (9,10). Fungi rely on spore formation and hyphal tip growth to extend the mycelium and colonize new niches (11).

Fungi live as heterotrophs, that is, as organisms that do not produce their own sustenance and, therefore, take up nutrients from external carbon sources. Since phagocytosis of food is not facilitated by the cell wall, fungi absorb nutrients after degrading complex polymers of the exterior environment with secreted enzymes (12).

Also a unique characteristic of fungi is that most have complex life cycles, with both sexual and asexual reproduction and production of spores (13). In the past, fungi have been classified based on their spore production. The asexual morph, that produces asexual spores, was called anamorph, while the sexual morph, that produces sexual spores, was called teleomorph. Today, such terminology is no longer used, and researchers are working on using only the name of the holomorph, the complete range of forms belonging to one fungus (14).

1.2. Pathogenicity in fungi

Fungi can be divided in three groups depending on how they obtain their nutrients: pathogens, symbionts and saprotrophs. While symbionts live in association with the host, encompassing a significant range of relationships (mutualism, commensalism and parasitism), and saprotrophs take advantage of dead material, decomposing it, pathogens might represent the biggest treat of all, causing damage on a huge variety of living organisms (15–17). This division is not always clear, since subtle genetic mutations or transcriptional alterations in the fungus and its interactor can trigger the transition to a pathogenic state (11). Similarly, some fungal species are not so easily categorized into these group because they display facultative trophic forms (17).

Although most authors define a pathogenic relationship as one that causes disease on the host (6,8), Casadevall and Pirofski (1999) have reasoned that this definition is far from precise. When we consider a pathogen as responsible for causing disease, we are missing possible qualities of both pathogen and host that can independently characterize the disease-causing potential of many organisms (18). Therefore a pathogen is defined as an organism that causes damage to the host during

the organism-host interaction or as consequence of it (1,18), and pathogenicity is the capacity of the organism to cause damage in a host (18).

Pathogens are traditionally seen as either obligate, facultative or opportunistic (1). Obligate pathogens usually are able to infect only a limited range of host species but can infect even when the host is completely healthy. Facultative pathogens also infect a limited range of host species but can survive outside the host. Opportunistic pathogens develop normally without dependency of a host but can infect a vast number of species. Usually, opportunistic pathogens express low virulence towards a host until a scenario where the host's immunity becomes compromised, time when the pathogen can attack aggressively, immediately causing severe disease, or progressively, causing initial soft to mild symptoms that gradually become severe (1).

There are also synergistic infections in which pathogens cause disease only in the presence of other pathogens (18), a situation that can involve both fungi and bacteria (19).

A disease state can be identified when the host suffers enough damage to disturb its homeostasis (18). While damage is the main characteristic of infectious diseases, it can be caused either by the pathogen (by means of toxins and virulence factors) or the host (through indirect mechanisms of response) (1). The nature and extent of host damage depends on its immunity condition, but most pathogen-host interactions are based on a continuum of host- and pathogen-mediated damage that leads to disease only when the nature of the damage impairs the normal function of the host. This means that disease is not exclusively of the pathogen's responsibility, and some pathogens might not even cause sufficient damage but illicit a response from the host that causes disease (18).

The immunological status of the host is a determining factor for the success of the infection process of fungal pathogens (18). But the very interaction of both parts depends upon "key-and-lock" situations, in the way that for a host to be susceptible to

infection, the genetic basis of both parts must be compatible and allow for the molecular interaction that defines the type of relationship (1).

Although pathogens can cause an array of diseases through multiple ways of damaging hosts of all species, the establishment of an infection in plants is always based on a few common steps (**Figure 2**) (1).

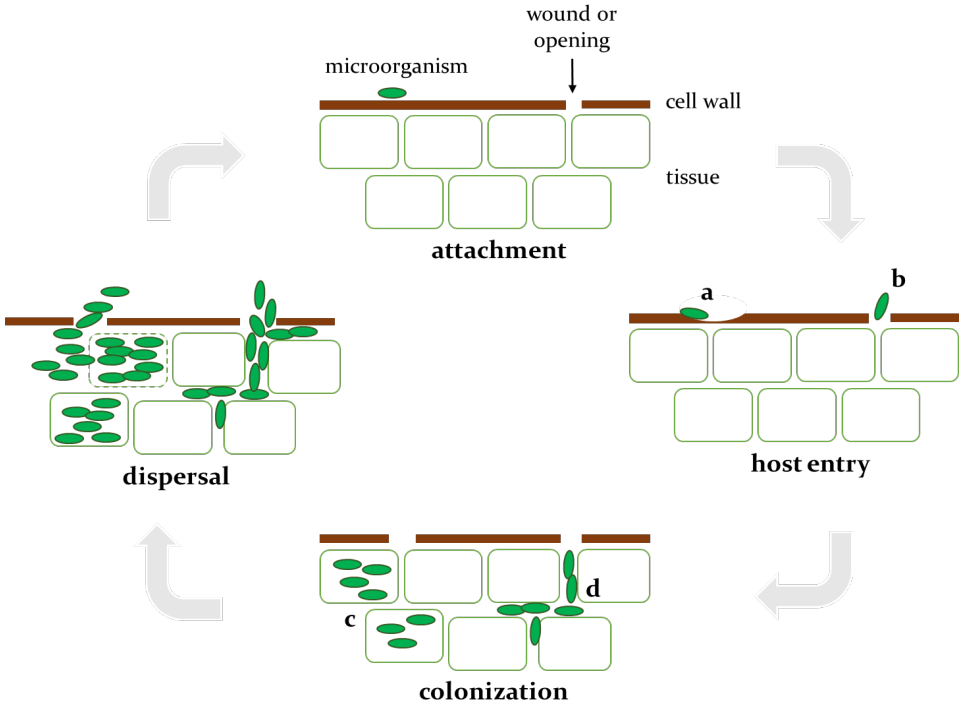

Figure 2 – General process of infection in plant hosts, adapted from van Baarlen et al. (2007) (1). Infection begins with the attachment of the microorganism to the exterior of the plant, it is followed by entry through active penetration strategies (**a**) or natural openings and existing wounds (**b**). Colonization of host tissues can be intracellular (**c**) or extracellular (**d**). Dispersal of cells allows for new infection.

The first step of the infection process is the adhesion of the pathogen to the outer surface of the host cells or tissues. This might require the use of adhesins or specialized adherence proteins that allow firm attachment and enable the

microorganism to resist dislodgment caused by climatic factors (1,3). In this situation, it is assumed that the development of fungi outside the host tissue is favored by environmental conditions such as humidity, light and temperature (20).

Following adhesion, the microorganism enters the host, using active penetration strategies or through wounds and natural openings. Phytopathogenic fungi are known to use specialized structures called appressoria to force their entry inside the plant host (1,21,22). These modified hyphae usually have melanized walls and exert high turgor pressure that facilitates penetration (21,23). Appressoria increase the fungus-plant contact area by attaching themselves firmly to the host. A penetration hyphae (or infection peg) grows from a pore in the base of the appressoria and goes directly into the host tissues, penetrating the cuticle and cell wall (20).

When not using specialized hyphae, fungi might produce cuticle- and cell wall degrading enzymes (CWDEs), but both strategies are frequently used in combination. Degrading the cell wall requires the combined action of multiple families of enzymes, including cellulases, xylanases, proteases and pectic enzymes (20,24).

Most pathogenic fungi are able to penetrate living tissues, but some prefer to enter through existing wounds that favor spore germination because of conditions such as humidity or presence of nutrients (20). Other pathogens prefer to enter through natural openings, such as stomata, pores on the epidermis of leaves that allow for the exchange of gases involved in respiration and transpiration, and lenticels, big portions of porous tissue present on the bark of some trees that enable direct exchange of gases (1,20). All efforts used on adhesion and penetration have evolved to cause minimal damage to the host tissues and minimize the chances of host immune activation (23).

Naturally, the fungus can, from this point on, colonize the host in order to feed and replicate. The colonization can happen intracellularly or extracellularly depending on the pathogen (1). Sometimes, the fungus can persist asymptomatically inside the host for some time, resisting elimination by the immune system and only causing infection when the immune state of the host is deteriorated (11).

The final step is the release and dispersal of reproduction cells, such as fungal spores, so that new infection can take place (1). Because the process of infection is highly regulated at every stage, it requires fungi to be in constant sensing and signaling of the external environment (22).

The permanence within a host offers benefits beyond an easier and assured nutrient uptake, providing protection from the external environment (8). Nevertheless, when a pathogen develops within a host it releases pathogen-associated molecular patterns (PAMPs) that directly result from its activity or are the product of its pathogenicity towards the host (25). Plants have specific receptors for PAMPs, called pattern recognition receptors (PRRs), that can activate immune defense pathways (25).

1.2.1. Phytopathogenic fungi

Most fungi are adapted to grow in association with a plant host, being that 90% of higher plants are associated with fungi at their roots (11), in a symbiotic relation termed mycorrhizae (8). Consequently only about 6000 species (out of an estimated 1.5 million) are known as phytopathogenic, taking advantage of a plant's resources and causing severe disease or even leading to death (11,26). Although they represent a minority in their kingdom, phytopathogenic fungi are responsible for more than 70% of all crop diseases (6).

When focusing on the nutritional relationship of plant pathogenic interactions, there are necrotrophic and biotrophic pathogens (1,6). Biotrophic pathogens feed on living tissues with the help of structures that can absorb nutrients, such as haustoria, specialized in feeding and suppressing host defense mechanisms. Necrotrophic pathogens cause death to then feed on dead tissues, by invasion and production of enzymes and toxins (1). Intermediate forms are called hemibiotrophic, initially feeding on living tissues but eventually invading them and causing death (6,23). Necrotrophic organisms usually do not bear sophisticated mechanisms for host immune response suppression. These organisms cause infections that are termed chronic, when a

persisting pathogen causes a long-term infection, or acute, when the pathogen rapidly develops and spreads within the host (1).

In order to successfully develop within a host, biotrophic pathogens developed certain features: the continuous suppression of host defense mechanisms; a limited use of secretory enzymes; an interfacial multi-layer between fungal and plant plasma membrane that is rich in lipids as well as in carbohydrates and proteins; and the development of specialized infection structures, in some species including haustoria, specialized hyphae that allow the absorption of nutrients from plant tissues (23).

1.2.2. Virulence and pathogenicity factors

Virulence is the means through which organisms express their pathogenicity, that is, the relative capacity to cause damage to a host (1,18). Therefore virulence is a property of the pathogen, although it is modulated by host susceptibility and resistance (18).

Pathogenic fungi produce a vast array of extracellular enzymes that enable them to enter and prosper within the host, being involved in the synthesis of toxins (6,26). These kind of components that can damage the host and that may or may not be essential for the pathogen's viability are called virulence factors (18). They are expressed from specific genes that give pathogenic species the ability to infect their hosts (26). Other examples of virulence factors are melanin production, CWDEs and the ability to grow at 37°C (7).

The production and release of degradative enzymes is crucial at the time the fungus is entering the host (27). These extracellular hydrolytic enzymes contribute to the pathogenicity of the fungus since they promote the destruction of plant tissues, and often lead to the activation of the host immune response mechanisms (24,28).

1.2.3. Cross-kingdom host jumps

In order to benefit from successful colonization, it is usual for a pathogen to specifically infect just a few species that are phylogenetically related or morphologically similar. However, some organisms have the ability to infect a variety of host species, sometimes even from different kingdoms of life. When a microorganism infects a species from a taxonomic kingdom but gains the ability to repeatedly colonize a species from another kingdom, it is called a cross-kingdom host jump (1).

It is estimated that only about 150 to 400 species of fungi are pathogenic to humans (11). Most of these fungi did not evolve to infect humans, but rather began as environmental fungi that lived outside the human body and accidentally caused exogenous infections (11).

There is interest in understanding the underlying mechanisms of cross-kingdom host jumps because the environment to which fungi must adapt to are so different. Human pathogenic fungi have to survive and prosper at temperatures higher than phytopathogenic fungi, although they are more protected from the external temperature variation that naturally occurs in the environment (29). Nevertheless, pH inside the human body can vary from 2 to 8 depending on the cellular compartment, although most niches are neutral to mild alkaline. Fungi prefer low pH values, meaning they don't usually adapt to the human pH but rather manipulate it by the production of lactic acid and fatty acids (11).

1.3. The *Lasiodiplodia* genus

Lasiodiplodia genus belongs to the family Botryosphaeriaceae. The species included in this genus are phytopathogens frequently associated to dieback, a disease that commonly affects grapevines and other plant hosts. The genus *Lasiodiplodia* is typically found in warmer climates, such as tropical and subtropical regions (30,31). It is characterized morphologically by thick-walled conidia that mature slowly, eventually

depositing melanin pigments on the inner surface of the wall and forming longitudinal striations (31,32).

Phylogeny and species identification in the family Botryosphaeriaceae has long been a difficult process (30,33). In the last years, enormous advances have been possible in species identification due to the rise of molecular genetics techniques (32).

1.3.1. *Lasiodiplodia theobromae*

Lasiodiplodia theobromae (Pat.) Griffon e Maubl. is a phytopathogenic fungus that can cause severe disease in various plant hosts, besides having been reported to cause, on several occasions, infections in humans, making it a human opportunistic pathogen (34). *Lasiodiplodia theobromae* is described by Úrbez-Torres (2011) as a plurivorous fungal species for living on several hosts, known to infect about 500 plant species but humans as well (31). Usually the hosts of this species are woody plants or fruit trees, where infection by *L. theobromae* leads to dieback, cankers and fruit, leaf or root rot (30,35–39). In humans, infections by this fungi have led to cases of fungal keratitis and phaeohyphomycosis, among others (40,41).

Lasiodiplodia theobromae can also behave as a latent pathogen, since it has the ability to colonize a healthy host without causing symptoms. The fungus can be isolated from the plant tissues and only start to cause disease symptoms when the host is under stress (38).

Regarding morphology, *L. theobromae* develops pycnidial, uniloculate conidiomata that are dark-brown to black. Paraphyses are hyaline, septate and cylindrical with rounded ends, occasionally branched. Conidia are subovoid to ellipsoid-ovoid and thick-walled with granular contents. Initially hyaline and aseptate to later become dark-brown and one-septate (32).

When in culture, *L. theobromae* initially develops a white cotton-like mycelium that progressively becomes greyish, being black in reverse (39).

1.3.1.1. The effect of temperature on *Lasiodiplodia* growth

Like most Botryosphaeriaceae species, *L. theobromae* shows a broad range of distribution worldwide, being able to adapt to a vast variety of environments (30). Although it is commonly associated to warmer regions, with optimal growth between 27 and 33°C, it can grow under temperatures from 9 to 39°C (42).

Eight *Lasiodiplodia* species analyzed by Correia et al. (2016) in a grapevine dieback study were isolated in northeastern Brazil, having the optimum temperature for mycelium growth varying between 29.9 and 31.2°C. (43). In a similar study regarding mango dieback, seven *Lasiodiplodia* species showed optimal mycelium growth between 28 and 31°C (36). In both studies, all species could grow at 10°C.

Although this Ascomycete occurs mostly in tropical and subtropical regions, being well adapted to high environmental temperatures, *L. theobromae* has a high adaptation capacity and has been reported to infect hosts of both warm and cold climates. In fact, temperature modulates the extracellular protein production as well as the metabolome of *L. theobromae*. These differences can be related to adaptation to specific host conditions (34).

1.3.1.2. Plant hosts of *Lasiodiplodia theobromae*

Lasiodiplodia theobromae has long been known to infect a vast number of plant hosts (39,44,45). It has been reported as the causal agent of dieback and the major pathogen in various plant species, including grapevines (37,43,46), mango trees (36,47), banana trees (48) and seedlings of yellow mombin, cashew, soursop and Brazil plum (45), sometimes alongside other species from the family Botryosphaeriaceae (**Table 1**).

Table 1 – Listing of examples of identification reports of *Lasiodiplodia theobromae* infections in plant hosts.

Host	**Location**	**Identification**	**Reference**

Vitis vinifera	Mexico	Morphological characterization, β-tubulin gene, ITS, tef1-α	J. R. Úrbez-Torres et al., 2008
Mangifera indica	Brazil	ITS, tef1-α	Marques et al., 2013
Banana (species not specified)	India	Morphological characterization, RAPD	Sangeetha et al., 2012
Mangifera indica	Peru	ITS, tef1-α	Edgar Rodríguez-Gálvez et al., 2017
Vitis vinifera	Peru	Morphological characterization, ITS, tef1-α	E. Rodríguez-Gálvez et al., 2015
Vitis vinifera	Brazil	Morphological characterization, ITS, tef1-α	Correia et al., 2016
Spondias mombin ***Anacardium occidentale*** ***Annona muricata*** ***Spondias tuberosa***	Brazil	Morphological characterization	Lima et al., 2013

Legend: ITS – internal transcribed spacer, region; tef1-α – translation elongation factor 1-α, gene; RAPD – Random amplified polymorphic DNA, markers for genetic diversity

1.3.1.3. Humans as hosts of *Lasiodiplodia theobromae*

Although rarely, *L. theobromae* has been reported to infect human tissues. Out of the most common diseases caused by this species, is fungal keratitis, a damaging infection of the cornea and one of the main causes for ocular morbidity, especially in developing countries (40,49–51). Other diseases caused by *L. theobromae* are fungal

sinusitis (52), in this case associated to a neck lymph node, and fungal maxillary sinusitis (53). Phaeohyphomycosis is a fungal disease caused by the production of dark, melanized filaments in human tissue, and has also been associated to infection by *L. theobromae* (41). A summary of identification reports of human infections is listed in **Table 2**.

Table 2 – Listing of examples of identification reports of *Lasiodiplodia theobromae* infections in human hosts.

Disease	Location	Identification	Reference
Fungal keratitis	Brazil, India	Morphological characterization, ITS	(40,49–51)
Invasive fungal sinusitis with neck lymph node	South Korea	ITS	(52)
Fungal maxillary sinusitis	India	Morphological characterization	(53)
Phaeohyphomycosis	Jamaica	Morphological characterization	(41)

Legend: ITS – internal transcribed spacer, region

1.3.2. *Lasiodiplodia hormozganensis*

Lasiodiplodia hormozganensis Abdollahzadeh, Zare & A.J.L. Phillips was first described in 2010, among isolates similar to *L. theobromae* collected from various tree species showing signs of dieback (35). This species was described as having stromatic, pycnidial *conidiomata* that are dark-brown to black and covered with a dense mycelium. *Paraphyses* are hyaline, cylindrical and thin-walled. *Conidia* were initially

hyaline and aseptate, ellipsoid to cylindrical with granular content, becoming dark brown, ellipsoid to ovoid with longitudinal striations (35).

When in culture, there is the development of abundant aerial mycelium whose surface is grey, being the reverse greenish grey to dark blue (35).

Lasiodiplodia hormozganensis has been associated to grapevine and mango dieback in northeastern Brazil (36,43). In both studies, identification was performed recurring to molecular analyses of the ITS region and *tefi-α* gene, along with morphological characterization. This was the first time *L. hormozganensis* was reported in gravepine worldwide. In mango (*Mangifera indica*), *L. hormozganensis* was not only first reported but one of the most virulent species of the study (36). It was also reported as an endophyte in *Ficus krishnae,* without causing apparent disease (54).

Recently, *L. hormozganensis* was reported as a human opportunistic pathogen for the first time (55). Sequencing of the genome of the clinical strain CBS339.90, isolated from a phaeohyphomycotic cyst and identified as *L. theobromae*, showed that the strain had been misidentified and was in fact *L. hormozganensis*. Genomic, transcriptomic and proteomic data have confirmed *L. hormozganensis* as a cross-kingdom pathogen that has the ability to express virulence towards humans and plants (55).

1.4. Lipidomics

We know today that to accurately understand nature we must not only focus in one detail at a time but to understand the interactions that make the whole. Therefore, systems biology developed as an interdisciplinary field that collects input from various scientific areas in order to systematically study the complex interactions that compose biological systems (56). Being lipids some of the most relevant organic compounds found in living cells, it was imperative to establish a scientific field focused on their investigation. Lipidomics is a recent field, integrated in systems biology, that aims to analyze the whole lipidome of a certain species (56,57). The lipidome can be defined as

the complete lipid profile of a cell or organism at a certain time and is a subset of the metabolome, which includes all the metabolites produced in cells, such as proteins, nucleic acids and carbohydrates (57).

The term “lipidomics” encompasses the techniques used to study the pathways of cellular lipids using mass spectrometry (MS) (58). It is due to the recent developments in MS technique, such as increase in sensitivity and resolution, that lipidomics is now facing a huge progress (56,58,59), with great aid coming from “soft” ionization techniques like electrospray ionization (ESI) and also of exact mass resolution, provided by newly high resolution instruments (58). Lipidomic analyses comprise the identification and quantification of the lipid species present in sample, along with their interactions with other molecules. This includes the determination of functions and structures and the analysis of cellular dynamics and any changes that happen in a disturbed system (57). Understandably, this kind of analyses take a long time and always generate enormous amounts of data. Recent advances in bioinformatics have also helped lipidomics by facilitating statistical analyses and selecting important information that can provide biological insight (56,58).

Commonly seen as hydrophobic compounds, lipids are not always insoluble in water and soluble in organic solvents. The International Lipid Classification and Nomenclature Committee has described lipids as “hydrophobic or amphipathic small molecules that may originate entirely or in part by carbanion-based condensation of thioester (fatty acyls, glycerolipids, glycerophospholipids, sphingolipids, saccharolipids, and polyketides) and/or by carbocation-based condensations of isoprene units (prenol lipids and sterol lipids) (58).

Lipids can be divided into eight categories: fatty acids, glycerolipids, glycerophospholipds, polyketides, prenol lipids, saccharolipids, sphingolipids, and sterol lipids, each forming distinct classes and subclasses of their own (56,57). The major component of a lipid is a long, aliphatic, hydrocarbon-type chain which is usually bound to a polar head group (57). There is a huge diversity and complexity in lipids

that is justified by the endless combinations of polar moieties, fatty acyl chains and backbone structures, but that is also responsible for the various challenges imposed on the field (56). The diversity of structures is also connected with a vast range of functions, although lipids are commonly addressed as an energy source and constituents of the plasma membrane (57).

The cellular functions of lipids are vast and include: the structural integrity of eukaryotic plasma membranes, where glycerophospholipids and sphingolipids are highly abundant; signal transduction, where, for example, lipid mediators are formed by phospholipases or oxidative modifications on structural lipids; and regulation of membrane trafficking, where lipids work together with proteins to regulate the assembly of protein complexes (2,56). It is also accepted today that lipids play roles in apoptosis, inflammation and immunity (2,58). In all these processes, lipid metabolism is subjected to change when the organism's condition is altered, for example in a virulent state. Although the importance of lipids in cellular dynamics, whole lipidomic analysis of fungi are still rare in literature (57,60).

1.4.1. Methods in lipidomics

To first assess any information on the lipid species present in a cell or organism, one should start by obtaining a high purity sample of lipids from this source (56). It is important that the homogenization steps are able to break down all subcellular organelles without disrupting any vesicular organelles that contain lipases. Sample preparation should also be quick and performed at low temperatures to minimize undesired enzymatic activity (56). The procedure of lipid extraction should extract cellular lipids quantitatively while not contaminating the sample with non-lipidic components (56). Lipid extraction, particularly in fungi, is usually based on the methods of Folch et al. (1957) with some adaptations (61). Initial steps of lipids extraction from fungal tissues often requires mechanical strategies such as using glass beads to break the fungal cell wall (62). A nonpolar solvent is necessary, in which most

lipid compounds are reasonably soluble, but a polar solvent is also present among the blend of solvents, to denature proteins. The extraction is typically done on dry biomass, either thermally or by lyophilization. Extraction of lipids from wet biomass requires extra steps of preparation that may endanger the yield of lipids obtained after the process (62). Traditional lipid analysis used to involve thin-layer chromatography (TLC) and gas chromatography (GC) coupled to mass spectrometry (MS). With the development and advance of MS techniques, lipidomics emerged as a part of metabolomics, and with it new methods have arisen (58). A typical workflow in lipidomics can be observed in **Figure 3**.

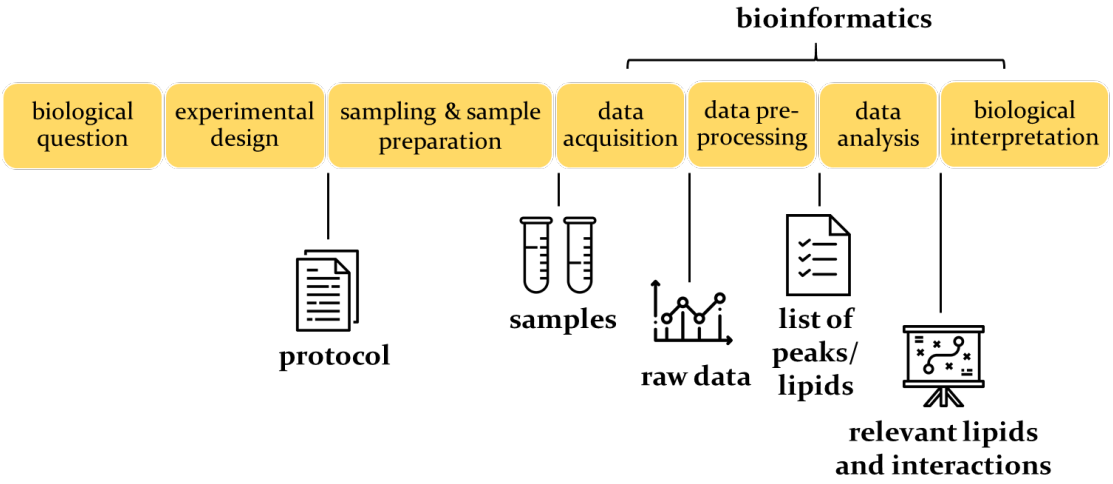

Figure 3 – Lipidomics workflow, adapted from Vaz et al. (2014) (58). It starts with the formulation of the biological question, followed by the design of the experiment and establishment of a protocol. After obtaining samples and data acquisition, bioinformatic techniques allow the analysis of raw data to finally obtain lipids' identification and biological function assignment.

Mass spectrometry analysis relies on the ionization of molecules in the gaseous phase and their separation of the ions in electric fields, which depends on their mass-to-charge ratio (*m*/*z*) (63). A mass spectrometer consists of an ionization source, a mass analyzer that measures the m/z of the ionized analytes, a detector that registers the number of ions at each m/z value, and a computer to control the settings, as well as to

perform data acquisition, analysis, storage and retrieval (64). In lipidomics, mass spectrometry is usually coupled to liquid chromatography that allows the separation of lipids from different classes. Identification of lipid species is based on three factors: the identification of retention time, the identification of the ions formed in the LC-MS data and the analysis of typical fragmentation observed in LC-MS/MS mass spectra (65).

1.4.2. Fungal lipids

The lipids of fungal species mostly function in cell membranes or as energy storage (66), but recent studies suggest an additional role in host-pathogen relationships, where lipids are involved in cell signaling (67). Lipids produced by fungi can vary deeply between species and strains and even be affected by growth conditions and life cycle phases, among other reasons (62,68). The type of lipid present in each area of the cell can also vary and be dependent of environmental cues (69). Fungal lipids can also work as pathogenicity and virulence factors or as allergens (29,67).

Fungi infecting animals or plants often accumulate lipids like triacylglycerols and fatty acids that serve mainly as metabolic energy sources (69). Fungal lipids are commonly the target of antifungals, because lipids constitute the plasma membrane and pathogenic fungi often accumulate specific lipids while infecting the host (2,29).

Most antifungals are carefully thought out to disrupt the lipidic metabolism in certain steps of a pathway, which can effectively cease pathogen-caused damage. Antifungal drugs like the azoles, allylamines and morpholines work by inhibiting certain enzymes involved in ergosterol synthesis: the azoles inhibit cytochrome P450-dependent lanosterol 14α-demethylase, allylamines inhibit squalene epoxidase and morpholines inhibit sterol Δ14-reductase and sterol Δ8,Δ7-isomerase (2). Regarding phospholipids, many enzymes involved in the synthesis of phosphatidylcholines (PC) show potential to become antifungal targets because higher eukaryotes use the Kennedy pathway to produce PC, instead of the methylation pathway used by fungi (2).

As some fungi are more prone to produce oils than others, some are called oleaginous. These organisms are specially known for their ability to produce and accumulate amounts of lipid higher that 20% w/w of their dry cell weight (DCW) during growth on glucose or similarly catabolized compounds (62). The accumulation of lipids in oleaginous organisms, fungi included, is usually triggered by the scarcity of nitrogen in the culture medium (70). In this scenario, excess carbon sources in the medium are converted into storage lipids (fatty acids and triacylglycerols).

There are two types of lipids usually found in fungi: polar lipids (phospholipids) and neutral lipids (fatty acyls) (29,62).

Phospholipids (PL) are the lipids found in the plasma membrane of fungi and eukaryotes and are some of the most commonly found lipids in lipidomic analyses of fungi. These are also the most sensitive lipids to alterations in the extracellular medium (71). Among them, phosphatidylcholines (PC) and phosphatidylethanolamines (PE) are the most common and abundant, followed by smaller amounts of phosphatidylinositol (PI), phosphatidylserine (PS) and diphosphatidylglycerol (DPG) (61,62,70). PC and PE are closely related since the first is synthesized from the second as can be seen in the schematic representation of the metabolic network of phospholipids in **Figure 4**. The ratio between PC and PE is important for membrane stability and cell function, since PC stabilizes the bilayer of the cell membrane while PE is prone to form non-bilayer hexagonal phases (61). PG, PI and PS are also correlated, since all require the same precursor, and PS is a precursor to PE and thus PC synthesis (72,73). In yeast, PS is found uniquely in the inner surface of the plasma membrane, while PI is used as a precursor for complex sphingolipids and is therefore essential for growth and metabolism (61). PI also has important roles in signal transduction, mRNA export from the nucleus and glycolipid anchoring of plasma membrane proteins (73).

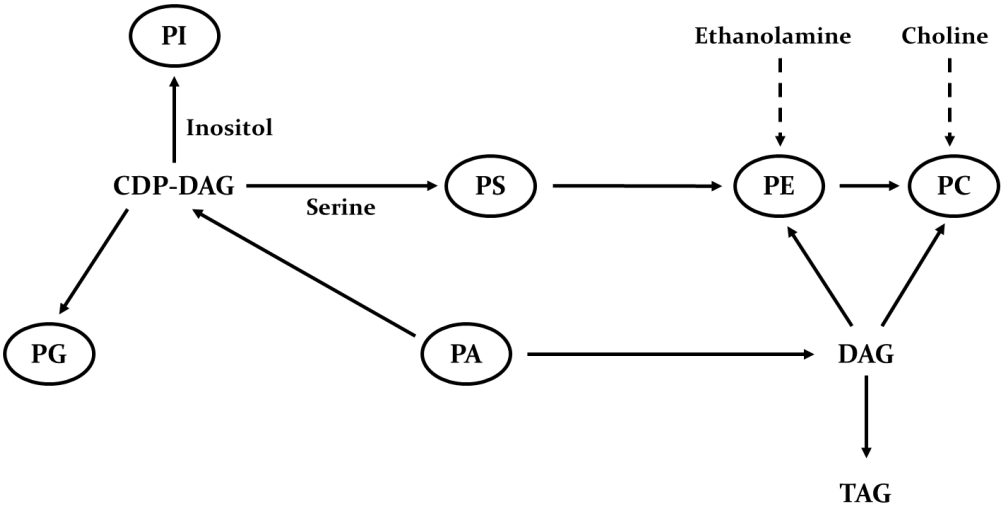

Figure 4 – Metabolic network of phospholipids in *S. cerevisiae*, adapted from Xia et al. (2011) (72). CDP-DAG – citidyldiphosphate; DAG – diacylglycerol; PA – phosphatidic acid; PC – phosphatidylcholine; PE – phosphatidylethanolamine; PG – phosphatidylglycerol ; PI - phosphatidylinositol; PS – phosphatidylserine ; TAG – triacylglycerol.

On the other hand, neutral lipids (NL) compose a major part of the storage lipids in filamentous fungi. Triacylglycerols (TG) and fatty acids (FA) are the most common, while monoacylglycerols, diacylglycerols (DAG) and steryl-esters are scarce compounds (60,62). Non polar lipids are commonly found as oil droplets in the cell (especially in oleaginous microorganisms) since they are highly reactive and can bind to and inactivate enzymes and proteins (2,67,69).

Storage lipids such as FA provide large amounts of ATP when β-oxidized and are stored in the form of TGs and sterol esters (STE) when in excess intracellularly (2). FA also have important roles in the host-pathogen relationship, as the fatty acid composition of both plants and fungi is reported to suffer alteration when the pathogen adheres to the host (67).

Fungi produce also a variety of sphingolipids, such as inositolphosphoryl ceramides (IPC) and hexosylceramides like glucosylceramides (GlcCer) and galactosylceramides (GalCer) (62,67,74,75). Ceramides are sphingolipids with a R group

consisting of a hydrogen atom. Sphingolipids are important in the growth and development of eukaryotic species and can be involved in a variety of roles in fungi such as heat stress response, signal transduction and phagocytosis (76). Nonetheless, lipids such as IPC and GlcCer play a determinant role in virulence and pathogenicity of fungi (67,74,77). GluCer is important in phytopathogenesis, inducing the defense mechanisms of plant species (78). Lipid rafts (LR), signaling structures of the cell membrane, are mainly composed by sphingolipids and sterols, and can play a role in fungal pathogenicity (2,67). Through these structures, virulence factors may be presented and biophysicial properties of the plasma membrane may be altered. The defining features of LR are the alteration of plasma membrane thickness and lipid composition, which is fundamental for the exchange of toxins (67).

Sterols are some of the most important components of the fungal lipidome, modulating membrane fluidity and taking an active part of the cell membrane (75,78). They have a distinct chemical structure, when compared to other lipids, because they are formed through complex reactions from isoprene precursors (75). Ergosterol is the most common sterol found in fungi, as mentioned before, and because its biosynthesis pathway is different from the mammalian cholesterol synthesis, its pathway is a known target for antifungals (2,75).

Although the analysis of the metabolome of a species can lead to a better understanding of the host-pathogen relationship, lipidomic studies on fungi remain scarce (55). Kohlwein (2017) has addressed the challenges of analyzing the lipidome of yeast species, making remarks on the highly diverse chemical structures, the abrupt difference in abundance from one class to another, and a complex variation in acyl chain composition of the molecular species (75).

The genetic analysis of the plant pathogen *Fusarium graminearum* on phospholipid biosynthesis-related genes has revealed that PE and PC are essential for the vegetative growth of the species (79). Mutants for three genes involved in the *de*

novo pathway of phospholipid biosynthesis have shown that this pathway is crucial for toxin production and full virulence.

Characterization of fatty acid derivatives of *L. theobromae* by nuclear magnetic resonance (NMR) and gas-chromatography-mass spectrometry (GC-MS) identified ethyl linoleate (linoleate ethyl ester or LAEE) as one of the most abundant fatty acid esters produced by this fungal species. Ethyl palmitate (palmitate ethyl ester or PAEE), stearate ethyl ester (SAEE) and oleate ethyl ester (OAEE) were also identified in the samples. In this study, ethyl linoleate was shown to regulate the growth of tobacco seedlings, providing a new understanding of the importance of naturally esterified fatty acids when produced by phytopathogenic fungi (80). Other than this, there are no studies characterizing the lipidome of *L. theobromae* or *L. hormozganensis*.

1.5. Objectives

The impact of pathogenic fungi on the environment and in world economy is well known today. This subject has gained increased attention over the years, particularly in the scientific community, and all strategies are welcome when fighting such an issue. The fungal genus *Lasiodiplodia*, of the family Botryosphaeriaceae, is known for its pathogenicity to both plants and humans. Thorough investigation on the molecular and systems biology of the cross-kingdom pathogen *L. theobromae* has been performed in the recent past, leading to the discovery of the first clinical report of the plant pathogen *L. hormozganensis*. These two species are related in the way that they are morphologically very similar and have similar pathogenic behaviors.

Although the genome, transcriptome, proteome and metabolome of these species has been previously characterized (34,81), whole lipidomic analyses have not been performed on these species or any other species in the genus *Lasiodiplodia*. It is important to identify and characterize the lipid profile of these species not only to complete the contribution that has been made to systems biology but also due to the significance that lipids have in fungal cells, as seen before. The lipids identified in both

fungi can help to differentiate the two species or elucidate on the mechanisms used to cross-kingdom host jump.

Since the lipidomic characterization of filamentous fungi using modern mass spectrometry techniques is still a field under initial development, this research could build awareness as to what to expect when analyzing the lipids of fungal species. Furthermore, the identification of lipids of pathogenic fungi can lead to the suggestion of possible targets for antifungal drugs. This investigation can also elucidate on lipids with relevant bioactivity that can be of biotechnological value.

The aim of this study is to fully characterize the lipidome of *L. theobromae* and of *L. hormozganensis*, using advanced liquid chromatography mass spectrometry and gas chromatography-mass spectrometry approaches and to compare the lipids produced by the two species.

2. Methods and materials

2.1. Fungal species and isolates

In this study, an environmental strain of *Lasiodiplodia theobromae*, LA-SOL3, was used. This strain was isolated from *Vitis vinifera* in Peru and showed to be the most aggressive in artificial inoculations trials of cv. Red Globe plants (55).

A clinical strain of *Lasiodiplodia hormozganensis*, CBS339.90, obtained from the CBS collection of then Westerdijk Fungal Biodiversity Centre, was also used in this study. This strain was initially isolated from a phaeohyphomycotic cyst of a patient from Jamaica and identified as *L. theobromae*, but further analysis by sequencing of different loci confirmed it as *L. hormozganensis* (55).

2.2. Culture conditions

Cultures were maintained in solid medium (Potato Dextrose Agar, Merck) at room temperature (±25 °C). The medium was autoclaved for a period of 20 minutes at 121 °C after preparation and poured into sterile 45 mm Petri dishes. Inoculation was performed by placing a plug (5 mm diameter) of a living culture in the center of the dish.

Liquid growth was used to obtain the fungal mycelium and easily separate it from the culture medium. For liquid growth, two plugs of an actively growing culture (incubated for 5 days) were inoculated into 50 mL of liquid medium (Potato Dextrose Broth, Merck) in 250 mL flasks and incubated at 37 °C for 7 days. The liquid medium was previously prepared and autoclaved for a period of 20 minutes at 121 °C.

All assays were performed in triplicate. The mycelium was collected by gravitational filtration through filter paper and stored at -80 °C in 50 mL tubes until maceration.

2.3. Maceration of the mycelium

To obtain a powder-like sample for lipid extraction, the frozen mycelium obtained by filtration was macerated with liquid nitrogen. A ceramic mortar and pestle, along with a stainless-steel tweezer and long spoon were used, being priorly disinfected with 96% ethanol. The powder-like sample was stored at -80 °C in 50 mL tubes.

2.4. Lipid extraction of filamentous fungi

The total fungal lipids were extracted from the samples previously stored at –80 °C, following the Bligh and Dyer method (82). 3.75 mL of dichloromethane/methanol (1:2, v/v) were added to 300 mg of fungal biomass, in glass centrifuge tubes. To homogenize the mixture, the tubes were vortexed and sonicated before incubating on ice for 60 min, vortexing every 10 minutes and sonicating for 10 minutes after 30 minutes. 1.25 mL of dichloromethane was added and the tubes were vortexed. The samples were centrifuged at 2000 rpm for 10 minutes at room temperature and the supernatant was transferred to a clean glass tube and dried under a nitrogen stream. The extraction step was repeated, adding 3.75 mL of dichloromethane/methanol (1:2, v/v) and 1.25 mL of dichloromethane to the pellet, followed by vortex and centrifuging. The supernatant was added to the previous tube and dried under a nitrogen stream. 3.75 mL of dichloromethane/methanol (1:2, v/v), 1.25 mL of methanol and 2.25 mL of Milli-Q water were added to the supernatant, followed by vortex after each addition and centrifuging. Two phases were formed, the upper being the aqueous phase and the lower being the organic phase, that contains the extracted lipids. The organic phase was transferred to a clean glass tube and 1.88 mL of dichloromethane was added to the aqueous phase to wash. The tubes were vortex and centrifuged, before transferring the organic phase. The washing step was repeated and the extracted lipids were dried under a nitrogen stream. Dichloromethane was added to transfer the extracted lipids to

2 mL amber glass vials. The lipids were dried under a nitrogen stream and stored under a nitrogen atmosphere at –20 °C.

2.5. Quantification of phospholipids by phosphorus assay

The quantification of phospholipids was performed by measuring the phosphorus amount in the total lipid extracts, as described by Lopes et al. (2019) (83). The extracted lipids were resuspended in dichloromethane and 10 µL was transferred to a glass tube. After drying the lipids under a nitrogen stream, 125 µL of 70% perchloric acid was added to both samples and phosphate standards (100 µg mL^{-1} of sodium phosphate dibasic dihydrate, ranging from 0.10 to 2.00 µg of phosphorus). The samples were heated at 180 °C for 40 min, or until clear, and cooled down until room temperature. 825 µL of Milli-Q water, 125 µL of 2.5% ammonium molybdate and 125 µL of 10% ascorbic acid were added to both samples and phosphate standards, followed by vortex after each addition. All tubes were incubated in a water bath for 10 min at 100 °C and cooled down in cold water afterward. 200 µL of samples and standards were transferred (in duplicate) to a 96-well plate and the absorbance of was measured at 797 nm, at room temperature, in a microplate UV-Vis spectrophotometer.

2.6. Separation of lipids by thin-layer chromatography

Lipids from the total lipid extract were separated by thin-layer chromatography (TLC) using silica gel plates (**Supplementary Material 1 and 2**). The plates were washed with chloroform/methanol (1:1, v/v) prior to the separation and placed in an oven at 100 °C for 15 minutes to dry. Spots containing 20 mg of lipids were applied to the plates and developed using hexane/ether/acetic acid (80:20:1, v/v/v) as a solvent mixture. Separated lipid spots were revealed by exposing the plates to sprayed primuline (50 mg/100 mL acetone/water, 80:20, v/v) and visualized under a UV lamp (254 and 366 nm; Camag, Berlin, Germany). Fractions of polar and neutral lipids were obtained. The spots were scraped off the plates and extracted from silica with

dichloromethane/methanol (2:1, v/v) and the fractions of PL were quantified by the phosphorus assay.

2.7. Polar Lipid Analysis by Hydrophilic Interaction Liquid Chromatography – Electrospray Ionization – Mass Spectrometry

Polar lipids were analyzed by hydrophilic interaction liquid chromatography – electrospray ionization – mass spectrometry (HILC-ESI-MS) on a Thermo Scientific Accela™ High-Performance Liquid Chromatography (HPLC) system with an autosampler online coupled to a QExactive® mass spectrometer with Orbitrap® technology (Thermo Fisher, Scientifc, Bremen, Germany). The solvent system consisted of two mobile phases: mobile phase A was acetonitrile/methanol/water, 50:25:25 per volume, with 1 mM ammonium acetate, and mobile phase B was acetonitrile/methanol, 60:40 per volume, with 1 mM ammonium acetate. Initially, 0% of mobile phase B was held isocratically for 8 min, followed by a linear increase to 50% of A and an increase to 70% of B within 5 min, followed by a maintenance period of 2 min, returning to the initial conditions in 3 min. A volume of 10 µL of each sample containing 10 µg of lipid extract and 190 µL of eluent B was introduced into the Ascentis®Si column (15 cm × 1 mm, 3 µm, Sigma-Aldrich) with a flow rate of 200 µL min^{-1} and at 35 °C.

The mass spectrometer with Orbitrap®technology was operated simultaneously in positive (electrospray voltage 3.0 kV) and negative (electrospray voltage –2.7 kV) modes with a resolution of 70,000 and automatic gain control (AGC) target of 1×10^6, the capillary temperature was 250 °C and the sheath gas flow was 15 U. In MS/MS experiments, a resolution of 17,500 and AGC target of 1×10^5 were used. Cycles consisted of one full scan mass spectrum and ten data-dependent MS/MS scans were repeated continuously throughout the experiments with the dynamic exclusion of 60 s and intensity threshold of 2×10^4. Normalized collision energy™ (CE) ranged between 25, 30 and 35 eV. Data acquisition was carried out using the Xcalibur data system (V2.2

SP1.48, Thermo Fisher Scientific, USA). Six replicates were performed, corresponding to three analytical replicates of two lipid extracts (total of six replicates, N = 3 × 2).

Manual injection of the triacylglyceride fractions was also performed and analyzed by direct infusion ESI-MS in positive mode in the ESI- QExactive® mass spectrometer with Orbitrap® technology (Thermo Fisher, Scientifc, Bremen, Germany). operating in similar conditions. For ESI-MS analysis, 2 µL of each sample containing 2 µg of TG extract (plus 998 µL of eluent B and 100 µL of ammonium acetate) was injected.

The identification of molecular species of polar lipids was based on the LC retention time, mass accuracy and detailed structural information inferred by MS/MS data. Accurate mass measurements (≤5 ppm) were used to confirm the elemental composition calculation of empirical formula. Structural characterization of molecular species was based on tandem mass spectra interpretation to confirm polar head group and fatty acyl chains.

2.8. Fatty Acid Analysis by Gas Chromatography – Mass Spectrometry

The total fatty acyl substituents were analyzed after transmethylation of total lipid extracts (10 µg), fractions of phospholipid (20 µg) and fractions of triacylglyceride (10 µg). Fatty acid methyl esters (FAMEs) were prepared using a methanolic solution of potassium hydroxide (2.0 M) and saturated sodium chloride solution, according to the methodology previously described by Aued-Pimentel et al. (2004) (84). Volumes of 2.0 µL of hexane solution containing the FAME were subjected to analysis by gas chromatography – mass spectrometry (GC–MS) on an Agilent Technologies 6890 N Network (Santa Clara, CA, USA) equipped with a DB-FFAP column with 30 m of length, 0.32 mm of internal diameter, and 0.25 µm of film thickness (J&W Scientific, Folsom, CA, USA). The GC equipment was connected to an Agilent 5973 Network Mass Selective Detector operating with an electron impact mode at 70 eV and scanning the range m/z 40–500 in a 1-s cycle in a full scan mode acquisition. The oven temperature

was programmed from an initial temperature of 80 °C, a standing at this temperature for 3 min, a linear increase to 160 °C at 25 °C/min, followed by a linear increase to 190 °C at 2°C/min. The injector and detector temperatures were 220 and 280 °C, respectively. Helium was used as a carrier gas at a flow rate of 1.4 mL/min. Eighteen replicates were performed, corresponding to three analytical replicates of two lipid extracts, divided into three lipid fractions (total lipid extract, phospholipid fraction and triacylglyceride fraction, N = 3 × 2 x 3). Data acquisition and analysis was carried out using the Qualitative Analysis MassHunter Workstation (V10.0, Agilent Technologies, USA) against the NIST14.L database. The sum of the areas of the peaks assigned as FA in the chromatogram was considered as the total amount of FA. To determine the relative content of each FA, areas of each individual peak were divided by the sum of the area of all the peaks identified allowing us to determine the relative content of each FA.

3. Results and discussion

3.1. Identification and characterization of the phospholipid profile of *Lasiodiplodia theobromae* and *Lasiodiplodia hormozganensis*

Identification of the polar lipid profile at the molecular level was performed by liquid chromatography-mass spectrometry (LC-MS) and LC-MS/MS. The interpretation of the mass spectrometry data collected for fungal total lipid extracts allowed the identification of 147 phospholipid (PL) species, most of them present in both fungi. Fifty one (51) PL species were present either in the lipidome of *L. theobromae* or *L. hormozganensis*. In total, 108 molecular species of PL were identified in *L. theobromae* and 135 were identified in *L. hormozganensis*, representing 243 new identifications. The criteria for identifying lipids from each PL class included the accuracy of the mass measurements (< 5 ppm), the LC retention time (within the characteristic range for each class), and the characteristics of the MS/MS spectra (manual analysis allowed the confirmation of the polar head, characteristic ions and fatty acyl composition).

A total ion chromatogram (TIC) is a time-dependent representation of the relative abundance of molecular species in a sample. A TIC of PL species can be observed in **Figure 5.** In **Figure 6** are reconstructed-ion chromatograms (RIC), a mass-dependent representation of the relative abundance of molecular species that display a representative MS spectrum of each class identified.

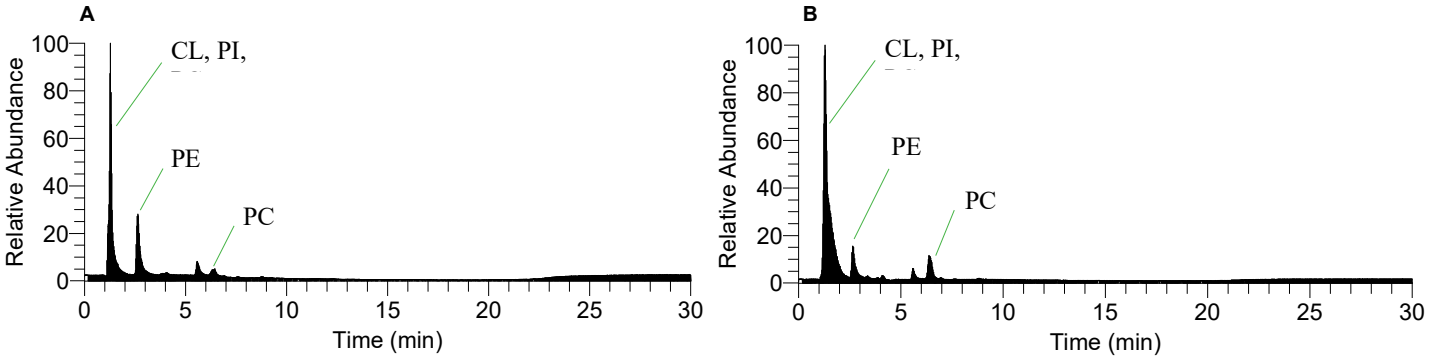

Figure 5 – Representative TIC of the phospholipids in a sample of *Lasiodiplodia theobromae* (A) and *Lasiodiplodia hormozganensis* (B). CL – cardiolipin; PC – phosphatidylcholine; PE – phosphatidylethanolamine; PI – phosphatidylinositol.

Regarding the phospholipid profile of *L. theobromae*, 108 molecular species (m/z ions) from 11 classes were identified: phosphatidylcholine (PC, 27 species) and lyso-PC (LPC, 4 species) (**Table 3**), phosphatidylethanolamine (PE, 19 species) and lyso-PE (LPE, 10 species) (**Table 5**), sphingomyelin (SM, 1 species) (**Table 8**), phosphatidic acid (PA, 13 species) and lyso-PA (LPA, 1 species) (**Table 10**), cardiolipin (CL, 17 species) (**Table 12**), phosphatidylinositol (PI, 7 species) and lyso-PI (LPI, 4 species) (**Table 14**), phosphatidylglycerol (PG, 3 species) (**Table 16**) and phosphatidylserine (PS, 2 species) (**Table 18**). Two ceramides (Cer, 2 species) were also identified (**Table 7**).

Regarding the phospholipid profile of *L. hormozganensis*, 135 molecular species from 11 classes were identified: phosphatidylcholine (PC, 35 species) and lyso-PC (LPC, 6 species) (**Table 4**), phosphatidylethanolamine (PE, 28 species) and lyso-PE (LPE, 15 species) (**Table 6**), sphingomyelin (SM, 2 species) (**Table 9**), phosphatidic acid (PA, 13 species) and lyso-PA (LPA, 1 species) (**Table 11**), cardiolipin (CL, 18 species) (**Table 13**), phosphatidylinositol (PI, 10 species) (**Table 15**), phosphatidylglycerol (PG, 6 species) (**Table 17**) and phosphatidylserine (PS, 1 species) (**Table 19**).

The PC and LPC species were identified in the mass spectra as $[M + H]^+$ and $[M + CH_3COO]^-$ molecular ions and PE, LPE and PS were identified as $[M + H]^+$ and $[M – H]^-$ ions. PAs were identified as $[M + NH_4]^+$ and $[M-H]^-$ ions. Ceramides and sphingomyelins were identified as $[M + H]^+$ ions. The remaining classes were assigned as $[M – H]^-$ ions. All species were first identified by the LC retention time and by mass accuracy. After this step, the tandem mass spectra of each match were analyzed to confirm the polar head group. In the MS/MS spectra it was also possible to identify the fatty acyl chains that compose the phospholipids, mainly in the negative ion mode, in the form of carboxylate anions ($RCOO^-$ ions). Information on the fatty acid

composition of the lipids identified can be observed in the tables of this chapter. The most abundant lipid species is presented in bold.

Phosphatidylcholines

Phosphatidylcholines (PC) and lyso-phosphatidylcholines (LPC) were identified in the positive ion mode as $[M + H]^+$ ions (**Table 3** and **Table 4**). Species of this class were identified in the MS/MS spectra by the presence of the ion of the phosphocholine polar head group, at m/z 184. PC and LPC can also be identified in the negative ion mode as $[M + CH_3COO]^-$ ions, which represents a mass shift of plus 58 Da in comparison with the $[M+H]^+$ ions. Here, species were identified by MS//MS analysis, by the neutral loss of 74 Da and the fragment ion at m/z 168, corresponding to the demethylated phosphocholine polar head group. The most abundant PC molecular species in the lipidome of *L. theobromae* and *L. hormozganensis* were identified in the positive ion mode at m/z 758.5699, PC(34:2), and m/z 782.5693, PC(36:4), respectively.

The LC-MS spectra showing the representative profile of the PC class of both fungi can be observed in **Figure 6**, along with MS/MS spectra of two abundant molecular species of this class, both in positive and negative ion mode.

Table 3 – Phosphatidylcholine identified in *Lasiodiplodia theobromae* by LC-MS and LC-MS/MS (mass error < 5 ppm).

Observed *m/z*	**Lipid species (C:N)**	**Fatty acyl chains**
	PC identified as $[M+H]^+$	
496.3401	LPC(16:0)	16:0
524.3713	LPC(18:0)	**
522.3561	LPC(18:1)	18:1
520.3396	LPC(18:2)	18:2
718.5377	PC(31:1)	**
714.5088	PC(31:3)	*
734.5703	PC(32:0)	**
732.5518	PC(32:1)	*
730.5389	PC(32:2)	**

744.5535	PC(33:2)	**
760.5856	PC(34:1)	(16:0/18:1)
758.5699	**PC(34:2)**	**(16:0/18:2) and (16:1/18:1)**
756.5548	PC(34:3)	(16:0/18:3) and (16:1/18:2)
754.53386	PC(34:4)	*
752.5223	PC(34:5)	*
772.5865	PC(35:2)	**
770.5696	PC(35:3)	**
788.6152	PC(36:1)	*
786.6012	PC(36:2)	(18:1/18:1) and (18:0/18:2)
784.5850	PC(36:3)	(18:1/18:2) and (18:0/18:3
782.5703	PC(36:4)	(18:2/18:2) and (18:1/18:3)
780.5519	PC(36:5)	*
778.5362	PC(36:6)	*
800.6152	PC(37:2)	**
814.6317	PC(38:2)	*
812.6164	PC(38:3)	(18:2/20:1) and (18:1/20:2)
802.5359	PC(38:8)	*
844.6781	PC(40:1)	**
856.6785	PC(41:2)	**
870.6954	PC(42:2)	**
PC identified as $[M + CH_3COO]^-$		
868.6078	PC(38:4)	(18:2/20:2)

Legend: C – number of carbon atoms; N – number of double bonds on the fatty acyl chains; *molecular species confirmed by the LC retention time and exact mass; **molecular species confirmed by the LC retention time, exact mass and the polar head ion

Table 4 – Phosphatidylcholine identified in *Lasiodiplodia hormozganensis* by LC-MS and LC-MS/MS (mass error < 5 ppm).

Observed m/z	**Lipid species (C:N)**	**Fatty acyl chains**
PC identified as $[M+H]^+$		
496.3399	LPC(16:0)	16:0
510.3568	LPC(17:0)	*
524.3723	LPC(18:0)	18:0
520.3402	LPC(18:2)	18:2
518.3244	LPC(18:3)	18:3
676.4904	PC(28:1)	*
706.5391	PC(30:0)	*
720.5515	PC(31:0)	*

718.5394	PC(31:1)	(18:1/13:0) and (18:0/13:1)
714.5064	PC(31:3)	(18:2/13:1)
734.5701	PC(32:0)	**
730.5391	PC(32:2)	**
744.5546	PC(33:2)	*
760.5848	PC(34:1)	(16:0/18:1)
758.5702	PC(34:2)	(16:0/18:2) and (16:1/18:1)
756.5546	PC(34:3)	(16:0/18:3) and (16:1/18:2)
754.5386	PC(34:4)	**
752.5224	PC(34:5)	*
774.5997	PC(35:1)	*
772.5855	PC(35:2)	**
770.5698	PC(35:3)	**
768.5536	PC(35:4)	**
788.6144	PC(36:1)	**
786.5995	PC(36:2)	(18:1/18:1) and (18:0/18:2)
784.5856	PC(36:3)	(18:1/18:2) and (18:0/18:3)
782.5693	**PC(36:4)**	**(18:2/18:2) and (18:1/18:3)**
780.5540	PC(36:5)	**
778.5383	PC(36:6)	**
798.6002	PC(37:3)	**
814.6304	PC(38:2)	*
812.6165	PC(38:3)	(18:2/20:1) and (18:1/20:2)
810.6022	PC(38:4)	(18:2/20:2)
802.5364	PC(38:8)	**
800.5201	PC(38:9)	*
844.6779	PC(40:1)	**
834.5985	PC(40:6)	*
856.6795	PC(41:2)	**
870.6956	PC(42:2)	**
868.6797	PC(42:3)	**
884.7120	PC(43:2)	**
PC identified as [M + CH_3COO]-		
580.3627	LPC(18:1)	18:1

Legend: C – number of carbon atoms; N – number of double bonds on the fatty acyl chains; *molecular species confirmed by the LC retention time and exact mass; **molecular species confirmed by the LC retention time, exact mass and the polar head ion

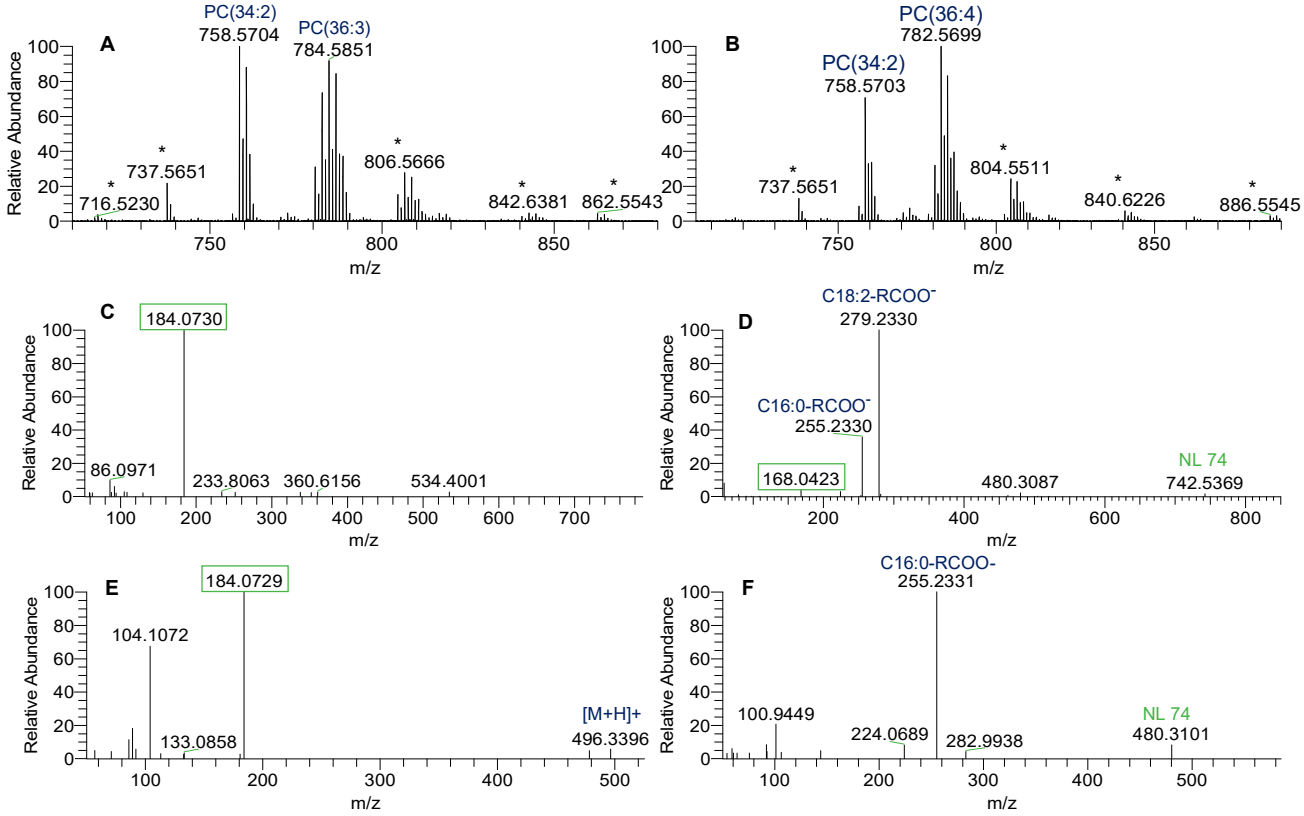

Figure 6 – LC-MS spectrum representative of the phospholipid subclass phosphatidylcholine (PC) of *L. theobromae* (A) and *L. hormozganensis* (B), identified as $[M+H]^+$ ions. ESI-MS/MS spectra of $[M+H]^+$ ions at m/z 758.57 (C) and $[M+CH_3COO]^-$ ions at m/z 816.58 (D), corresponding to PC(34:2). ESI-MS/MS spectra of $[M+H]^+$ ions at m/z 496.34 (E) and $[M+CH_3COO]^-$ ions at m/z 554.35 (F), corresponding to LPC(16:0). *background

In sum, 37 individual molecular species were identified for the PC class: 25 were found in both fungi and 12 were observed isolated in one species or another (**Figure 7**). *Lasiodiplodia hormozganensis* was the species with larger number of phosphatidylcholines, with 10 additional new identifications in addition to the 25 that are common to both fungi. Two molecular species PC(32:1) and PC(37:2) were identified in the samples of *L. theobromae*, but not in *L. hormozganensis*.

LPC were also more abundant in *L. hormozganensis*, with 6 identifications, while in *L. theobromae* only 4 molecular species were found and all are present in *L. hormozganensis*.

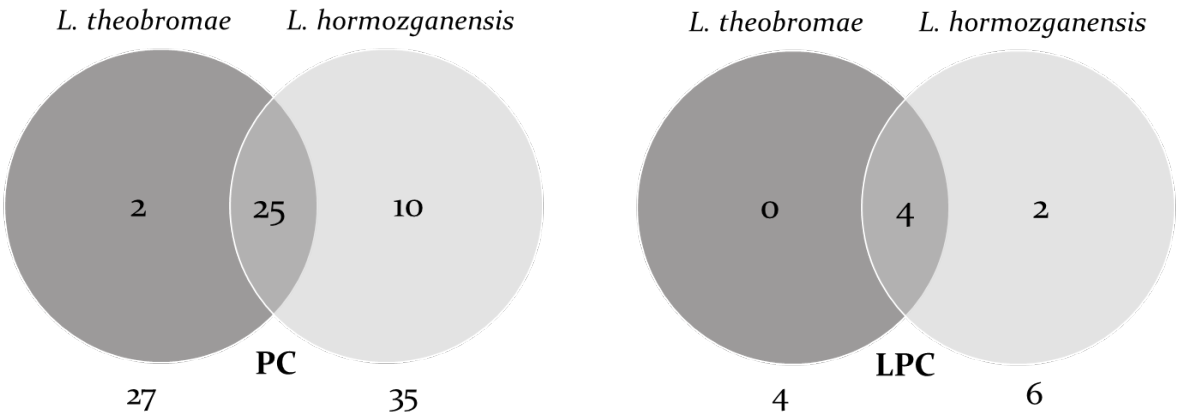

Figure 7 – Venn diagram of PC and LPC present in the lipidomic profile of *Lasiodiplodia theobromae* and *Lasiodiplodia hormozganensis*.

PC and PE have been reported as the most abundant lipids of fungal species in several studies (66,85–87), although most identify a much smaller number of molecular species or do not have information for fatty acyl composition. These are the most commonly found classes of phospholipids. In phytopathogenic fungi, PC and PE have been reported as essential for growth and their pathway as crucial for toxin production and full virulence (79).

Phosphatidilethanolamines

Phosphatidylethanolamines (PE) and lyso-phosphatidylethanolamines (LPE) were identified in the positive ion mode as $[M + H]^+$ ions (**Table 5** and **Table 6**). Species of this class were confirmed by the neutral loss of 141 Da observed in the ESI-MS/MS spectra, which corresponds to the neutral loss of the phosphoethanolamine polar head group. PE and LPE can also be identified in the negative ion mode as $[M – H]^-$ molecular ions. In this mode, molecular species were identified by the fragment ions at m/z 140, corresponding to the phosphoethanolamine polar head group, and the abundant ion at m/z 196. The most abundant PE molecular species in the lipidome of *L. theobromae* and *L. hormozganensis* were identified in the positive ion mode at m/z 716.5236 and m/z 716.5234 [PE(34:2)], respectively.

A LC-MS spectra of PE species of both fungi can be observed in **Figure 8**, along with MS/MS spectra of two abundant molecular species of this class, in both positive and negative ion mode.

Table 5 – Phosphatidylethanolamine identified in *Lasiodiplodia theobromae* by LC-MS and LC-MS/MS (mass error < 5 ppm).

Observed *m/z*	**Lipid species (C:N)**	**Fatty acyl chains**
	PE identified as $[M+H]^+$	
426.2618	LPE(14:0)	*
454.2933	LPE(16:0)	16:0
468.3092	LPE(17:0)	17:0
466.2935	LPE(17:1)	17:1
482.3261	LPE(18:0)	*
480.3091	LPE(18:1)	18:1
478.2934	LPE(18:2)	18:2
476.2755	LPE(18:3)	*
508.3405	LPE(20:1)	*
504.3078	LPE(20:3)	*
634.4459	PE(28:0)	*
692.5232	PE(32:0)	*
690.5077	PE(32:1)	*
688.4911	PE(32:2)	(14:0/18:2)
704.5258	PE(33:1)	(15:0/18:1) and (16:0/17:1)
718.5391	PE(34:1)	(16:0/18:1)
716.5236	**PE(34:2)**	**(16:0/18:2)**
714.5077	PE(34:3)	(16:0/18:3) and (16:1/18:2)
730.5389	PE(35:2)	*
728.5228	PE(35:3)	(17:1/18:2)
746.5674	PE(36:1)	*
744.5545	PE(36:2)	(18:1/18:1)
742.5380	PE(36:3)	(18:2/18:1)
740.5231	PE(36:4)	(18:2/18:2)
770.5713	PE(38:3)	**
	PE identified as $[M-H]^-$	
772.5826	PE(38:1)	*
770.5707	PE(38:2)	(18:1/20:1) and (20:0/18:2)
766.5393	PE(38:4)	*

764.5202	PE(38:5)	*

Legend: C – number of carbon atoms; N – number of double bonds on the fatty acyl chains; *molecular species confirmed by the LC retention time and exact mass; **molecular species confirmed by the LC retention time, exact mass and the polar head ion

Table 6 – Phosphatidylethanolamine identified in *Lasiodiplodia hormozganensis* by LC-MS and LC-MS/MS (mass error < 5 ppm).

Observed *m/z*	**Lipid species (C:N)**	**Fatty acyl chains**
	PE identified as $[M+H]^+$	
426.2615	LPE(14:0)	*
454.2934	LPE(16:0)	16:0
452.2778	LPE(16:1)	16:1
468.3091	LPE(17:0)	17:0
466.2934	LPE(17:1)	17:1
482.3261	LPE(18:0)	*
480.3092	LPE(18:1)	18:1
478.2936	LPE(18:2)	18:2
476.2756	LPE(18:3)	18:3
508.3405	LPE(20:1)	20:1
506.3258	LPE(20:2)	20:2
504.3080	LPE(20:3)	*
502.2912	LPE(20:4)	20:4
500.2753	LPE(20:5)	*
692.5232	PE(32:0)	(16:0/16:0)
690.5078	PE(32:1)	(14:0/18:1) and (16:1/16:0)
688.4909	PE(32:2)	(14:0/18:2)
704.5243	PE(33:1)	(18:1/15:0) and (17:1/16:0)
700.4940	PE(33:3)	**
718.5377	PE(34:1)	(16:0/18:1)
716.5234	**PE(34:2)**	**(16:0/18:2)**
714.5077	PE(34:3)	(16:0/18:3)
712.4935	PE(34:4)	*
728.5224	PE(35:3)	(18:2/17:1)
746.5671	PE(36:1)	*
744.5547	PE(36:2)	(18:1/18:1), (16:0/20:2) and (18:0/18:2)
742.5380	PE(36:3)	(18:1/18:2) and (18:0/18:3)
740.5213	PE(36:4)	(18:2/18:2)
738.5054	PE(36:5)	*
772.5857	PE(38:2)	(18:1/20:1)

770.5696	PE(38:3)	(18:1/20:2) and (18:2/20:1)
768.5524	PE(38:4)	(18:2/20:2), (18:1/20:3) and (18:3/20:1)
766.5359	PE(38:5)	*
764.5201	PE(38:6)	*
794.5675	PE(40:5)	*
792.5517	PE(40:6)	*
PE identified as [M-H]$^-$		
438.2632	LPE(15:0)	15:0
634.4460	PE(28:0)	*
700.4948	PE(33:2)	(16:0/17:2) and (15:0/18:2)
728.5247	PE(35:2)	(17:0/18:2) and (17:1/18:1)
734.4789	PE(36:6)	(18:3/18:3) and (18:3O)
756.5534	PE (37:2)	(18:1/19:1)
754.5375	PE (37:3)	(18:2/19:1)

Legend: C – number of carbon atoms; N – number of double bonds on the fatty acyl chains; *molecular species confirmed by the LC retention time and exact mass; **molecular species confirmed by the LC retention time, exact mass and the polar head ion

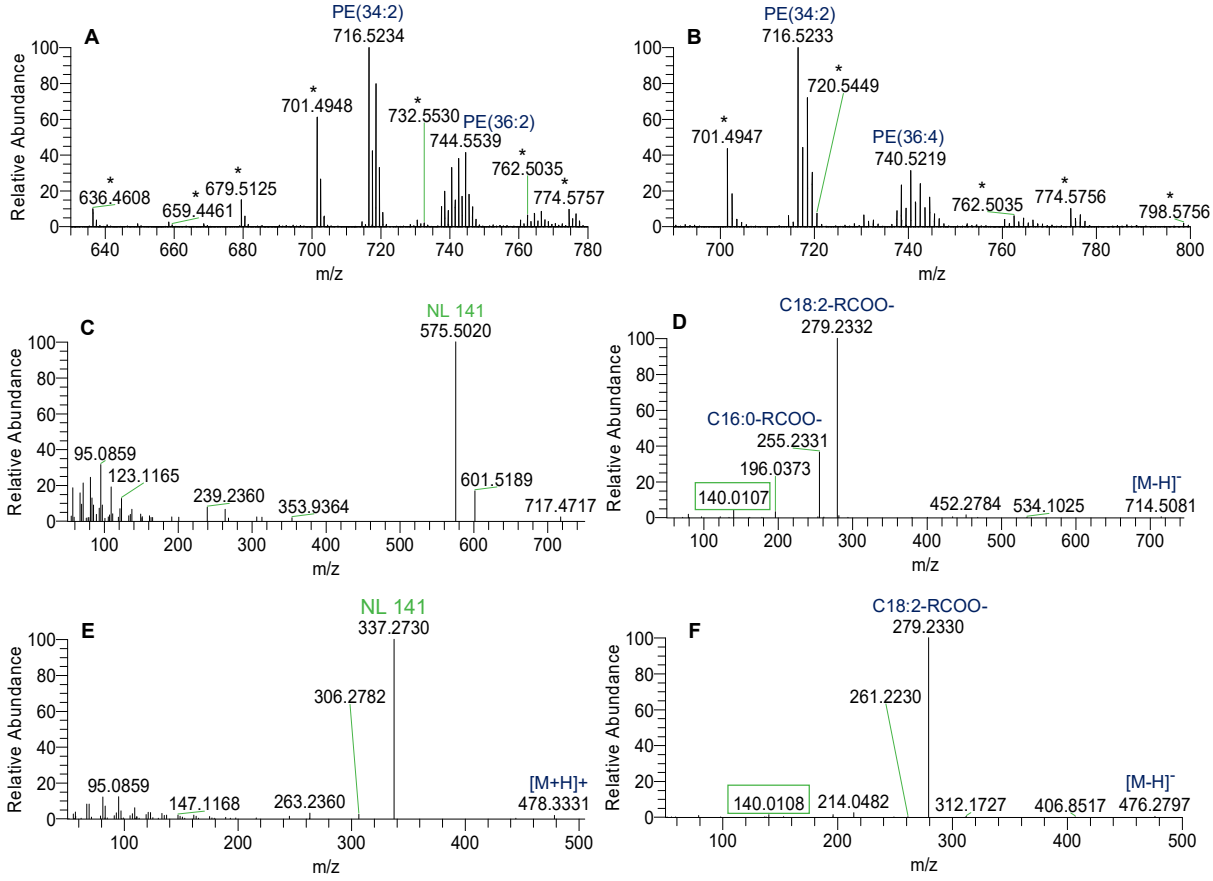

Figure 8 – LC-MS spectra representative of the phospholipid subclass phosphatidylethanolamine (PE) of *L. theobromae* (A) and *L. hormozganensis* (B), identified as $[M+H]^+$ ions; ESI-MS/MS spectra of PE(34:2), of the corresponding $[M+H]^+$ ions at m/z 716.52 (C) and $[M-H]^-$ ions at m/z 714.51 (D). ESI-MS/MS spectrum of LPE(18:2), of the corresponding $[M+H]^+$ ions at m/z 478.29 (E) and $[M-H]^-$ ions at m/z 476.28 (F). *background

In sum, 29 individual molecular species were identified for the PE class, 18 of those found in both fungi (**Figure 9**). *Lasiodiplodia hormozganensis* was the species with larger number of phosphatidylcholines, with 10 additional new identifications in addition to the 18 that are common to both fungi. One molecular species, PE(38:1), was identified in the samples of *L. theobromae*, but not in *L. hormozganensis*.

LPE were also more abundant in *L. hormozganensis*, with 15 identifications, while in *L. theobromae* only 10 molecular species were found and all are present in *L. hormozganensis*.

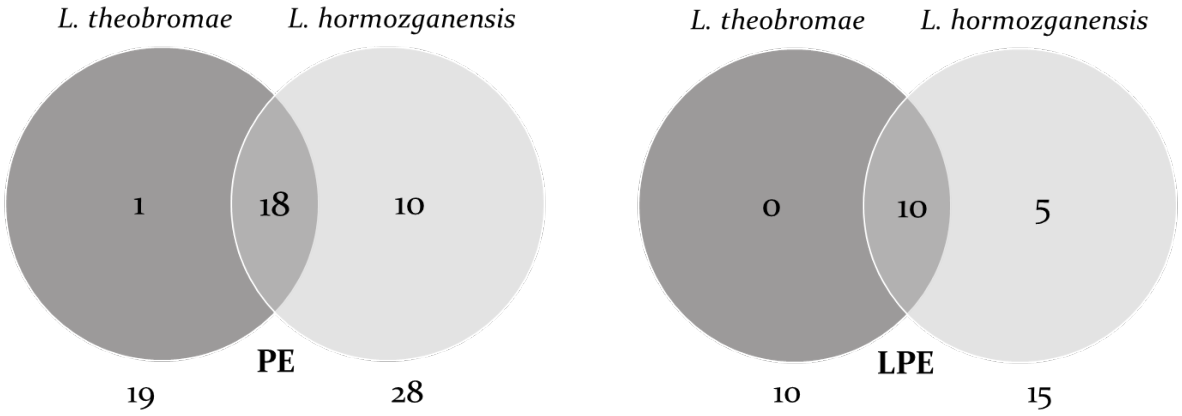

Figure 9 – Venn diagram of PE and LPE present in the lipidomic profile of *L. theobromae* and *L. hormozganensis*.

Ceramides and sphingomyelins

Ceramides and sphingomyelins were identified in the positive mode as $[M + H]^+$ ions (**Table 7**, **Table 8** and **Table 9**). In the ESI-MS/MS spectrum, ceramides were identified by the fragment ions of the sphingoid base and ions of the FA amide substituent. Only two molecular species of Cer were identified, in the lipidome of *L. theobromae*. The most abundant was identified at m/z 668.6553 [Cer(42:0)] and can be observed in **Figure 10**.

Sphingomyelins were identified in the ESI-MS/MS spectrum by the abundant ion at m/z 184, corresponding to the phosphocholine polar head group. The most abundant SM molecular species identified was in the lipidome of *L. hormozganensis*, at m/z 717.5904 [SM(d35:1)]. An MS/MS spectrum of SM(d34:1), identified in *L. hormozganensis*, can be observed in **Figure 11**.

Table 7 – Ceramides identified in *Lasiodiplodia theobromae* by LC-MS and LC-MS/MS (mass error < 5 ppm).

Observed m/z	Lipid species (C:N)	Fatty acyl chains
Ceramides identified as [M+H]+		
568.5662	Cer(d36:0)	*
668.6553	**Cer(t42:0)**	**(18:0/24:0)**

Legend: C – number of carbon atoms; N – number of double bonds on the fatty acyl chains; *molecular species confirmed by the LC retention time and exact mass

Table 8 – Sphingomyelins (SM) identified in *Lasiodiplodia theobromae* by LC-MS and LC-MS/MS (mass error < 5 ppm).

Observed *m/z*	Lipid species (C:N)	Fatty acyl chains
Sphingomyelins identified as [M+H]+		
717.5905	SM(d35:1)	*

Legend: C – number of carbon atoms; N – number of double bonds on the fatty acyl chains; *molecular species confirmed by the LC retention time and exact mass

Table 9 – Sphingomyelins (SM) identified in *Lasiodiplodia hormozganensis* by LC-MS and LC-MS/MS (mass error < 5 ppm).

Observed *m/z*	Lipid species (C:N)	Fatty acyl chains
Sphingomyelins identified as [M+H]+		
703.5750	SM(d34:1)	**
717.5904	**SM(d35:1)**	*

Legend: C – number of carbon atoms; N – number of double bonds on the fatty acyl chains; *molecular species confirmed by the LC retention time and exact mass; **molecular species confirmed by the LC retention time, exact mass and the polar head ion

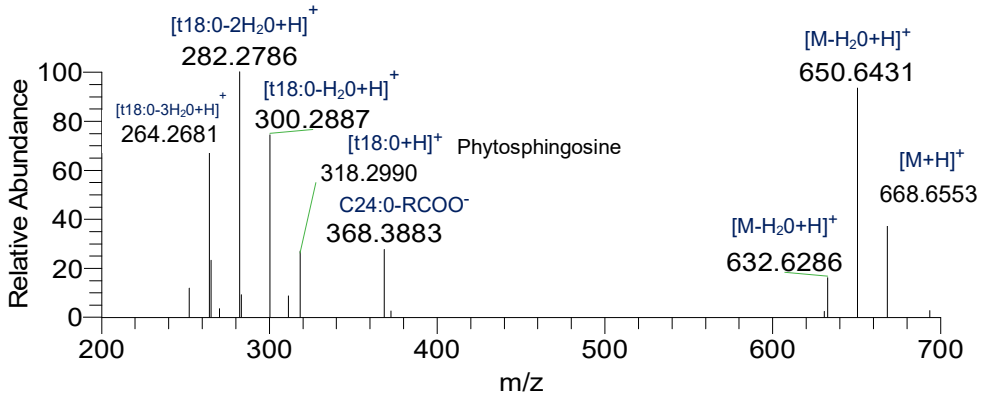

Figure 10 – ESI-MS/MS spectrum of Cer(t42:0), of corresponding $[M+H]^+$ ions at m/z 668.65. The successive loss of three molecules of H_2O allows for the identification of the sphingoid base as a phytosphingosine.

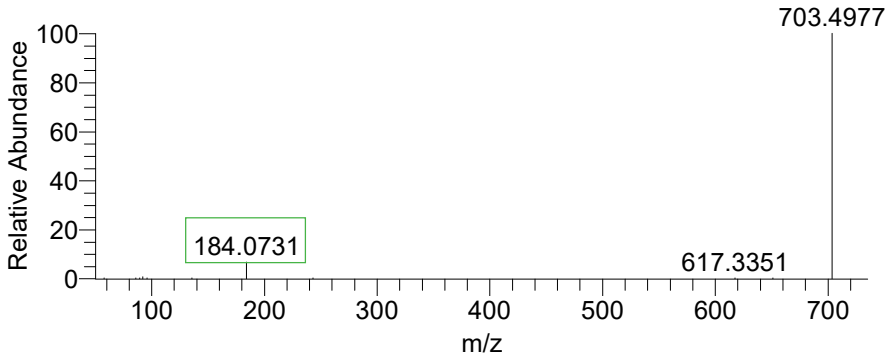

Figure 11 – ESI-MS/MS spectrum of SM(d34:1), of corresponding $[M+H]^+$ ions at m/z 703.5751.

Only two individual molecular species were identified for the SM subclass among the lipidomes of *L. theobromae* and *L. hormozganensis*, respectively one and two, but one sphingomyelin was common to both species (**Figure 12**).

Sphingomyelins have not been reported before in fungi.

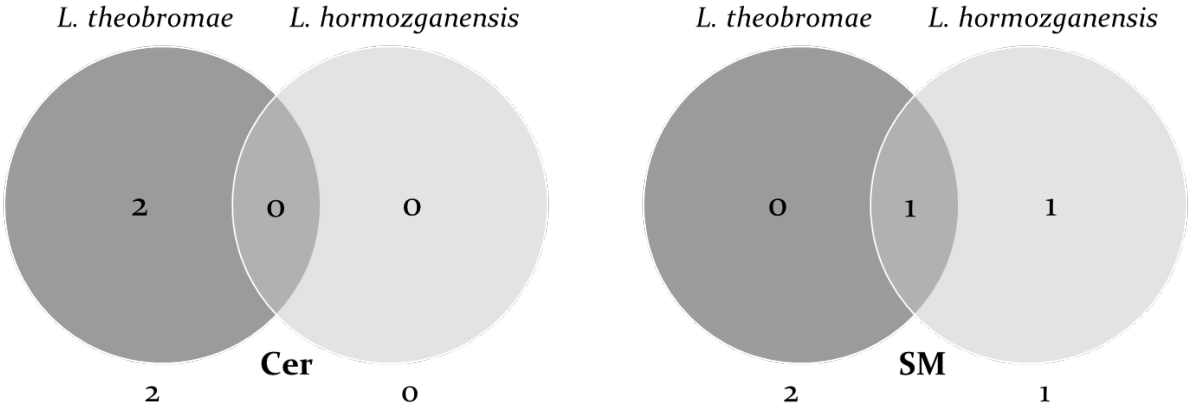

Figure 12 – Venn diagram of Cer and SM present in the lipidomic profile of *L. theobromae* and *L. hormozganensis*.

Phosphatidic acids

Phosphatidic acids (PA) were identified in the negative ion mode as $[M-H]^-$ ions (**Table 10** and **Table 11**) and confirmed in the ESI-MS/MS spectrum by the abundant ion at m/z 153. PA can also be identified in the positive ion mode as $[M + NH_4]^+$ molecular ions, by the neutral loss of 115 Da observed in the ESI-MS/MS spectrum (88). The most abundant PA molecular species in the lipidome of *L. theobromae* and *L. hormozganensis* were identified in the negative ion mode at m/z 671.4667 [PA(34:2)] and m/z 695.4668 [PA(36:4)], respectively.

A LC-MS spectra of PA species of both fungi can be observed in **Figure 13**, along with MS/MS spectra of two abundant molecular species of this class, PA(36:4) in the negative ion mode and PA(28:0) in the positive ion mode.

Table 10 – Phosphatidic acid identified in *Lasiodiplodia theobromae* by LC-MS and LC-MS/MS (mass error < 5 ppm).

Observed *m/z*	Lipid species (C:N)	Fatty acyl chains
	PA identified as $[M+NH_4]^+$	
610.4453	PA(28:0)	**
650.4401	PA(30:2(OH))	**

690.4716	PA(33:3(OH))	**
	PA identified as [M-H]$^-$	
433.2360	LPA(18:2)	*
673.4817	PA(34:1)	*
671.4667	**PA(34:2)**	**(16:0/18:2)**
669.4506	PA(34:3)	(16:1/18:2)
701.5107	PA(36:1)	(18:0/18:1)
699.4972	PA(36:2)	(18:1/18:1) and (18:0/18:2)
697.4818	PA(36:3)	(18:1/18:2)
695.4664	PA(36:4)	(18:2/18:2)
693.4508	PA(36:5)	*
727.5272	PA(38:2)	*
725.5133	PA(38:3)	*

Legend: C – number of carbon atoms; N – number of double bonds on the fatty acyl chains; *molecular species confirmed by the LC retention time and exact mass; **molecular species confirmed by the LC retention time, exact mass and the polar head ion

Table 11 – Phosphatidic acid identified in *Lasiodiplodia hormozganensis* by LC-MS and LC-MS/MS (mass error < 5 ppm).

Observed *m/z*	**Lipid species (C:N)**	**Fatty acyl chains**
	PA identified as [M-H]$^-$	
433.2358	LPA(18:2)	18:2
673.4818	PA(34:1)	*
671.4669	PA(34:2)	(16:0/18:2)
669.4514	PA(34:3)	(16:0/18:3) and (16:1/18:2)
701.5101	PA(36:1)	(18:0/18:1)
699.4981	PA(36:2)	(18:1/18:1) and (18:0/18:2)
697.4822	PA(36:3)	*
695.4668	**PA(36:4)**	**(18:2/18:2) and (18:1/18:3)**
693.4512	PA(36:5)	(18:2/18:3)
691.4359	PA(36:6)	(18:3/18:3)
685.4819	PA(35:2)	(17:0/18:2) and (17:1/18:1)
683.4667	PA(35:3)	(17:1/18:2)
727.5272	PA(38:2)	*
725.5145	PA(38:3)	*

Legend: C – number of carbon atoms; N – number of double bonds on the fatty acyl chains; *molecular species confirmed by the LC retention time and exact mass

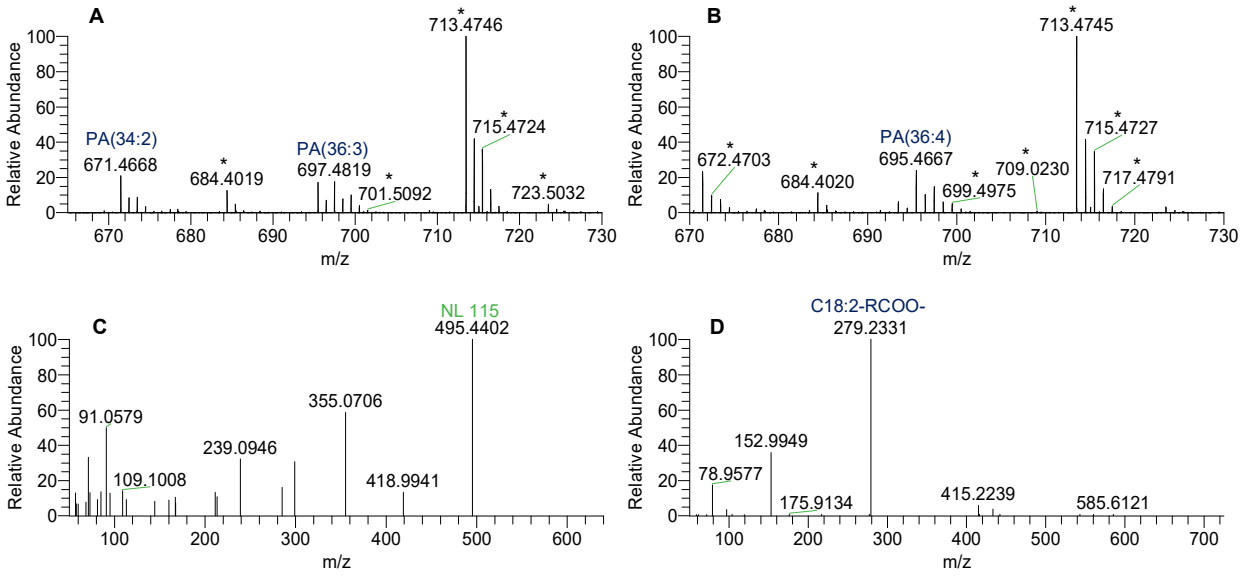

Figure 13 – LC-MS spectra representative of the phospholipid subclass phosphatidic acid (PA) of *L. theobromae* (A) and *L. hormozganensis* (B), identified as $[M-H]^-$ ions; ESI-MS/MS spectra of PA(28:0), corresponding of $[M+NH_4]^+$ ions at m/z 610.45 (C). MS/MS spectra of PA(36:4), corresponding of [M-H]- ions at m/z 695.47 (D). *background

In sum, 16 individual molecular species were identified for the PA subclass, meaning that 10 were found in both fungi and 6 were observed isolated in one species or another (**Figure 14**). Both species had the same number of phosphatidic acids and both had 3 additional new identifications in addition to the 10 that are common. Two oxidated species [PA(30:2(OH))and PA(33:3(OH))] were identified in the samples of *L. theobromae*, but not in *L. hormozganensis*.

Regarding LPAs, only one species was identified in both fungi, LPA(18:2).

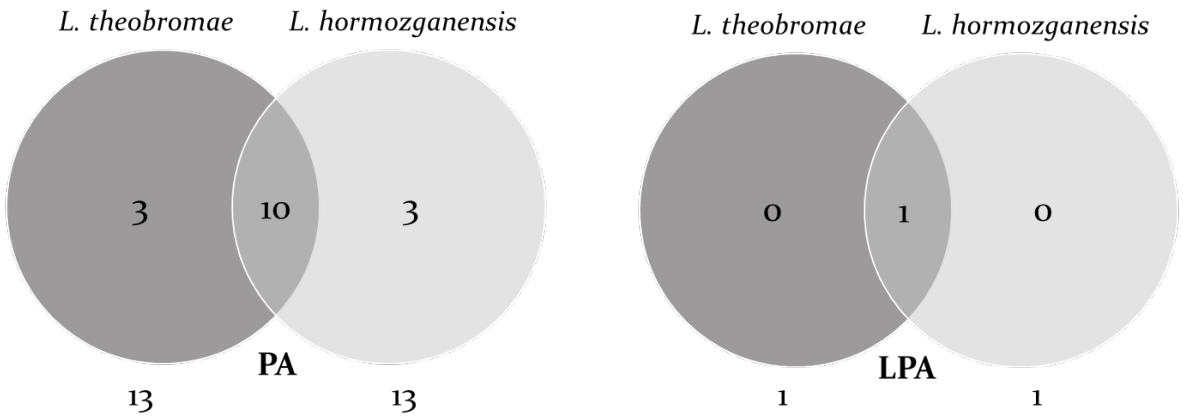

Figure 14 – Venn diagram of PA and LPA present in the lipidomic profiles of *L. theobromae* and *L. hormozganensis*.

Cardiolipins

Cardiolipins (CL) were identified in the mass spectra as $[M - H]^-$ ions (**Table 12** and **Table 13**). CL were identified by the fragment ions at m/z values of 415, 695 and 831. The most abundant CL molecular species in the lipidome of *L. theobromae* and *L. hormozganensis* were identified at m/z 1451.9941 [CL(72:6)] and m/z 1449.9796 [CL(72:7)], respectively.

A LC-MS spectra of CL species of both fungi can be observed in **Figure 15**, along with MS/MS spectra of two abundant molecular species of this class.

Table 12 – Cardiolipins identified in *Lasiodiplodia theobromae* by LC-MS and LC-MS/MS (mass error < 5 ppm).

Observed *m/z*	**Lipid species (C:N)**	**Fatty acyl chains**
	CL identified as $[M-H]^-$	
1185.7344	CL(54:6)	(16:0/18:2/18:1)
1379.9906	CL(66:0)	*
1432.0247	CL(70:2)	*
1430.0097	CL(70:3)	*
1427.9942	CL(70:4)	*
1425.9761	CL(70:5)	(16:0/18:2/18:2/18:2) and (16:1/18:3/18:1/18:0)

1423.9673	CL(70:6)	(16:0/18:2/18:2/18:2)
1456.0237	CL(72:4)	(18:1/18:1/18:1/18:1)
1454.0084	CL(72:5)	(18:1/18:2/18:1/18:1)
1451.9941	**CL(72:6)**	*
1449.9781	CL(72:7)	(18:0/18:2/18:2/18:3) and (18:1/18:1/18:2/18:3)
1447.9640	CL(72:8)	(18:1/18:1/18:2/18:3)
1471.9605	CL(74:10)	*
1469.9451	CL(74:11)	*
1478.0070	CL(74:7)	*
1475.9913	CL(74:8)	*
1473.9763	CL(74:9)	*

Legend: C – number of carbon atoms; N – number of double bonds on the fatty acyl chains; *molecular species confirmed by the LC retention time and exact mass

Table 13 – Cardiolipins identified in *Lasiodiplodia hormozganensis* by LC-MS and LC-MS/MS (mass error < 5 ppm).

Observed *m/z*	**Lipid species (C:N)**	**Fatty acyl chains**
	CL identified as $[M-H]^-$	
1185.7350	CL(54:6)	*
1379.9904	CL(66:0)	*
1432.0208	CL(70:2)	*
1430.0063	CL(70:3)	*
1427.9900	CL(70:4)	*
1425.9766	CL(70:5)	(16:0/18:1/18:2/18:2), (16:0/18:0/18:2/18:3), (16:1/18:0/18:2/18:2) and (17:0/17:0/18:2/18:3)
1423.9548	CL(70:6)	(16:0/18:2/18:2/18:2) and (16:1/18:1/18:2/18:2) (16:0/18:1/18:2/18:3)
1458.0359	CL(72:3)	*
1456.0214	CL(72:4)	(18:0/18:0/18:1/18:3), (18:0/18:1/18:1/18:2) and (18:1/18:1/18:1/18:1)
1454.0123	CL(72:5)	(18:1/18:1/18:1/18:2)
1451.9946	CL(72:6)	*
1449.9834	**CL(72:7)**	**(18:0/18:2/18:2/18:3) and (18:1/18:1/18:2/18:3)**
1447.9646	CL(72:8)	(18:1/18:1/18:2/18:3)
1445.9451	CL(72:9)	(18:2/18:2/18:2/18:3)

1471.9594	CL(74:10)	*
1469.9456	CL(74:11)	*
1478.0049	CL(74:7)	*
1473.9757	CL(74:9)	*

Legend: C – number of carbon atoms; N – number of double bonds on the fatty acyl chains; *molecular species confirmed by the LC retention time and exact mass

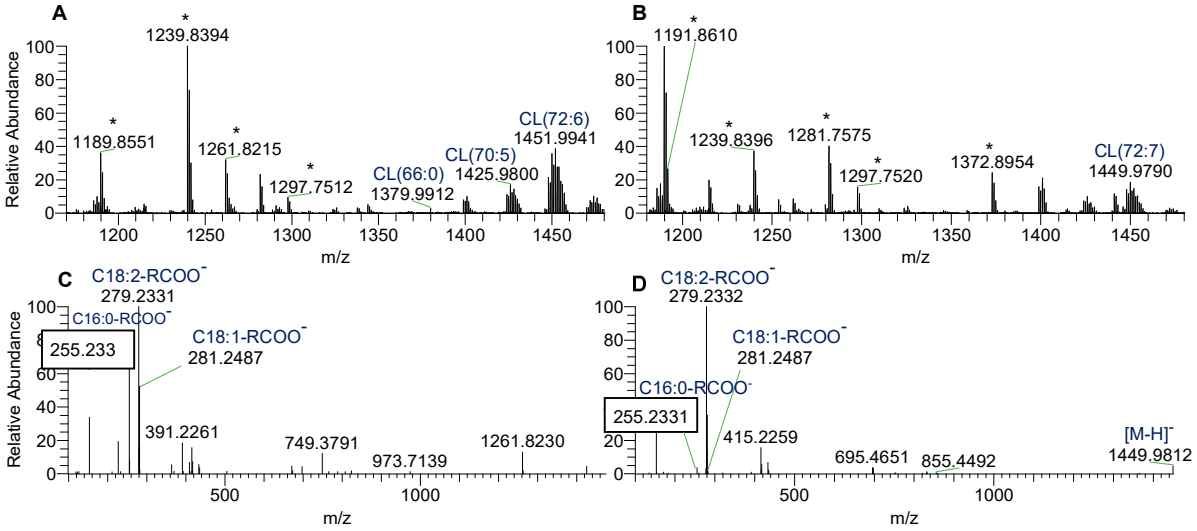

Figure 15 – LC-MS spectra representative of the phospholipid subclass cardiolipin (CL) of *L. theobromae* (A) and *L. hormozganensis* (B), identified as $[M-H]^-$ ions; ESI-MS/MS spectra of $[M-H]^-$ ions at m/z 1425.98 [CL(70:5)] of *L. theobromae* (C) and of $[M-H]^-$ ions at m/z 1449.9834 [CL(72:7)] of *L. hormozganensis* (D). *background

In sum, 19 individual molecular species were identified for the CL subclass, meaning that 16 were found in both fungi and 3 were observed isolated in one species or another (**Figure 16**). In the lipidome of *L. theobromae*, 17 identifications were made, while in *L. hormozganensis* there were 18. Respectively, each species had one and two CLs identified, in addition to the common 16 molecular species.

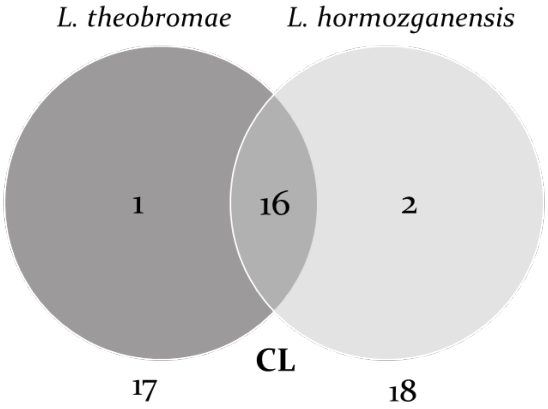

Figure 16 – Venn diagram of CL present in the lipidomic profiles of *L. theobromae* and *L. hormozganensis*.

Phosphatidylinositols

Phosphatidylinositols (PI) were identified in the mass spectra as $[M-H]^-$ molecular ions (**Table 14** and **Table 15**). In the ESI-MS/MS spectra, PI were identified by the fragment ion at m/z 241, corresponding to the phosphatidylinositol polar head group, and the abundant ion at m/z 153. The most abundant PI molecular species in the lipidome of *L. theobromae* and *L. hormozganensis* were identified at m/z 833.5193 and m/z 833.5192 [PC(34:2)], respectively.

The LC-MS spectra of PI species of both fungi can be observed in **Figure 17**, along with MS/MS spectra of two abundant molecular species of this class.

Table 14 – Phosphatidylinositol identified in *Lasiodiplodia theobromae* by LC-MS and LC-MS/MS (mass error < 5 ppm).

Observed *m/z*	Lipid species (C:N)	Fatty acyl chains
	PI identified as $[M-H]^-$	
571.2892	LPI(16:0)	16:0
599.3200	LPI(18:0)	*
597.3062	LPI(18:1)	18:1
595.2899	LPI(18:2)	18:2
833.5193	**PI(34:2)**	**(16:0/18:2) and (16:1/18:1)**

831.5058	PI(34:3)	(16:0/18:3) and (16:1/18:2)
847.5349	PI(35:2)	(17:0/18:2)
863.5639	PI(36:1)	*
861.5493	PI(36:2)	(18:1/18:1) and (18:0/18:2)
859.5341	PI(36:3)	(18:1/18:2) and (18:0/18:3)
857.5181	PI(36:4)	(18:2/18:2) and (18:1/18:3)

Legend: C – number of carbon atoms; N – number of double bonds on the fatty acyl chains; *molecular species confirmed by the LC retention time and exact mass

Table 15 – Phosphatidylinositol identified in *Lasiodiplodia hormozganensis* by LC-MS and LC-MS/MS (mass error < 5 ppm).

Observed *m/z*	**Lipid species (C:N)**	**Fatty acyl chains**
	PI identified as $[M-H]^-$	
835.5349	PI(34:1)	*
833.5192	**PI(34:2)**	**(16:0/18:2) and (16:1/18:1)**
831.5031	PI(34:3)	(16:0/18:3) and (16:1/18:2)
849.5491	PI(35:1)	(17:0/18:1) and (16:0/19:1)
847.5348	PI(35:2)	(17:1/18:1) and (17:0/18:2)
865.5803	PI(36:0)	*
863.5674	PI(36:1)	(18:0/18:1)
861.5513	PI(36:2)	(18:1/18:1) and (18:0/18:2)
859.5356	PI(36:3)	(18:1/18:2) and (18:0/18:3)
857.5200	PI(36:4)	(18:2/18:2) and (18:1/18:3)

Legend: C – number of carbon atoms; N – number of double bonds on the fatty acyl chains; *molecular species confirmed by the LC retention time and exact mass

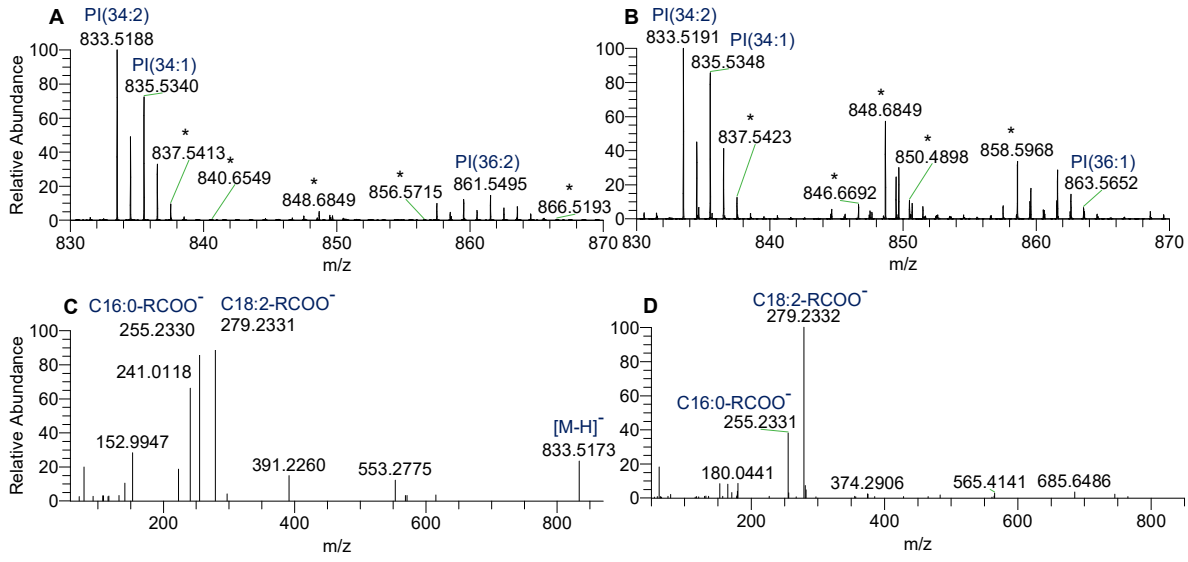

Figure 17 – LC-MS spectrum representative of the phospholipid subclass phosphatidylinositol (PI) of *L. theobromae* (A) and *L. hormozganensis* (B), identified as $[M-H]^-$ ions; ESI-MS/MS spectra of $[M-H]^-$ ions at m/z 833.52 [PI(34:2)] of *L. theobromae* (C) and *L. hormozganensis* (D). *background

Hence, 10 individual molecular species were identified for the PI subclass, being that 7 were found in both fungi and 3 were observed uniquely in the lipidome of *L. hormozganensis* (**Figure 18**). Regarding LPIs, 4 molecular species were exclusively identified in the lipidome of *L. theobromae*.

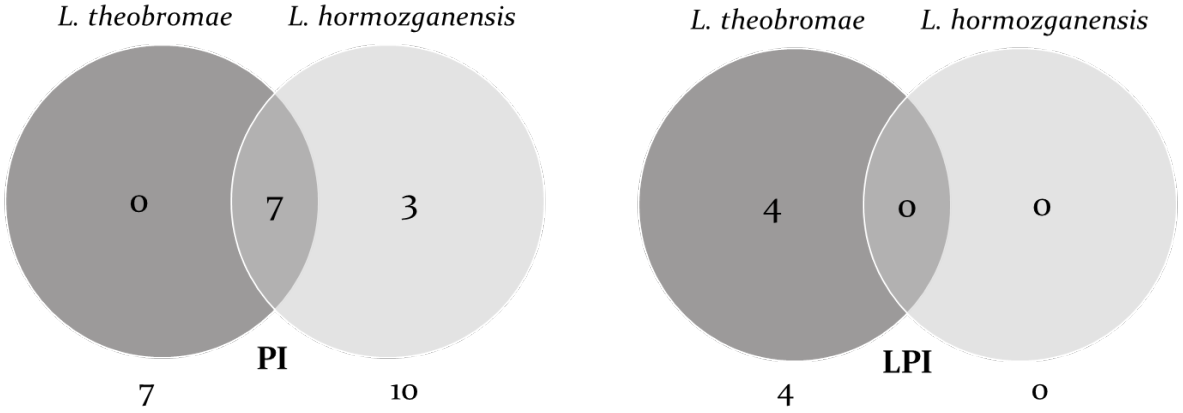

Figure 18 – Venn diagram of PI and LPI present in the lipidomic profile of *L. theobromae* and *L. hormozganensis*.

Phosphatidylglycerols

Phosphatidylglycerols (PG) were identified in the mass spectra as $[M-H]^-$ molecular ions (**Table 16** and **Table 17**). In the MS/MS spectra, PG were identified by the fragment ion at m/z 171, corresponding to the phosphoglycerol group. The most abundant PG molecular species in the lipidome of *L. theobromae* and *L. hormozganensis* were identified at m/z 745.5038 and m/z 745.5031 [PG(34:2)], respectively.

The LC-MS of PG species of both fungi can be observed in **Figure 19**, along with MS/MS spectra of two abundant molecular species of this class.

Table 16 – Phosphatidylglycerol identified in *Lasiodiplodia theobromae* by LC-MS and LC-MS/MS (mass error < 5 ppm).

Observed *m/z*	Lipid species (C:N)	Fatty acyl chains
	PG identified as $[M-H]^-$	
747.5186	PG(34:1)	(16:0/18:1)
745.5038	**PG(34:2)**	**(16:0/18:2)**
769.5016	PG(36:4)	*

Legend: C – number of carbon atoms; N – number of double bonds on the fatty acyl chains; *molecular species confirmed by the LC retention time and exact mass

Table 17 – Phosphatidylglycerol identified in *Lasiodiplodia hormozganensis* by LC-MS and LC-MS/MS (mass error < 5 ppm).

Observed *m/z*	Lipid species (C:N)	Fatty acyl chains
	PG identified as $[M-H]^-$	
747.5179	PG(34:1)	*
745.5031	**PG(34:2)**	**(16:0/18:2) and (16:1/18:1)**
773.5329	PG(36:2)	*
771.5178	PG(36:3)	(18:1/18:2) and (18:0/18:3)
769.5029	PG(36:4)	*
767.4874	PG(36:5)	*

Legend: C – number of carbon atoms; N – number of double bonds on the fatty acyl chains; *molecular species confirmed by the LC retention time and exact mass

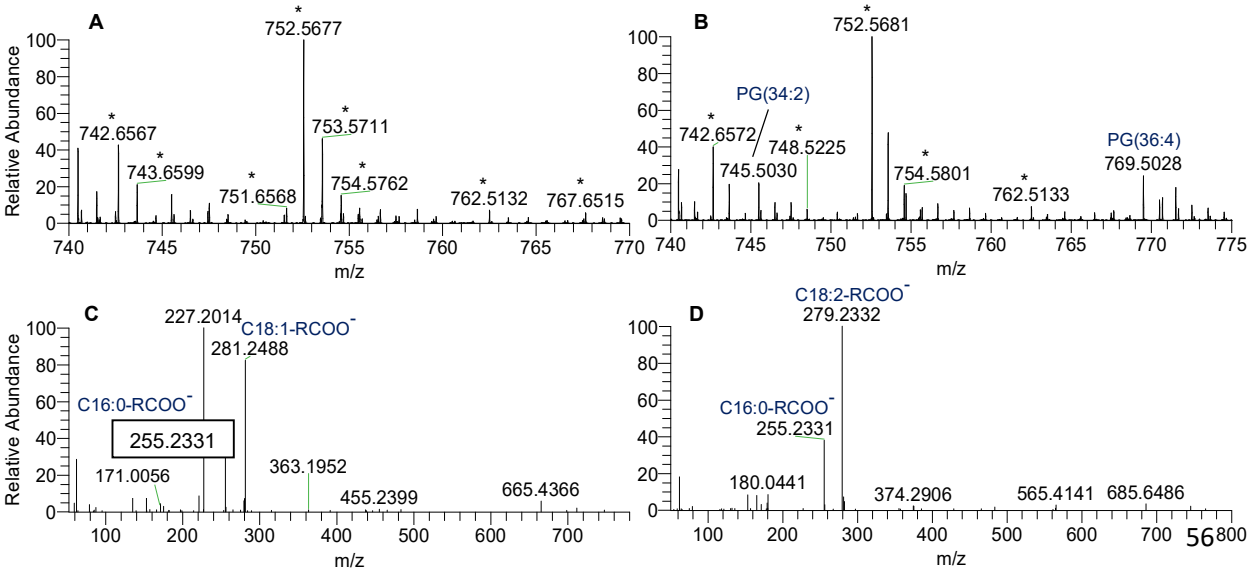

Figure 19 – LC-MS spectra representative of the phospholipid subclass phosphatidylglycerol (PG) of *L. theobromae* (A) and *L. hormozganensis* (B), identified as $[M-H]^-$ ions; ESI-MS/MS spectra of $[M-H]^-$ ions at m/z 747.52 [PG(34:1)] of *L. theobromae* (C) and of $[M-H]^-$ ions at m/z 745.50 [PG(34:2)] of *L. hormozganensis* (D). *background

Results show that 6 individual PG molecular species were identified, 6 in both fungi and 3 belonging to the lipidome of *L. hormozganensis* (**Figure 20**).

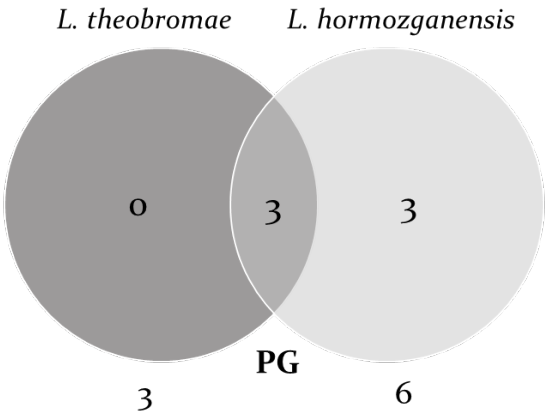

Figure 20 – Venn diagram of PG present in the lipidomic profiles of *L. theobromae* and *L. hormozganensis*.

Phosphatidylserines

Phosphatidylserines (PS) were identified in the positive ion mode as $[M + H]^+$ ions (**Table 18** and **Table 19**) and confirmed by the neutral loss of 185 Da observed in the MS/MS spectrum, corresponding to the neutral loss of phosphoserine polar head. PS can also be identified in the negative ion mode, by the neutral loss of 87 Da, which corresponds to the serine of the polar head group. The most abundant PS molecular species in the lipidome of *L. theobromae* and *L. hormozganensis* were identified in the negative ion mode at m/z 758.4980 and m/z 758.4983 [PC(34:2)], respectively, and can be observed in **Figure 21**.

Table 18 – Phosphatidylserine identified in *Lasiodiplodia theobromae* by LC-MS and LC-MS/MS (mass error < 5 ppm).

Observed *m/z*	Lipid species (C:N)	Fatty acyl chains
	PS identified as $[M-H]^-$	
758.4980	**PS(34:2)**	**(16:0/18:2)**
786.5292	PS(36:2)	(18:1/18:1)

Legend: C – number of carbon atoms; N – number of double bonds on the fatty acyl chains

Table 19 – Phosphatidylserine identified in *Lasiodiplodia hormozganensis* by LC-MS and LC-MS/MS (mass error < 5 ppm).

Observed *m/z*	Lipid species (C:N)	Fatty acyl chains
	PS identified as $[M-H]^-$	
758.4983	PS(34:2)	(16:0/18:2)

Legend: C – number of carbon atoms; N – number of double bonds on the fatty acyl chains

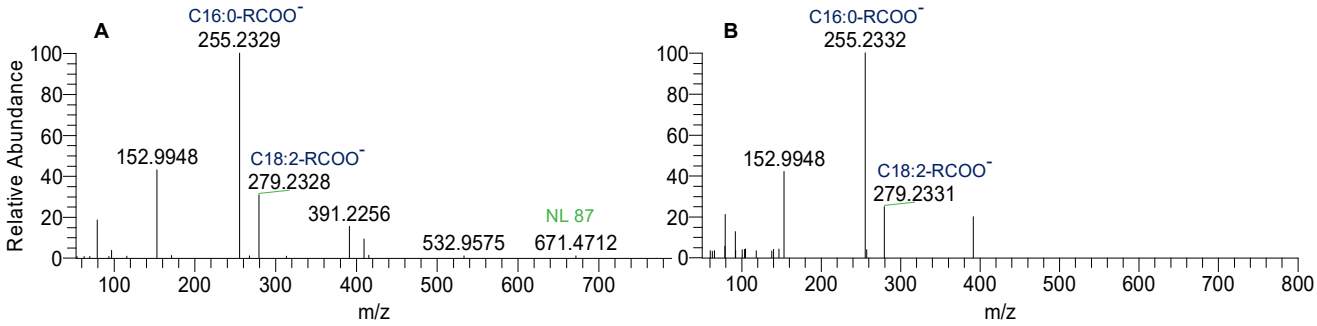

Figure 21 – ESI-MS/MS spectra of $[M-H]^-$ ions at m/z 758.50 [PS(34:2)] of *L. theobromae* (A) and *L. hormozganensis* (B).

Only two distinct molecular species were found in the lipidome of both *L. theobromae* and *L. hormozganensis* that belonged to the PS subclass, being PS(34:2) common to both species and PS(36:2) found only in *L. theobromae*.

Classes of phospholipid identified in *L. theobromae* and *L. hormozganensis* were similar to the PL profiles of yeasts (61,85,89) and filamentous fungi (86,87), but yeast species have in general a lower amount of identified molecular species. In the studies mentioned, PC and PE are the most abundant classes of lipids found, followed by PI, PS, PA, PG and CL at different orders.

The lipidome of *L. hormozganensis* is richer than the one of *L. theobromae*, which may be explained by the temperature at which both fungi were cultured – 37°C – a temperature at which *L. hormozganensis* grows better. Despite this, *L. theobromae* had a larger amount of PL when quantification of phosphate was performed (**Table 20**) and is known for growing at a vast range of temperatures (55).

Table 20 – Quantity of PL present in *Lasiodiplodia theobromae* and *Lasiodiplodia hormozganensis*, determined by quantification of phosphate and presented as mean ± standard deviation.

	Lasiodiplodia theobromae	***Lasiodiplodia hormozganensis***
PL (µg)	158.42 ± 33.8	62.78 ± 11.4

3.2. Identification and characterization of the triacylglycerol profile of *Lasiodiplodia theobromae* and *Lasiodiplodia hormozganensis*

Identification of the triacylglycerol (TG) profile at the molecular level was performed by direct infusion ESI-mass spectrometry (ESI-MS) and ESI-MS/MS. The manual injection of fractions of neutral lipids (obtained by thin-layer chromatography) and interpretation of the mass spectrometry data allowed for the identification of 83 different TG species. In total, 78 molecular species of TG were identified in *L. theobromae* (**Table 21**), and 58 were identified in *L. hormozganensis* (**Table 22**), representing a total of 136 new identifications. The criteria for identifying triacylglycerols included the accuracy of the mass measurements (< 5 ppm), the LC retention time (within the characteristic range), and the characteristics of the MS/MS spectra (manual analysis allowed the confirmation of characteristic ions and fatty acyl composition).

Triacylglycerols were identified in the mass spectra as $[M+NH_4]^+$ molecular ions. In the MS/MS spectra, TGs were identified by the neutral loss of 17 Da, corresponding to the loss of ammonium ($-NH_3$), plus the neutral loss of the fatty acyl chains, represented by diacyl ions. The most abundant TG molecular species in the lipidome of *L. theobromae* and *L. hormozganensis* were identified at m/z 876.7983 [TG(52:2)] and m/z 898.7829 [TG(54:5)], respectively.

An ESI-MS spectra of TG species of both fungi can be observed in **Figure 22**, along with ESI-MS/MS spectra of two abundant molecular species of this class.

Table 21 – Triacylglycerols identified in *Lasiodiplodia theobromae* by LC-MS and LC-MS/MS (mass error < 5 ppm).

Observed *m/z*	Lipid species (C:N)	Fatty acyl chains
TG identified as $[M+NH_4]^+$		
802.6956	TG(47:4)	*
808.7364	TG(47:1)	*
810.7514	TG(47:0)	*

816.7104	TG(48:4)	*
820.7358	TG(48:2)	*
822.7512	TG(48:1)	*
824.7668	TG(48:0)	*
830.727	TG(49:4)	*
834.7512	TG(49:2)	*
838.7823	TG(49:0)	*
840.7108	TG(50:6)	*
842.7268	TG(50:5)	*
844.7391	TG(50:4)	*
846.7508	TG(50:3)	*
848.7689	TG(50:2)	(14:0/18:2/20:0), (16:0/16:1/18:1) and (16:0/16:0/18:2)
850.7847	TG(50:1)	(18:1/16:0/16:0) and (16:1/16:0/18:0)
858.7579	TG(51:4)	*
860.7671	TG(51:3)	*
862.7831	TG(51:2)	*
864.7981	TG(51:1)	*
866.7255	TG(52:7)	*
868.7417	TG(52:6)	*
870.755	TG(52:5)	*
872.7676	TG(52:4)	(16:0/18:2/18:2), (16:0/18:1/18:3) and (16:1/18:1/18:2)
874.7827	TG(52:3)	(16:0/18:1/18:2) and (16:1/18:1/18:1)
876.7983	**TG(52:2)**	**(16:0/18:0/18:2) and (16:1/18:0/18:1)**
878.7272	TG(53:8)	*
878.8131	TG(52:1)	(16:0/18:0/18:1)
880.7420	TG(53:7)	*
882.7574	TG(53:6)	*
884.7724	TG(53:5)	*
886.7892	TG(53:4)	*
888.7975	TG(53:3)	*
890.7234	TG(54:9)	*
890.8134	TG(53:2)	(17:0/18:1/18:1), (17:1/18:1/18:0) and (17:0/18:2/18:0)
892.7408	TG(54:8)	*
892.8308	TG(53:1)	*
894.7556	TG(54:7)	*
896.7675	TG(54:6)	*
898.7823	TG(54:5)	*

900.7974	TG(54:4)	(18:1/18:1/18:2) and (18:0/18:2/18:2)
902.7249	TG(55:10)	*
902.813	TG(54:3)	(18:1/18:0/18:2) and (18:1/18:1/18:1)
904.7412	TG(55:9)	*
904.8286	TG(54:2)	(18:0/18:1/18:1), (18:0/18:0/18:2), (16:0/20:0/18:2) and (16:0/18:1/20:1)
906.7572	TG(55:8)	*
906.8444	TG(54:1)	(18:0/18:0/18:1), (16:0/20:0/18:1)
908.7728	TG(55:7)	*
910.7882	TG(55:6)	*
912.8037	TG(55:5)	*
914.8195	TG(55:4)	*
926.8138	TG(56:5)	*
932.8603	TG(56:2)	*
934.8756	TG(56:1)	*
936.8054	TG(57:7)	*
948.8927	TG(57:1)	*
952.8304	TG(58:6)	*
954.8493	TG(58:5)	*
956.8611	TG(58:4)	*
960.8916	TG(58:2)	*
962.9069	TG(58:1)	*
964.8357	TG(59:7)	*
966.8508	TG(59:6)	*
968.8661	TG(59:5)	*
970.8801	TG(59:4)	*
972.8909	TG(59:3)	*
974.9061	TG(59:2)	*
976.9225	TG(59:1)	*
982.8800	TG(60:5)	*
984.8923	TG(60:4)	*
986.9068	TG(60:3)	*
988.9224	TG(60:2)	*
990.9378	TG(60:1)	*
992.8673	TG(61:7)	*
994.8821	TG(61:6)	*
996.8972	TG(61:5)	*
998.9078	TG(61:4)	*
1000.9222	TG(61:3)	*

Legend: C – number of carbon atoms; N – number of double bonds on the fatty acyl chains; *molecular species confirmed by the LC retention time and exact mass

Table 22 – Triacylglycerols identified in *Lasiodiplodia hormozganensis* by LC-MS and LC-MS/MS (mass error < 5 ppm).

Observed *m/z*	Lipid species (C:N)	Fatty acyl chains
TG identified as $[M+NH_4]^+$		
808.7375	TG(47:1)	*
810.7535	TG(47:0)	*
822.7516	TG(48:1)	*
824.7674	TG(48:0)	*
834.7523	TG(49:2)	*
836.7678	TG(49:1)	*
844.737	TG(50:4)	*
846.7521	TG(50:3)	*
848.7683	TG(50:2)	*
850.7839	TG(50:1)	(16:0/16:0/18:1), (18:0/18:1/14:0), (16:0/16:1/18:0), (15:0/15:0/20:0), (15:0/17:0/18:1) and (16:1/17:0/17:0)
854.7279	TG(51:6)	*
856.7406	TG(51:5)	*
858.7538	TG(51:4)	*
860.7678	TG(51:3)	*
862.7836	TG(51:2)	*
864.7987	TG(51:1)	*
868.7382	TG(52:6)	*
870.7522	TG(52:5)	*
872.7679	TG(52:4)	*
874.7835	TG(52:3)	(18:1/18:2/16:0), (18:1/18:1/16:1) and (18:0/18:2/16:1)
876.7983	TG(52:2)	*
878.8139	TG(52:1)	*
880.7430	TG(53:7)	*
882.7564	TG(53:6)	*
884.7742	TG(53:5)	(17:0/18:2/18:3)
886.7842	TG(53:4)	*
888.7989	TG(53:3)	*
890.8144	TG(53:2)	*
892.8308	TG(53:1)	*

892.7391	TG(54:8)	*
894.7525	TG(54:7)	*
896.7678	TG(54:6)	*
898.7829	**TG(54:5)**	**(18:2/18:2/18:1), (18:1/18:1/18:3) and (18:0/18:2/18:3)**
900.7982	TG(54:4)	(18:1/18:1/18:2)
902.7282	TG(55:10)	*
902.8136	TG(54:3)	(18:0/18:1/18:2), (18:0/18:1/18:2), (18:0/18:0/18:3), (16:0/20:0/18:3), (16:1/20:1/18:1), (16:0/20:1/18:2) and (16:1/20:0/18:2)
904.7428	TG(55:9)	*
904.8292	TG(54:2)	(18:0/18:1/18:1) and (20:0/18:2/16:0)
906.7589	TG(55:8)	*
906.8454	TG(54:1)	(18:0/18:0/18:1) and (16:0/18:1/20:0)
908.7740	TG(55:7)	(17:1/18:1/20:5), (17:0/18:2/20:5), (17:2/18:3/20:2) and (17:1/18:3/20:2)
910.7905	TG(55:6)	*
930.8449	TG(56:3)	*
932.8613	TG(56:2)	*
934.8772	TG(56:1)	*
948.8929	TG(57:1)	*
954.8466	TG(58:5)	*
958.8760	TG(58:3)	*
960.8930	TG(58:2)	*
962.9084	TG(58:1)	*
970.8783	TG(59:4)	*
974.9076	TG(59:2)	*
976.9238	TG(59:1)	*
982.8777	TG(60:5)	*
984.8932	TG(60:4)	*
986.9084	TG(60:3)	*
988.9249	TG(60:2)	*
990.9392	TG(60:1)	*

Legend: C – number of carbon atoms; N – number of double bonds on the fatty acyl chains; *molecular species confirmed by the LC retention time and exact mass

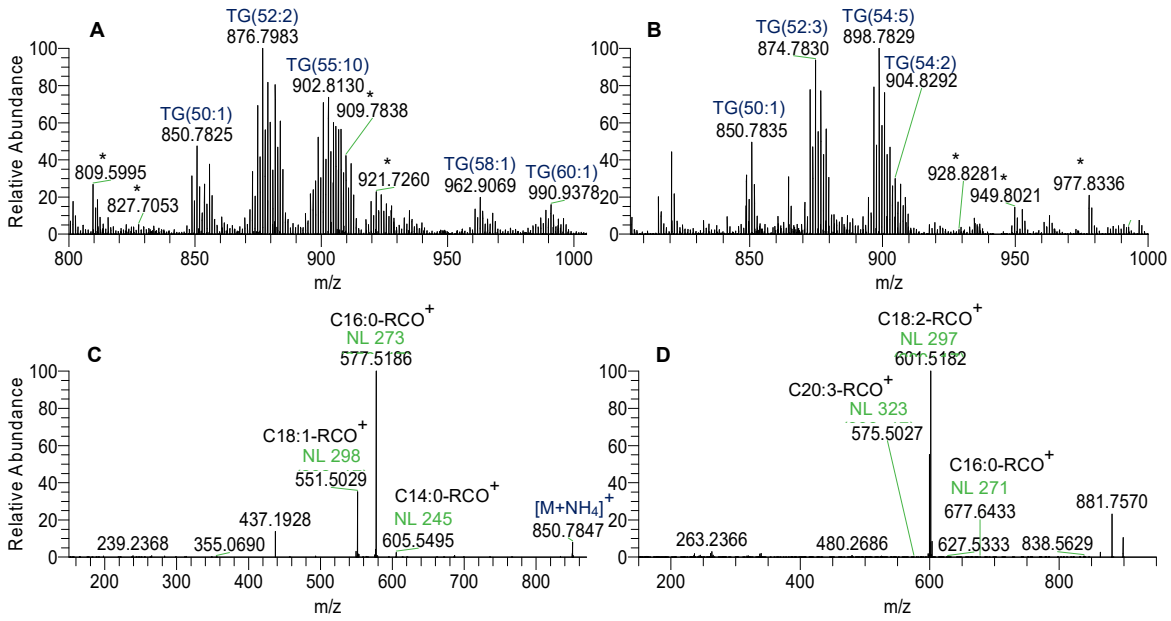

Figure 22 – LC-MS spectrum representative of the triacylglyceride (TG) profile of *L. theobromae* (A) and *L. hormozganensis* (B), identified as $[M+NH_4]^+$ ions; ESI-MS/MS spectra of $[M+NH_4]^+$ ions at m/z 850.78 [TG(50:1)] of *L. theobromae* (C) and of $[M+NH_4]^+$ ions at m/z 898.78 [TG(54:5)] of *L. hormozganensis* (D). *background

The triacylglycerol profile of both fungi is very similar, with 53 molecular species in common. In addition to the 53 triacylglycerols, *L. theobromae* had 25 more molecular species, while *L. hormozganensis* had only 5 specific triacylglycerols (**Figure 23**). The most abundant TG species in the total lipid extracts of both *L. theobromae* and *L. hormozganensis* had either 2 C18 and 1 C16 or 3 C18.

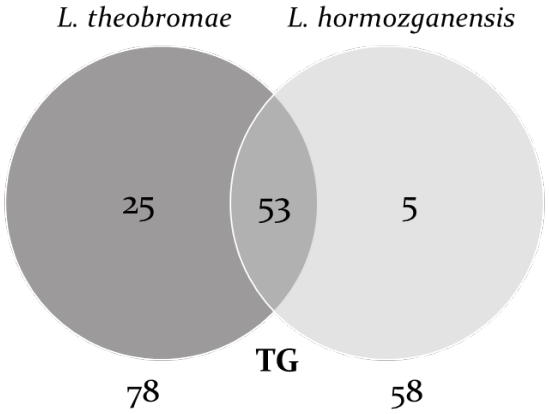

Figure 23 – Venn diagram of TG present in the lipidomic profiles of *L. theobromae* and *L. hormozganensis*.

With 83 species identified in total, the triacylglycerols constitute one of the most abundant lipid classes in these species. In fact, the initial separation procedures (TLC) had already showed that neutral lipids constituted the largest portion of lipids in the species studied (**Supplementary material 1 and 2**).

In fungi, TG is usually the most abundant lipid class (90) and its accumulation in fungal cells often happens in the later stages of growth (86,91). The abundancy of triacylglycerols in the lipidome may be explained by the importance of these lipids as carbon sources, being used in the production of other lipid molecules (92). Because *L. theobromae* has a richer TG profile that when compared to *L. hormozganensis*, this might indicate that *L. theobromae* is at a later stage of growth that *L. hormozganensis* when both species are grown at 37 °C for 7 days. Nevertheless, it would be relevant to compare the abundances of the molecular species for this matter. Contrary to the PL profile, in this case the number of species identified is smaller for the lipidome of *L. hormozganensis*.

3.3. Identification of the fatty acid profile of *Lasiodiplodia theobromae* and *Lasiodiplodia hormozganensis*

Identification of the fatty acid (FA) profile at the molecular level was performed by gas-chromatography-mass spectrometry (GC-MS.) The interpretation of the mass spectrometry data collected for fractions of fatty acids (obtained by TLC), after methylation of the samples, allowed the identification of 23 fatty acid species. In total, 23 molecular species of FA were identified in *L. theobromae* (**Table 23**), and 21 were identified in *L. hormozganensis* (**Table 24**), representing a total of 44 identifications. The criteria for identifying fatty acids included the GC retention time, when compared to the retention time of lipid standards, and the characteristics of the GC-EI-MS spectra.

Fatty acids were identified as fatty acid methyl esters (FAME), being observed in the mass spectra as M^+ molecular ions. Typical characteristics looked for in the MS spectra were the neutral loss of 31 Da, corresponding to the loss of the methoxyl group, which confirms it as a methyl ester, and the McLafferty rearrangement ion at m/z 74. The neutral loss of 43 is also characteristic, representing the loss of a C_3 unit (carbons 2 to 4). The most abundant FA molecular species in the lipidome of *L. theobromae* and *L. hormozganensis* was identified at m/z 270.24, corresponding to palmitic acid [FA(16:0)], for both species.

A RIC of FA species of both fungi can be observed in **Figure 24**, along with MS/MS spectra of two abundant molecular species of this class.

Table 23 – Fatty acids identified in *Lasiodiplodia theobromae* by GC-MS.

Observed *m/z*	Lipid species (C:N)	Fatty acid
	FA identified as FAMEs	
242.21	FA(14:0)	Isotridecanoate
256.21	FA(15:0)	Isotetradecanoate
256.21	FA(15:0)	9-methyltetradecanoate
270.24	**FA(16:0)**	**Hexadecanoate**

268.18	FA(9-16:1)	9-hexadecenoate
268.18	FA(11-16:1)	11-hexadecenoate
284.24	FA(17:0)	Isoheptadecanoate
284.25	FA(17:0)	Heptadecanoate
282.24	FA(9-17:1)	9-heptadecenoate
282.21	FA(8-17:1)	8-heptadecenoate
298.27	FA(18:0)	Octadecanoate
296.26	FA(13-18:1)	13-octadecenoate
294.24	**FA(7,12-18:2)**	**7,12-octadecadienoate**
312.28	FA(19:0)	Nonadecanoate
292.21	FA((18:3)*n-3*)	9,12,15-octadecatrienoate
326.29	FA(20:0)	Eicosanoate
324.26	FA(9-20:1)	9-eicosanoate
322.23	FA((20:2)*n-6*)	11,14-eicosadienoate
354.32	FA(22:0)	Isoheneicosanoate
354.32	FA(22:0)	Docosanoate
368.34	FA(23:0)	21-methyldocosanoate
368.34	FA(23:0)	Tricosanoate
382.36	FA(24:0)	Tetracosanoate

Legend: C – number of carbon atoms; N – number of double bonds on the fatty acyl chains

Table 24 – Fatty acids identified in *Lasiodiplodia hormozganensis* by GC-MS.

Observed *m/z*	**Lipid species (C:N)**	**Fatty acid**
	FA identified as FAMEs	
242.21	FA(14:0)	Isotridecanoate
256.21	FA(15:0)	9-methyltetradecanoate
256.21	FA(15:0)	Isotetradecanoate
270.24	**FA(16:0)**	**Hexadecanoate**
268.15	FA(11-16:1)	11-hexadecenoate
268.20	FA(9-16:1)	9-hexadecenoate
284.25	FA(17:0)	Isoheptadecanoate
284.26	FA(17:0)	Heptadecanoate
282.14	FA(9-17:1)	9-heptadecenoate
282.24	FA(8-17:1)	8-heptadecenoate
298.27	FA(18:0)	Octadecanoate
296.23	FA(13-18:1)	13-octadecenoate
294.24	**FA(7,12-18:2)**	**7,12-octadecadienoate**
312.29	FA(19:0)	Nonadecanoate
292.21	FA((18:3)n-3)	9,12,15-octadecatrienoate

326.29	FA(20:0)	Eicosanoate
324.26	FA(9-20:1)	9-eicosanoate
322.21	FA((20:2)n-6)	11,14-eicosadienoate
354.32	FA(22:0)	Isoheneicosanoate
368.33	FA(23:0)	Tricosanoate
382.36	FA(24:0)	Tetracosanoate

Legend: C – number of carbon atoms; N – number of double bonds on the fatty acyl chains

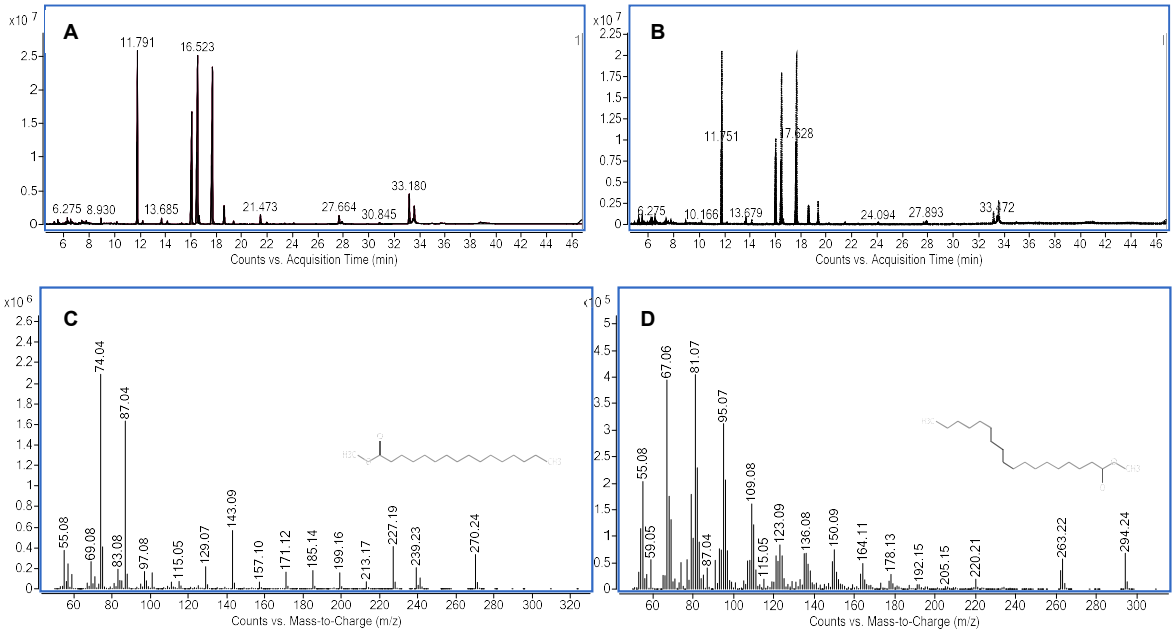

Figure 24 – GC-MS spectrum representative of the fatty acid (FA) profile of *L. theobromae* (A) and *L. hormozganensis* (B), identified as FAMEs; GC-MS spectra of $[M]^+$ ions at m/z 270.24 (hexadecanoate methyl ester), corresponding to hexadecanoate or palmitic acid [FA(16:0)] of *L. theobromae* (C) and of $[M]^+$ ions at m/z 294.24 (methyl 9-*cis*,11-*trans*-octadecadienoate), corresponding to 7,12-octadecadienoate or rumenic acid [FA(7,12-18:2)] of *L. hormozganensis* (D).

Considering the profiles of both fungi, almost the same fatty acids were identified in the two species (**Figure 25**).

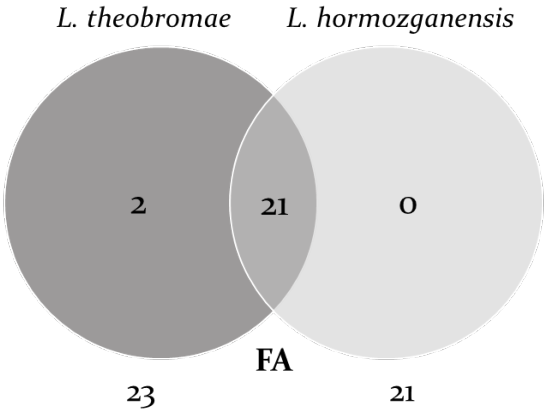

Figure 25 – Venn diagram of FA present in the lipidomic profiles of *L. theobromae* and *L. hormozganensis*.

Similar FA profiles were observed in yeast species (61,85,91,93) and fungi of the phylum Ascomycota (66,94–97), with C16:0, C18:0, C18:1, C18:2 and C18:3 being the most abundant fatty acids. But the fatty acid composition of *L. theobromae* and *L. hormozganensis* seems to be distinct from the one of oleaginous fungi, whose abundant FA are 6,9,12-18:3 and 20:4(n-6) (68).

Although not common among all organisms, odd-chain fatty acids (OCFA) such as C15:0, C17:0 and C17:1 have been identified in some species of fungi (66,94,97), in accordance to our results. OCFA are receiving increasing attention in the last few years, since serum levels of these compounds have been associated to a lower risk of obesity and cardiovascular diseases (98). Because of this, efforts to produce OCFA through fermentation and genetic engineering are being developed. However, the reason why OCFA are associated to human health remains unclear. It is interesting to point out that phytosphingosine, the sphingoid base of one ceramide identified in *L. theobromae* (**Figure 10**), can be metabolized to FA C15:0 and incorporated into glycerophospholipids. This has been observed in both yeasts and mammals (98).

A study characterizing the fatty acid profile of two species of the family Botryosphaeriaceae identified C16:0, C16:1, C18:0, C18:1 and C18:2 in the secretome of *Neofusicoccum vitifusiforme* and C18:0, C18:1 and C18:2 in the secretome of *N. parvum* (99). The authors identified C18:2 as the most abundant FA, but recognized that fungi of different species can have very distinct lipidomic profiles.

A somehow balanced ratio of saturated to unsaturated FA species is observed in the two fungi studied, since this ratio is essential for membrane stability (67). As observed previously in the fatty acyl chains of phospholipids and triacylglycerols, the number of unsaturation bonds is always lower than 4.

Something to take into consideration, since it was reported by numerous studies, is that the fatty acid composition of yeast species varies depending on growth conditions such as temperature and growth phase (66,91,94,95,100,101) and genetic background (89). The extent of the alterations depends on each species and although the diversity of molecular species usually remains the same, relative amounts may differ (95) and it might affect the degree of unsaturation of FA and the ratio of iso/anteiso (94,95). Stahl & Klug (1996) have made the correlation that the lower the temperature, the higher the unsaturation of fatty acyl chains (95). In fungi, saturated fatty acids are used to produce unsaturated species through desaturation (61).

Fatty acids and modified fatty acids have important roles in the colonization of host plants and can regulate plant growth, which may impact their virulence (80,99). Octadecenoid acids such as C18:2 and C18:3 are precursors of jasmonic acid, a plant hormone that can be phytotoxic and is known to be produced by pathogenic fungi (99,102–104).

Although the phospholipid profile is richer in *L. hormozganensis*, *L. theobromae* has a higher diversity of TG and FA species (**Table 25** and **Figure 26**). This may be because this species is at a later stage of growth, as previous studies have linked longer growth times to higher abundance of neutral lipids and less abundance of PL (86,95).

Table 25 – Lipid classes identified by LC and GC-MS in lipid extracts of *Lasiodiplodia theobromae* and *Lasiodiplodia hormozganensis*, with indication of the total number of lipid species identified in each class and the major lipid species per class.

	Lasiodiplodia theobromae		***Lasiodiplodia hormozganensis***	
Lipid class	**Number of lipid species**	**Major lipid species**	**Number of lipid species**	**Major lipid species**
PC	27	PC(34:2)	35	PC(36:4)
LPC	4	LPC(18:2)	6	LPC(18:2)
PE	19	PE(34:2)	28	PE(34:2)
LPE	10	LPE(16:0)	15	LPE(16:0)
SM	1	SM(d35:1)	2	SM(d35:1)
PA	13	PA(34:2)	13	PA(36:4)
LPA	1	LPA(18:2)	1	LPA(18:2)
CL	17	CL(72:6)	18	CL(72:7)
PI	7	PI(34:2)	10	PI(34:2)
LPI	4	LPI(16:0)	-	-
PG	3	PG(34:2)	6	PG(34:2)
PS	2	PS(34:2)	1	PS(34:2)
PL	108	-	135	-
Cer	2	Cer(t42:0)	-	-
TG	78	TG(52:2)	58	TG(54:4)
FA	23	FA(16:0)	21	FA(16:0)
Total	211	-	214	-

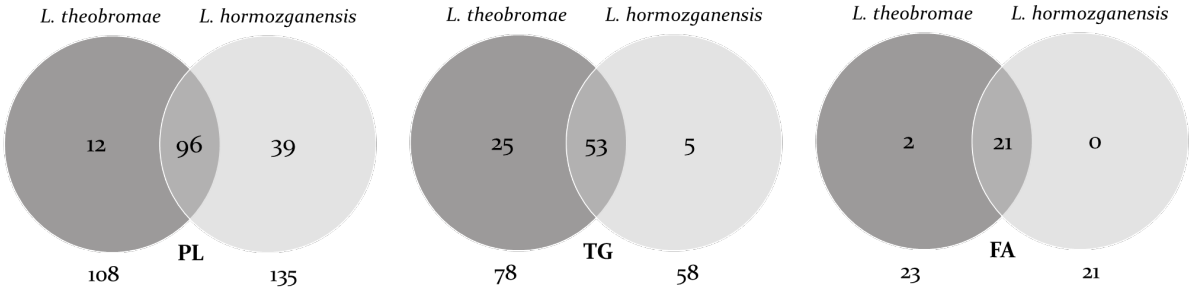

Figure 26 – Venn diagram of PL, TG and FA lipid species present in the lipidomic profile of *Lasiodiplodia theobromae* and *Lasiodiplodia hormozganensis*. The two ceramides identified in *L. theobromae* are not present in this representation.

Although described as highly abundant in fungi, sterols were not analyzed in this study (2,75). Due to their low volatility these compounds are usually analyzed by HPLC and may not be detected by LC or GC (97).

Most lipidomic studies involving fungal species are specially directed towards yeast (75,85,91,93), which are easier to grow and handle in the lab when compared to filamentous fungi. Nonetheless, yeast species represent a small portion of the enormous and diverse fungal kingdom. Lipidomic characterization of fungal spores is also abundantly found in literature (90,92,105), but the lipid composition of these structures differs from filamentous fungi in general and is therefore not much useful for comparison purposes.

4. Conclusions and Future work

In order to further understand the pathogenic behavior behind cross-kingdom host jumps of species of the *Lasiodiplodia* genus, the aim of this study was to fully characterize the lipidome of *L. theobromae* and *L. hormozganensis*, comparing the lipids produced by the two species.

To attain the objective of the investigation, liquid and gas chromatography coupled to mass spectrometry analysis was employed to identify phospholipids, triacylglycerols and fatty acids in the fungal samples.

While characterizing the lipidome of *L. theobromae* and *L. hormozganensis*, a total of 255 lipid species were identified: 147 phospholipids, including phosphatidylcholines (PC), lyso-phosphatidylcholines (LPC), phosphatidylethanolamines (PE), lyso-phosphatidylethanolamines (LPE), sphingomyelins (SM), phosphatidic acids (PA), lyso-phosphatidic acids (LPA), cardiolipins (CL), phosphatidylinositols (PI), lyso-phosphatidylinositols (LPI), phosphatidylglycerols (PG) and phosphatidylserines (PS); 2 ceramides (Cer); 83 triacylglycerols and 23 fatty acids. Because the two fungi share most of the lipids identified, this represents a total of 423 individual identifications. Lipids are highly abundant in the two fungal species, with PC and PE being the major classes of phospholipids; TG ranging from C47 to C61; and fatty acids of C14:0 to C24:0, with unsaturation bonds ranging from 0 to 3. We also discovered that *L. theobromae* and *L. hormozganensis* produce odd fatty acids such as C15:0, C17:0 and C19:0, along with unsaturated varieties. This is currently the most comprehensive description of the lipidome of species of the *Lasiodiplodia* genus.

Although the composition in lipids of both species is not sufficient to differentiate the two, this work has elucidated on the lipids that constitute filamentous fungi and provides useful information on the molecular and metabolic characterization of *Lasiodiplodia* species.

One of the limitations of this study was that the effect of temperature was not evaluated. An initial purpose that should be fulfilled in the future is to compare the lipidomes of the two species when grown at 25 and 37 °C, not only because these cross-

kingdom pathogens are able to adapt to the different temperatures, but because temperature is known to modulate the metabolites produced by these fungi.

In future work, it would be interesting to extend the analysis to more complex lipids, such as sphingolipids and glycolipids, that may be present in our samples but require a more dedicated approach. The bioactivity of lipids identified in this study can also be the subject of further investigation, with the prospect of finding compounds of biotechnological relevance.

In conclusion, these results enriched the field of fungal lipidomics and can open new paths for the study of plant pathogenic and human opportunist fungi.

5. References

1. van Baarlen P, van Belkum A, Summerbell RC, Crous PW, Thomma BPHJ. Molecular mechanisms of pathogenicity: how do pathogenic microorganisms develop cross-kingdom host jumps? *FEMS Microbiol Rev*. 2007 Apr;31(3):239–77.

2. Pan J, Hu C, Yu JH. Lipid biosynthesis as an antifungal target. *J Fungi*. 2018;4(2):1–13.

3. Gow NAR, Latge J-P, Munro CA. The Fungal Cell Wall: Structure, Biosynthesis, and Function. *Microbiol Spectr*. 2017 Jun 8;5(3):1–25.

4. Cortés JCG, Curto M-Á, Carvalho VSD, Pérez P, Ribas JC. The fungal cell wall as a target for the development of new antifungal therapies. *Biotechnol Adv*. 2019 Nov;37(6):107352.

5. Erwig LP, Gow NAR. Interactions of fungal pathogens with phagocytes. *Nat Rev Microbiol*. 2016;14(3):163–76.

6. Deacon JW. Fungal Biology. 4th ed. Wiley-Blackwell; 2005.

7. Rella A, Farnoud AM, Del Poeta M. Plasma membrane lipids and their role in fungal virulence. *Prog Lipid Res*. 2016;61:63–72.

8. Webster J, Weber R. Introduction to Fungi. 3rd ed. Cambridge University Press; 2007.

9. Luévano-Martínez LA, Caldeira da Silva CC, Nicastro GG, Schumacher RI, Kowaltowski AJ, Gomes SL. Mitochondrial alternative oxidase is determinant for growth and sporulation in the early diverging fungus *Blastocladiella emersonii*. *Fungal Biol*. 2019;123(1):59–65.

10. Gleason FH, Lilje O. Structure and function of fungal zoospores: ecological implications. *Fungal Ecol*. 2009;2(2):53–9.

11. Hube B. Fungal adaptation to the host environment. *Curr Opin Microbiol*. 2009;12(4):347–9.

12. Suryanarayanan TS, Thirunavukkarasu N, Govindarajulu MB, Gopalan V. Fungal endophytes: An untapped source of biocatalysts. *Fungal Divers*. 2012;54:19–30.

13. Nieuwenhuis BPS, James TY. The frequency of sex in fungi. *Philos Trans R Soc B Biol Sci*. 2016;371(1706).

14. Crous PW, Hawksworth DL, Wingfield MJ. Identifying and Naming Plant-Pathogenic Fungi: Past, Present, and Future. *Annu Rev Phytopathol*. 2015;53(1):247–67.

15. Dean R, Van Kan JAL, Pretorius ZA, Hammond-Kosack KE, Di Pietro A, Spanu PD, et al. The Top 10 fungal pathogens in molecular plant pathology. *Mol Plant Pathol*. 2012;13(4):414–30.

16. Bidartondo MI, Read DJ, Trappe JM, Merckx V, Ligrone R, Duckett JG. The dawn of symbiosis between plants and fungi. *Biol Lett*. 2011;7(4):574–7.

17. Koide RT, Sharda JN, Herr JR, Malcom GM. Ectomycorrhizal fungi and the biotrophy–saprotrophy continuum. *New Phytol*. 2008;178(2):230–3.

18. Casadevall A, Pirofski LA. Host-pathogen interactions: Redefining the basic concepts of virulence and pathogenicity. *Infect Immun*. 1999;67(8):3703–13.

19. Youker SR, Andreozzi RJ, Appelbaum PC, Credito K, Miller JJ. White piedra: further evidence of a synergistic infection. *J Am Acad Dermatol*. 2003 Oct;49(4):746–9.

20. Struck C. Infection strategies of plant parasitic fungi. In: Jones DG, Kaye B, editors. The Epidemiology of Plant Diseases. 2nd ed. Dordrecht: Kluwer Academic Publishers; 2006. p. 117–37.

21. Mendgen K, Hahn M, Deising H. Morphogenesis and Mechanisms of Penetration By Plant Pathogenic Fungi. *Annu Rev Phytopathol*. 1996;34(1):367–86.

22. van Kan JAL. Licensed to kill: the lifestyle of a necrotrophic plant pathogen. *Trends Plant Sci*. 2006;11(5):247–53.

23. Mendgen K, Hahn M. Plant infection and the establishment of fungal biotrophy. *Trends Plant Sci*. 2002;7(8):352–6.

24. Kikot GE, Hours RA, Alconada TM. Contribution of cell wall degrading enzymes to pathogenesis of *Fusarium graminearum*: A review. *J Basic Microbiol*. 2009;49(3):231–41.

25. Hématy K, Cherk C, Somerville S. Host-pathogen warfare at the plant cell wall. *Curr Opin Plant Biol*. 2009;12(4):406–13.

26. van der Does HC, Rep M. Virulence genes and the evolution of host specificity in plant-pathogenic fungi. *Mol Plant-Microbe Interact*. 2007;20(10):1175–82.

27. Esteves AC, Saraiva M, Correia A, Alves A. Botryosphaeriales fungi produce extracellular enzymes with biotechnological potential. *Can J Microbiol*. 2014;60(5):332–42.

28. Kubicek CP, Starr TL, Glass NL. Plant Cell Wall-Degrading Enzymes and Their Secretion in Plant-Pathogenic Fungi. *Annu Rev Phytopathol*. 2014;52:427–51.

29. Prasad R, Ghannoum MA. Lipids of Pathogenic Fungi. CRC Press; 1996. 291 p.

30. Úrbez-Torres JR. The status of Botryosphaeriaceae species infecting grapevines. *Phytopathol Mediterr*. 2011;50:S5–45.

31. Punithalingam E. *Botryodiplodia theobromae*.[Descriptions of Fungi and Bacteria]. IMI *Descr Fungi Bact*. 1976;52.

32. Alves A, Crous PW, Correia A, Phillips AJL. Morphological and molecular data reveal cryptic speciation in *Lasiodiplodia theobromae*. *Fungal Divers*. 2008;28:1–13.

33. Slippers B, Wingfield MJ. Botryosphaeriaceae as endophytes and latent pathogens of woody plants: diversity, ecology and impact. *Br Mycol Soc*. 2007;21:90–106.

34. Félix C, Duarte AS, Vitorino R, Guerreiro ACL, Domingues P, Correia ACM, et al. Temperature modulates the secretome of the phytopathogenic fungus *Lasiodiplodia theobromae*. *Front Plant Sci*. 2016;7(1096):1–12.

35. Abdollahzadeh J, Javadi A, Goltapeh EM, Zare R, Phillips AJL. Phylogeny and morphology of four new species of *Lasiodiplodia* from Iran. Persoonia - *Mol Phylogeny*

Evol Fungi. 2010 Dec 23;25(1):1–10.

36. Marques MW, Lima NB, De Morais MA, Barbosa MAG, Souza BO, Michereff SJ, et al. Species of *Lasiodiplodia* associated with mango in Brazil. *Fungal Divers*. 2013;61(1):181–93.

37. Úrbez-Torres JR, Leavitt GM, Guerrero JC, Guevara J, Gubler WD. Identification and pathogenicity of *Lasiodiplodia theobromae* and *Diplodia seriata*, the causal agents of bot canker disease of Grapevines in Mexico. *Plant Dis*. 2008;92(4):519–29.

38. Mullen JL, Gilliam CH, Hagan AK, Morgan-Jones G. Canker of Dogwood Caused by *Lasiodiplodia theobromae*, a Disease Influenced by Drought Stress or Cultivar Selection. *Plant Dis*. 1991;75(9):886–9.

39. Rodrigues R. Caracterização Morfológica e Patológica de *Lasiodiplodia theobromae* (Pat.) Griffon & Maubl., Agente Causal das Podridões de Tronco e Raízes da Videira. 2003.

40. Srinivasan M. Fungal keratitis. *Curr Opin Ophthamology*. 2004;15(4):321–7.

41. Summerbell RC, Krajden S, Levine R, Fuksa M. Subcutaneous phaeohyphomycosis caused by *Lasiodiplodia theobromae* and successfully treated surgically. *Med Mycol*. 2004;42(6):543–7.

42. Félix C. *Lasiodiplodia theobromae*: a phytopathogenic fungi that infect humans. Universidade de Aveiro; 2012.

43. Correia KC, Silva MA, de Morais MA, Armengol J, Phillips AJL, Câmara MPS, et al. Phylogeny, distribution and pathogenicity of *Lasiodiplodia* species associated with dieback of table grape in the main Brazilian exporting region. *Plant Pathol*. 2016;65(1):92–103.

44. Mohali S, Burgess TI, Wingfield MJ. Diversity and host association of the tropical tree endophyte *Lasiodiplodia theobromae* revealed using simple sequence repeat markers. *For Pathol*. 2005;35(6):385–96.

45. Lima JS, Moreira RC, Cardoso JE, Martins MVV, Viana FMP. Caracterização cultural,

morfológica e patogênica de *Lasiodiplodia theobromae* associado a frutíferas tropicais. *Summa Phytopathol*. 2013;39(2):81–8.

46. Rodríguez-Gálvez E, Maldonado E, Alves A. Identification and pathogenicity of *Lasiodiplodia theobromae* causing dieback of table grapes in Peru. *Eur J Plant Pathol*. 2015;141(3):477–89.

47. Rodríguez-Gálvez E, Guerrero P, Barradas C, Crous PW, Alves A. Phylogeny and pathogenicity of *Lasiodiplodia* species associated with dieback of mango in Peru. *Fungal Biol*. 2017;121(4):452–65.

48. Sangeetha G, Anandan A, Rani SU. Morphological and molecular characterisation of *Lasiodiplodia theobromae* from various banana cultivars causing crown rot disease in fruits. *Arch Phytopathol Plant Prot*. 2012;45(4):475–86.

49. Saha S, Sengupta J, Banerjee D, Khetan A. *Lasiodiplodia theobromae* Keratitis: A Case Report and Review of Literature. *Mycopathologia*. 2012 Oct 28;174(4):335–9.

50. Saha S, Sengupta J, Banerjee D, Khetan A. *Lasiodiplodia theobromae* keratitis: a rare fungi from eastern India. *Microbiol Res (Pavia)*. 2013 Jan 30;3(2):19.

51. da Rosa PD, Locatelli C, Scheid K, Marinho D, Kliemann L, Fuentefria A, et al. Antifungal Susceptibility, Morphological and Molecular Characterization of *Lasiodiplodia theobromae* Isolated from a Patient with Keratitis. *Mycopathologia*. 2018;183(3):565–71.

52. Gu HJ, Kim YJ, Lee HJ, Dong SH, Kim SW, Huh HJ, et al. Invasive Fungal Sinusitis by *Lasiodiplodia theobromae* in an Patient with Aplastic Anemia: An Extremely Rare Case Report and Literature Review. *Mycopathologia*. 2016;181(11–12):901–8.

53. Kindo AJ, Pramod C, Anita S, Mohanty S. Maxillary sinusitis caused by *Lasiodiplodia theobromae*. *Indian J Med Microbiol*. 2010;28(2):167–9.

54. Prasher IB, Dhanda RK. *Lasiodiplodia hormozganensis*: First report as an endophyte and a new record for India. *Kavaka*. 2017;48(2):59–60.

55. Félix C. Multi-omics approach to study responses to temperature in *Lasiodiplodia theobromae*, a human and plant fungal pathogen. Universidade de Aveiro; 2018.

56. Bou Khalil M, Hou W, Zhou H, Elisma F, Swayne LA, Blanchard AP, et al. Lipidomics era: Accomplishments and challenges. *Mass Spectrom Rev*. 2010 Nov;29(6):877–929.

57. Řezanka T, Kolouchová I, Gharwalová L, Palyzová A, Sigler K. Lipidomic Analysis: From Archaea to Mammals. *Lipids*. 2018;53(1):5–25.

58. Vaz FM, Pras-Raves M, Bootsma AH, van Kampen AHC. Principles and practice of lipidomics. *J Inherit Metab Dis*. 2014;38(1):41–52.

59. Bolla JR, Agasid MT, Mehmood S, Robinson C V. Membrane Protein–Lipid Interactions Probed Using Mass Spectrometry. *Annu Rev Biochem*. 2019 Jun 20;88(1):85–111.

60. Ratledge C. Yeasts, moulds, algae and bacteria as sources of lipids. In: *Technological Advances in Improved and Alternative Sources of Lipids*. Boston, MA: Springer; 1994. p. 235–91.

61. Bernat P, Gajewska E, Szewczyk R, Słaba M, Długoński J. Tributyltin (TBT) induces oxidative stress and modifies lipid profile in the filamentous fungus *Cunninghamella elegans*. *Environ Sci Pollut Res*. 2014 Mar 5;21(6):4228–35.

62. Athenaki M, Gardeli C, Diamantopoulou P, Tchakouteu SS, Sarris D, Philippoussis A, et al. Lipids from yeasts and fungi: physiology, production and analytical considerations. *J Appl Microbiol*. 2017;124(2):336–67.

63. Pomastowski P, Buszewski B. Two-dimensional gel electrophoresis in the light of new developments. *TrAC - Trends Anal Chem*. 2014;53:167–77.

64. Aebersold R, Mann M. Mass spectrometry-based proteomics. *Nature*. 2003;422(March):198–207.

65. Domingues MRM, Reis A, Domingues P. Mass spectrometry analysis of oxidized phospholipids. *Chem Phys Lipids*. 2008 Nov;156(1–2):1–12.

66. Gealt MA, Abdollahi A, Evans JL. Lipids and lipoidal mycotoxins of fungi. *Curr Top Med Mycol*. 1989;3(134):218–47.

67. Beccaccioli M, Reverberi M, Scala V. Fungal lipids: Biosynthesis and signalling during plant-pathogen interaction. *Front Biosci - Landmark*. 2019;24(1):172–85.

68. Subramaniam R, Dufreche S, Zappi M, Bajpai R. Microbial lipids from renewable resources: Production and characterization. *J Ind Microbiol Biotechnol*. 2010;37(12):1271–87.

69. Chopra A, Khuller GK. Lipids of pathogenic fungi. *Prog Lipid Res*. 1983;22(3):189–220.

70. Ratledge C, Wynn JP. The biochemistry and molecular biology of lipid accumulation in oleaginous microorganisms. *Adv Appl Microbiol*. 2002;51:1–52.

71. Dercová K, Čertík M, Maľová A, Sejáková Z. Effect of chlorophenols on the membrane lipids of bacterial cells. *Int Biodeterior Biodegrad*. 2004;54(4):251–4.

72. Xia J, Jones AD, Lau MW, Yuan YJ, Dale BE, Balan V. Comparative lipidomic profiling of xylose-metabolizing *S. cerevisiae* and its parental strain in different media reveals correlations between membrane lipids and fermentation capacity. *Biotechnol Bioeng*. 2011;108(1):12–21.

73. Gardocki ME, Jani N, Lopes JM. Phosphatidylinositol biosynthesis: Biochemistry and regulation. Biochim Biophys Acta - *Mol Cell Biol Lipids*. 2005;1735(2):89–100.

74. Rollin-Pinheiro R, Singh A, Barreto-Bergter E, Poeta M Del. Sphingolipids as targets for treatment of fungal infections. *Futur Med Chem*. 2016;8(12):1469–84.

75. Kohlwein SD. Analyzing and understanding lipids of yeast: A challenging endeavor. *Cold Spring Harb Protoc*. 2017;2017(5):373–8.

76. Singh A, Del Poeta M. Sphingolipidomics: An important mechanistic tool for studying fungal pathogens. *Front Microbiol*. 2016;7(APR):1–14.

77. Shea JM, Del Poeta M. Lipid signaling in pathogenic fungi. *Curr Opin Microbiol*. 2006;9(4):352–8.

78. Siebers M, Brands M, Wewer V, Duan Y, Hölzl G, Dörmann P. Lipids in plant–microbe interactions. Biochim Biophys Acta - *Mol Cell Biol Lipids*. 2016;1861(9):1379–95.

79. Wang J, Wang H, Zhang C, Wu T, Ma Z, Chen Y. Phospholipid homeostasis plays an important role in fungal development, fungicide resistance and virulence in *Fusarium graminearum*. *Phytopathol Res*. 2019;1(1):1–12.

80. Uranga CC, Beld J, Mrse A, Córdova-Guerrero I, Burkart MD, Hernández-Martínez R. Fatty acid esters produced by *Lasiodiplodia theobromae* function as growth regulators in tobacco seedlings. *Biochem Biophys Res Commun*. 2016;472(2):339–45.

81. Félix C, Meneses R, Gonçalves MFM, Tilleman L, Duarte AS, Jorrín-Novo J V., et al. A multi-omics analysis of the grapevine pathogen *Lasiodiplodia theobromae* reveals that temperature affects the expression of virulence- and pathogenicity-related genes. *Sci Rep*. 2019;9(1):1–12.

82. Bligh EG, Dyer WJ. A Rapid Method Of Total Lipid Extraction And Purification. *Can J Biochem Physiol*. 1959;37(8):911–7.

83. Lopes C, Barbosa J, Maciel E, da Costa E, Alves E, Domingues P, et al. Lipidomic signature of *Bacillus licheniformis* I89 during the different growth phases unravelled by high-resolution liquid chromatography-mass spectrometry. *Arch Biochem Biophys*. 2019;663(October 2018):83–94.

84. Aued-Pimentel S, Lago JHG, Chaves MH, Kumagai EE. Evaluation of a methylation procedure to determine cyclopropenoids fatty acids from *Sterculia striata* St. Hil. Et Nauds seed oil. *J Chromatogr A*. 2004;1054(1–2):235–9.

85. Turk M, Méjanelle L, Šentjurc M, Grimalt JO, Gunde-Cimerman N, Plemenitaš A. Salt-induced changes in lipid composition and membrane fluidity of halophilic yeast-like melanized fungi. *Extremophiles*. 2004;8(1):53–61.

86. Fakas S, Papanikolaou S, Galiotou-Panayotou M, Komaitis M, Aggelis G. Lipids of *Cunninghamella echinulata* with emphasis to γ-linolenic acid distribution among lipid classes. *Appl Microbiol Biotechnol*. 2006;73(3):676–83.

87. Stübiger G, Wuczkowski M, Mancera L, Lopandic K, Sterflinger K, Belgacem O. Characterization of Yeasts and Filamentous Fungi using MALDI Lipid Phenotyping. *J Microbiol Methods*. 2016;130:27–37.

88. Warren CR. A liquid chromatography-mass spectrometry method for analysis of intact fatty-acid-based lipids extracted from soil. *Eur J Soil Sci*. 2018 Sep;69(5):791–803.

89. Araújo ARD, Melo T, Maciel EA, Pereira C, Morais CM, Santinha DR, et al. Errors in protein synthesis increase the level of saturated fatty acids and affect the overall lipid profiles of yeast. *PLoS One*. 2018;13(8):1–28.

90. Beattie SE, Stafford AE, King AD. Triacylglycerol profiles of *Tilletia controversa* and *Tilletia tritici*. *Appl Environ Microbiol*. 1993;59(4):1054–7.

91. Klose C, Surma MA, Gerl MJ, Meyenhofer F, Shevchenko A, Simons K. Flexibility of a eukaryotic lipidome - insights from yeast lipidomics. *PLoS One*. 2012;7(4).

92. Gaspar ML, Pollero RJ, Cabello MN. Triacylglycerol consumption during spore germination of vesicular-arbuscular mycorrhizal fungi. *J Am Oil Chem Soc*. 1994;71(4):449–52.

93. Ejsing CS, Sampaio JL, Surendranath V, Duchoslav E, Ekroos K, Klemm RW, et al. Global analysis of the yeast lipidome by quantitative shotgun mass spectrometry. *Proc Natl Acad Sci U S A*. 2009;106(7):2136–41.

94. Zelles L. Phospholipid fatty acid profiles in selected members of soil microbial communities. *Chemosphere*. 1997;35(1–2):275–94.

95. Stahl PD, Klug MJ. Characterization and differentiation of filamentous fungi based on fatty acid composition. *Appl Environ Microbiol*. 1996;62(11):4136–46.

96. Ruess L, Häggblom MM, García Zapata EJ, Dighton J. Fatty acids of fungi and nematodes - Possible biomarkers in the soil food chain? *Soil Biol Biochem*. 2002;34(6):745–56.

97. Müller MM, Kantola R, Kitunen V. Combining sterol and fatty acid profiles for the characterization of fungi. *Mycol Res*. 1994;98(6):593–603.

98. Zhang LS, Liang S, Zong MH, Yang JG, Lou WY. Microbial synthesis of functional odd-chain fatty acids: a review. *World J Microbiol Biotechnol*. 2020;36(3):1–9.

99. Salvatore MM, Giambra S, Naviglio D, Dellagreca M, Salvatore F, Burruano S, et al. Fatty acids produced by *Neofusicoccum vitifusiforme* and *N. Parvum*, fungi associated with grapevine botryosphaeria dieback. *Agric*. 2018;8(12).

100. Daum G, Tuller G, Nemec T, Hrastnik C, Balliano G, Cattel L, et al. Systematic analysis of yeast strains with possible defects in lipid metabolism. *Yeast*. 1999;15(7):601–14.

101. Martin CE, Oh CS, Jiang Y. Regulation of long chain unsaturated fatty acid synthesis in yeast. Biochim Biophys Acta - *Mol Cell Biol Lipids*. 2007;1771(3):271–85.

102. Chanclud E, Morel JB. Plant hormones: a fungal point of view. *Mol Plant Pathol*. 2016;17(8):1289–97.

103. Husain A, Ahmad A, Agrawal PK. (-)-Jasmonic acid, a phytotoxic substance from *Botryodiplodia theobromae*: characterization by NMR spectroscopic methods. *J Nat Prod*. 1993;56(11):2008–11.

104. Andolfi A, Basso S, Giambra S, Conigliaro G, Lo Piccolo S, Alves A, et al. Lasiolactols A and B Produced by the Grapevine Fungal Pathogen *Lasiodiplodia mediterranea*. *Chem Biodivers*. 2016;13(4):395–402.

105. Graham JH, Hodge NC, Morton JB. Fatty acid methyl ester profiles for characterization of glomalean fungi and their endomycorrhizae. *Appl Environ Microbiol*. 1995;61(1):58–64.

6. Supplementary material

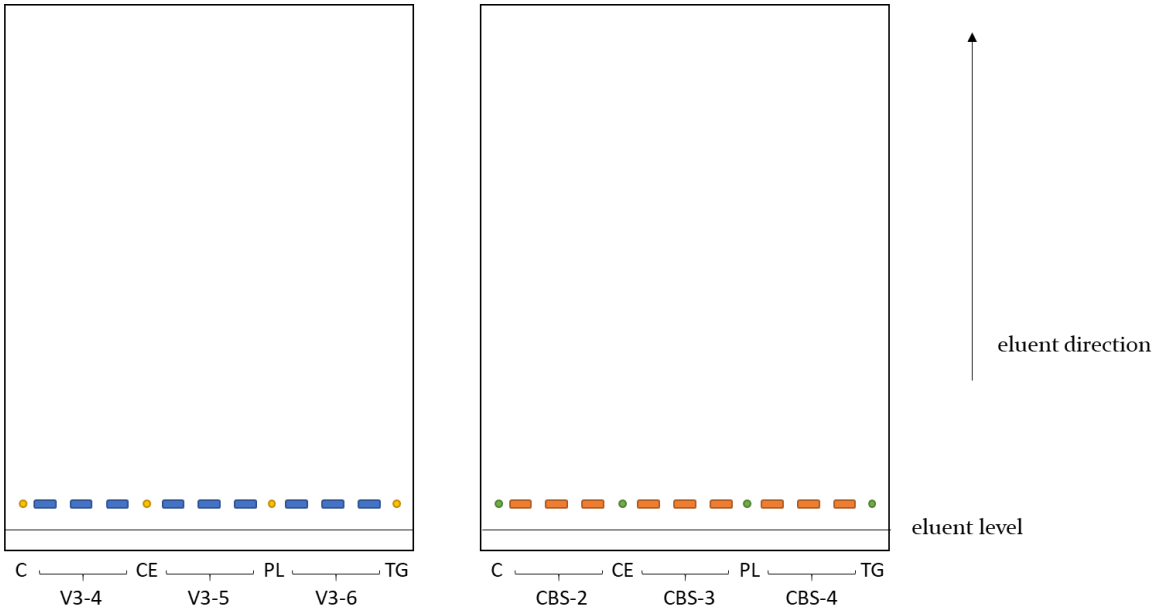

SM 1 – Schematic representation of the application of the samples in the thin-layer chromatography assay. V3 – lipid extract of strain LASOL3; CBS – lipid extract of strain CBS339.90

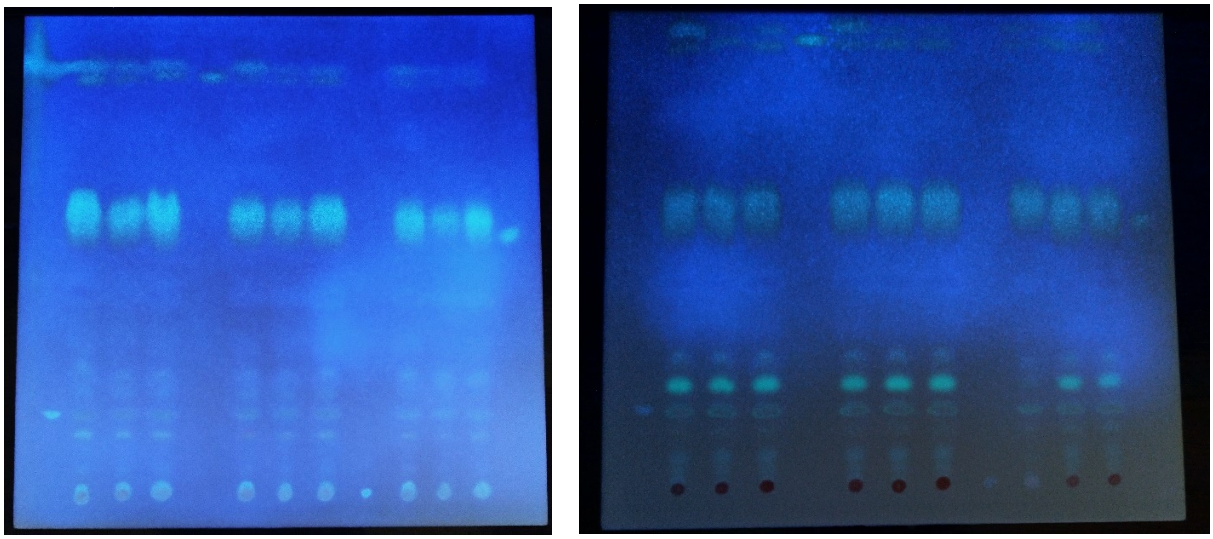

SM 2 – Thin layer chromatography plates after revelation with sprayed primuline. Left – *Lasiodiplodia theobromae*; Right – *Lasiodiplodia hormozganensis.*

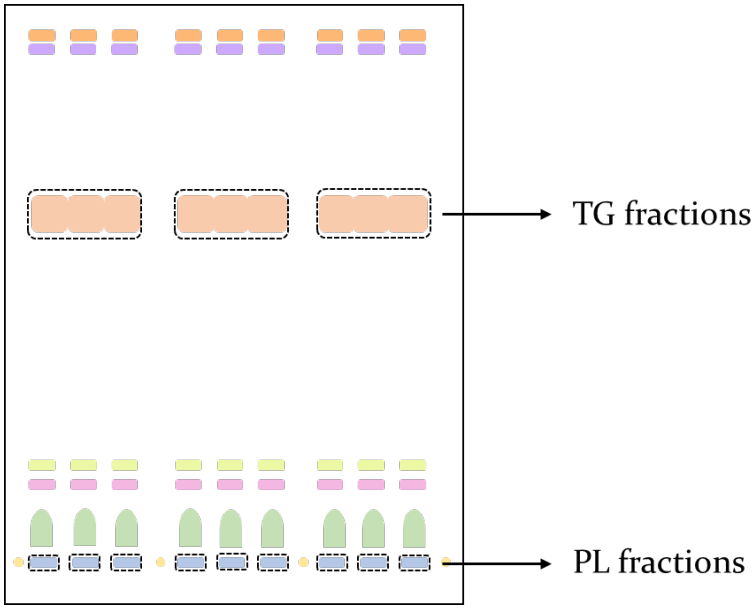

SM 3 – Schematic representation of the fractions obtained by thin-layer chromatography.

SM 4 – Phospholipids and sphingolipids (Cer) identified by LC-MS and LC-MS/MS of total lipid extracts of *Lasiodiplodia theobromae*, in the positive and negative ion modes. The complete list of PC, LPC, PE, LPE, SM and PA molecular species identified in positive mode, and PC, PE, PA, LPA, CL, PI, LPI, PG, PS and Cer molecular species identified in the negative mode, in MS and MS/MS spectra, are annotated. Data are presented as the respective sums of carbon atoms (C) and double bonds (N), followed by the calculated *m/z* values (ratios of mass to charge), plus the observed m/z values, followed by the error (< 5 ppm) and fatty acyl chains that compose the lipid, plus the respective formula.

Lipid species (C:N)	Calculated *m/z*	Observed *m/z*	Error (ppm)	Fatty acyl chains (C:N)	Formula
PC identified as $[M+H]^+$					
LPC(16:0)	496.3403	496.3401	-0.4352	16:0	C24H51NO7P
LPC(18:0)	524.3716	524.3713	-0.6045	**	C26H55NO7P
LPC(18:1)	522.3560	522.3561	0.2546	18:1	C26H53NO7P
LPC(18:2)	520.3403	520.3396	-1.3760	18:2	C26H51NO7P
PC(31:1)	718.5387	718.5377	-1.3667	**	C39H77NO8P
PC(31:3)	714.5074	714.5088	1.9846	*	C39H73NO8P
PC(32:0)	734.5700	734.5703	0.4329	**	C40H81NO8P
PC(32:1)	732.5543	732.5518	-3.4550	*	C40H79NO8P
PC(32:2)	730.5387	730.5389	0.2984	**	C40H77NO8P

PC(33:2)	744.5543	744.5535	-1.1161	**	C41H79NO8P
PC(34:1)	760.5856	760.5856	-0.0421	(16:0/18:1)	C42H83NO8P
PC(34:2)	758.5700	758.5699	-0.1081	(16:0/18:2) and (16:1/18:1)	C42H81NO8P
PC(34:3)	756.5543	756.5548	0.6199	(16:0/18:3) and (16:1/18:2)	C42H79NO8P
PC(34:4)	754.5387	754.5386	-0.1087	*	C42H77NO8P
PC(34:5)	752.5230	752.5223	-0.9727	*	C42H75NO8P
PC(35:2)	772.5856	772.5865	1.1235	**	C43H83NO8P
PC(35:3)	770.5700	770.5696	-0.4957	**	C43H81NO8P
PC(36:1)	788.6169	788.6152	-2.1963	*	C44H87NO8P
PC(36:2)	786.6013	786.6012	-0.1042	(18:1/18:1) and (18:0/18:2)	C44H85NO8P
PC(36:3)	784.5856	784.5850	-0.8055	(18:1/18:2) and (18:0/18:3)	C44H83NO8P
PC(36:4)	782.5700	782.5703	0.4064	(18:2/18:2) and (18:1/18:3)	C44H81NO8P
PC(36:5)	780.5543	780.5519	-3.1145	*	C44H79NO8P
PC(36:6)	778.5387	778.5362	-3.1880	*	C44H77NO8P
PC(37:2)	800.6169	800.6152	-2.1633	**	C45H87NO8P
PC(38:2)	814.6326	814.6317	-1.0827	*	C46H89NO8P
PC(38:3)	812.6169	812.6164	-0.6547	(18:2/20:1) and (18:1/20:2)	C46H87NO8P
PC(38:8)	802.5387	802.5359	-3.4665	*	C46H77NO8P
PC(40:1)	844.6795	844.6781	-1.6953	**	C48H95NO8P
PC(41:2)	856.6795	856.6785	-1.2047	**	C49H95NO8P
PC(42:2)	870.6952	870.6954	0.2515	**	C50H97NO8P
PC identified as $[M + CH_3COO]^-$					
PC(38:4)	868.6068	868.6078	-1.1950	(18:2/20:2)	C48H87NO10P
PE identified as $[M+H]^+$					
LPE(14:0)	426.2621	426.2618	-0.6264	*	C19H41NO7P
LPE(16:0)	454.2934	454.2933	-0.1475	16:0	C21H45NO7P
LPE(17:1)	466.2934	466.2935	0.2852	17:1	C22H45NO7P
LPE(17:0)	468.3090	468.3092	0.3908	17:0	C22H47NO7P
LPE(18:0)	482.3247	482.3261	2.9710	*	C23H49NO7P
LPE(18:1)	480.3090	480.3091	0.1728	18:1	C23H47NO7P
LPE(18:2)	478.2934	478.2934	0.0690	18:2	C23H45NO7P
LPE(18:3)	476.2777	476.2755	-4.6548	*	C23H43NO7P
LPE(20:1)	508.3403	508.3405	0.3620	*	C25H51NO7P
LPE(20:3)	504.3090	504.3078	-2.4132	*	C25H47NO7P
PE(28:0)	634.4448	634.4459	-1.7622	*	C33H65NO8P
PE(32:0)	692.5230	692.5232	0.2426	*	C37H75NO8P

PE(32:1)	690.5074	690.5077	0.4605	*	C37H73NO8P
PE(32:2)	688.4917	688.4911	-0.9179	(14:0/18:2)	C37H71O8NP
PE(33:1)	704.5230	704.5258	3.9289	(15:0/18:1) and (16:0/17:1)	C38H75NO8P
PE(34:1)	718.5387	718.5391	0.5817	(16:0/18:1)	C39H77NO8P
PE(34:2)	716.5230	716.5236	0.7927	(16:0/18:2)	C39H75NO8P
PE(34:3)	714.5074	714.5077	0.4451	(16:0/18:3) and (16:1/18:2)	C39H73O8NP
PE(35:2)	730.5387	730.5389	0.2984	*	C40H77NO8P
PE(35:3)	728.5230	728.5228	-0.3185	(17:1/18:2)	C40H75NO8P
PE(36:1)	746.5700	746.5674	-3.4585	*	C41H81O8NP
PE(36:2)	744.5543	744.5545	0.2270	(18:1/18:1)	C41H79O8NP
PE(36:3)	742.5387	742.5380	-0.9185	(18:2/18:1)	C41H77NO8P
PE(36:4)	740.5230	740.5231	0.0918	(18:2/18:2)	C41H75NO8P
PE(38:3)	770.5700	770.5713	1.7104	**	C43H81NO8P
PE identified as $[M-H]^-$					
PE(38:1)	772.5856	772.5826	3.9245	*	C43H83NO8P
PE(38:2)	770.5700	770.5707	-0.9318	(18:1/20:1) and (20:0/18:2)	C43H81O8NP
PE(38:4)	766.5387	766.5393	-0.8062	*	C43H77O8NP
PE(38:5)	764.5230	764.5202	3.7043	*	C43H75NO8P
SM identified as $[M+H]^+$					
SM(d35:1)	717.5911	717.5905	0.7678	*	C36H76N2O7P
PA identified as $[M+NH_4]^+$					
PA(28:0)	610.4448	610.4453	-0.8486	**	C31H65NO8P
PA(30:2(OH))	650.4397	650.4401	-0.6196	**	C33H65NO9P
PA(33:3(OH))	690.4710	690.4716	-0.8733	**	C36H69NO9P
PA identified as $[M-H]^-$					
LPA(18:2)	433.2355	433.2360	-1.1149	*	C21H38O7P
PA(34:1)	673.4808	673.4817	-1.2873	*	C37H70O8P
PA(34:2)	671.4652	671.4667	-2.2592	(16:0/18:2)	C37H68O8P
PA(34:3)	669.4495	669.4506	-1.5938	(16:1/18:2)	C37H66O8P
PA(36:1)	701.5121	701.5107	2.0427	(18:0/18:1)	C39H74O8P
PA(36:2)	699.4965	699.4972	-1.0250	(18:1/18:1) and (18:0/18:2)	C39H72O8P
PA(36:3)	697.4808	697.4818	-1.3864	(18:1/18:2)	C39H70O8P
PA(36:4)	695.4652	695.4664	-1.7499	(18:2/18:2)	C39H68O8P
PA(36:5)	693.4495	693.4508	-1.8271	*	C39H66O8P
PA(38:2)	727.5278	727.5272	0.8013	*	C41H76O8P
PA(38:3)	725.5121	725.5133	-1.6085	*	C41H74O8P
CL identified as $[M-H]^-$					

CL(54:6)	1185.7347	1185.7344	0.2876	(16:0/18:2/18:1)	C63H111O16P2
CL(66:0)	1379.9957	1379.9906	3.7000	*	C75H145O17P2
CL(70:2)	1432.0270	1432.0247	1.6103	*	C79H149O17P2
CL(70:3)	1430.0114	1430.0097	1.1580	*	C79H147O17P2
CL(70:4)	1427.9957	1427.9942	1.0546	*	C79H145O17P2
CL(70:5)	1425.9801	1425.9761	2.7735	(16:0/18:2/18:2/18:2) and (16:1/18:3/18:1/18:0)	C79H143O17P2
CL(70:6)	1423.9644	1423.9673	-2.0324	(16:0/18:2/18:2/18:2)	C79H141O17P2
CL(72:4)	1456.0270	1456.0237	2.2706	(18:1/18:1/18:1/18:1)	C81H149O17P2
CL(72:5)	1454.0114	1454.0084	2.0330	(18:1/18:2/18:1/18:1)	C81H147O17P2
CL(72:6)	1451.9957	1451.9941	1.1061	*	C81H145O17P2
CL(72:7)	1449.9801	1449.9781	1.3483	(18:0/18:2/18:2/18:3) and (18:1/18:1/18:2/18:3)	C81H143O17P2
CL(72:8)	1447.9644	1447.9640	0.2804	(18:1/18:1/18:2/18:3)	C81H141O17P2
CL(74:10)	1471.9644	1471.9605	2.6536	*	C83H141O17P2
CL(74:11)	1469.9488	1469.9451	2.4872	*	C83H139O17P2
CL(74:7)	1478.0114	1478.0070	2.9472	*	C83H147O17P2
CL(74:8)	1475.9957	1475.9913	2.9851	*	C83H145O17P2
CL(74:9)	1473.9801	1473.9763	2.5475	*	C83H143O17P2
PI identified as [M-H]$^-$					
LPI(16:0)	571.2883	571.2892	-1.5019	16:0	C25H48O12P
LPI(18:0)	599.3196	599.3200	-0.5957	*	C27H52O12P
LPI(18:1)	597.3040	597.3062	-3.6949	18:1	C27H50O12P
LPI(18:2)	595.2883	595.2899	-2.6172	18:2	C27H48O12P
PI(34:2)	833.5180	833.5193	-1.5501	(16:0/18:2) and (16:1/18:1)	C43H78O13P
PI(34:3)	831.5024	831.5058	-4.1395	(16:0/18:3) and (16:1/18:2)	C43H76O13P
PI(36:1)	863.5650	863.5639	1.2240	*	C45H84O13P
PI(36:2)	861.5493	861.5493	0.0093	(18:1/18:1) and (18:0/18:2)	C45H82O13P
PI(36:3)	859.5337	859.5341	-0.5142	(18:1/18:2) and (18:0/18:3)	C45H80O13P
PI(36:4)	857.5180	857.5181	-0.1073	(18:2/18:2) and (18:1/18:3)	C45H78O13P
PI(35:2)	847.5337	847.5349	-1.4654	(17:0/18:2)	C44H80O13P
PG identified as [M-H]$^-$					
PG(34:1)	747.5176	747.5186	-1.3204	(16:0/18:1)	C40H76O10P
PG(34:2)	745.5020	745.5038	-2.4655	(16:0/18:2)	C40H74O10P
PG(36:4)	769.5020	769.5016	0.4704	*	C42H74O10P

PS identified as [M-H]$^-$					
PS(34:2)	758.4972	758.4980	-1.0389	(16:0/18:2)	C40H73NO10P
PS(36:2)	786.5285	786.5292	-0.8747	(18:1/18:1)	C42H77NO10P
Ceramides identified as [M+H]$^+$					
Cer(d36:0)	568.5669	568.5662	1.1766	*	C36H74NO3
Cer(t42:0)	668.6557	668.6553	-0.5743	(18:0/24:0)	C42H86NO4

SM 5 – Phospholipids identified by LC-MS and LC-MS/MS of total lipid extracts of *Lasiodiplodia hormozganensis*, in the positive and negative ion modes. The complete list of PC, LPC, PE, LPE, SM and PA molecular species identified in positive mode, and PC, PE, PA, LPA, CL, PI, LPI, PG and PS molecular species identified in the negative mode, in MS and MS/MS spectra, are annotated. Data are presented as the respective sums of carbon atoms (C) and double bonds (N), followed by the calculated *m/z* values (ratios of mass to charge), plus the observed m/z values, followed by the error (< 5 ppm) and fatty acyl chains that compose the lipid, plus the respective formula.

Lipid species (C:N)	**Calculated *m/z***	**Observed *m/z***	**Error (ppm)**	**Fatty acyl chains (C:N)**	**Formula**
PC identified as [M+H]$^+$					
LPC(16:0)	496.3403	496.3399	-0.8381	16:0	C24H51NO7P
LPC(17:0)	510.3560	510.3568	1.6342	*	C25H53NO7P
LPC(18:0)	524.3716	524.3723	1.3025	18:0	C26H55NO7P
LPC(18:2)	520.3403	520.3402	-0.2229	18:2	C26H51NO7P
LPC(18:3)	518.3247	518.3244	-0.5151	18:3	C26H49NO7P
PC(28:1)	676.4917	676.4904	-1.9690	*	C36H71NO8P
PC(30:0)	706.5387	706.5391	0.5916	*	C38H77NO8P
PC(31:0)	720.5543	720.5515	-3.9289	*	C39H79NO8P
PC(31:1)	718.5387	718.5394	0.9993	(18:1/13:0) and (18:0/13:1)	C39H77NO8P
PC(31:3)	714.5074	714.5064	-1.3744	(18:2/13:1)	C39H73NO8P
PC(32:0)	734.5700	734.5701	0.1606	**	C40H81NO8P
PC(32:2)	730.5387	730.5391	0.5722	**	C40H77NO8P
PC(33:2)	744.5543	744.5546	0.3613	*	C41H79NO8P
PC(34:1)	760.5856	760.5848	-1.0939	(16:0/18:1)	C42H83NO8P
PC(34:2)	758.5700	758.5702	0.2874	(16:0/18:2) and (16:1/18:1)	C42H81NO8P
PC(34:3)	756.5543	756.5546	0.3556	(16:0/18:3) and (16:1/18:2)	C42H79NO8P
PC(34:4)	754.5387	754.5386	-0.1087	**	C42H77NO8P

PC(34:5)	752.5230	752.5224	-0.8398	*	C42H75NO8P
PC(35:1)	774.6013	774.5997	-2.0423	*	C43H85NO8P
PC(35:2)	772.5856	772.5855	-0.1709	**	C43H83NO8P
PC(35:3)	770.5700	770.5698	-0.2362	**	C43H81NO8P
PC(35:4)	768.5543	768.5536	-0.9511	**	C43H79NO8P
PC(36:1)	788.6169	788.6144	-3.2107	*	C44H87NO8P
PC(36:2)	786.6013	786.5995	-2.2654	(18:1/18:1) and (18:0/18:2)	C44H85NO8P
PC(36:3)	784.5856	784.5856	-0.0408	(18:1/18:2) and (18:0/18:3)	C44H83NO8P
PC(36:4)	782.5700	782.5693	-0.8715	(18:2/18:2) and (18:1/18:3)	C44H81NO8P
PC(36:5)	780.5543	780.5540	-0.4241	**	C44H79NO8P
PC(36:6)	778.5387	778.5383	-0.4907	**	C44H77NO8P
PC(37:3)	798.6013	798.6002	-1.3549	**	C45H85NO8P
PC(38:2)	814.6326	814.6304	-2.6785	*	C46H89NO8P
PC(38:3)	812.6169	812.6165	-0.5316	(18:2/20:1) and (18:1/20:2)	C46H87NO8P
PC(38:4)	810.6013	810.6022	1.1325	(18:2/20:2)	C46H85NO8P
PC(38:8)	802.5387	802.5364	-2.8435	**	C46H77NO8P
PC(38:9)	800.5230	800.5201	-3.6626	*	C46H75NO8P
PC(40:1)	844.6795	844.6779	-1.9321	**	C48H95NO8P
PC(40:6)	834.6013	834.5985	-3.3333	*	C48H85NO8P
PC(41:2)	856.6795	856.6795	-0.0374	**	C49H95NO8P
PC(42:2)	870.6952	870.6956	0.4812	**	C50H97NO8P
PC(42:3)	868.6795	868.6797	0.1934	**	C50H95NO8P
PC(43:2)	884.7108	884.7120	1.3202	**	C51H99NO8P
PC identified as $[M + CH_3COO]^-$					
LPC(18:1)	580.3614	580.3627	-2.1590	18:1	C28H55NO9P
PE identified as $[M+H]^+$					
LPE(14:0)	426.2621	426.2615	-1.3302	*	C19H41NO7P
LPE(16:0)	454.2934	454.2934	0.0726	16:0	C21H45NO7P
LPE(16:1)	452.2777	452.2778	0.1835	16:1	C21H43NO7P
LPE(17:0)	468.3090	468.3091	0.1772	17:0	C22H47NO7P
LPE(17:1)	466.2934	466.2934	0.0708	17:1	C22H45NO7P
LPE(18:0)	482.3247	482.3261	2.9710	*	C23H49NO7P
LPE(18:1)	480.3090	480.3092	0.3810	18:1	C23H47NO7P
LPE(18:2)	478.2934	478.2936	0.4871	18:2	C23H45NO7P
LPE(18:3)	476.2777	476.2756	-4.4449	18:3	C23H43NO7P
LPE(20:1)	508.3403	508.3405	0.3620	20:1	C25H51NO7P
LPE(20:2)	506.3247	506.3258	2.2377	20:2	C25H49NO7P

LPE(20:3)	504.3090	504.3080	-2.0166	*	C25H47NO7P
LPE(20:4)	502.2934	502.2912	-4.3142	20:4	C25H45NO7P
LPE(20:5)	500.2777	500.2753	-4.8313	*	C25H43NO7P
PE(32:0)	692.5230	692.5232	0.2426	(16:0/16:0)	C37H75NO8P
PE(32:1)	690.5074	690.5078	0.6054	(14:0/18:1) and (16:0/16:1)	C37H73NO8P
PE(32:2)	688.491732	688.4909	-1.2084	(14:0/18:2)	C37H71O8NP
PE(33:1)	704.5230	704.5243	1.7998	(18:1/15:0) and (17:1/16:0)	C38H75NO8P
PE(33:3)	700.4917	700.4940	3.2377	**	C38H71NO8P
PE(34:1)	718.5387	718.5377	-1.3667	(16:0/18:1)	C39H77NO8P
PE(34:2)	716.5230	716.5234	0.5136	(16:0/18:2)	C39H75NO8P
PE(34:3)	714.5074	714.5077	0.4451	(16:0/18:3)	C39H73O8NP
PE(34:4)	712.4917	712.4935	2.4814	*	C39H71NO8P
PE(35:3)	728.5230	728.5224	-0.8675	(18:2/17:1)	C40H75NO8P
PE(36:1)	746.5700	746.5671	-3.8603	*	C41H81O8NP
PE(36:2)	744.554331	744.5547	0.4956	(18:1/18:1), (16:0/20:2) and (18:0/18:2)	C41H79O8NP
PE(36:3)	742.538682	742.5380	-0.9185	(18:1/18:2) and (18:0/18:3)	C41H77NO8P
PE(36:4)	740.5230	740.5213	-2.3389	(18:2/18:2)	C41H75NO8P
PE(36:5)	738.507382	738.5054	-2.6838	*	C41H73O8NP
PE(38:2)	772.5856	772.5857	0.0880	(18:1/20:1)	C43H83O8NP
PE(38:3)	770.5700	770.5696	-0.4957	(18:1/20:2) and (18:2/20:1)	C43H81NO8P
PE(38:4)	768.5543	768.5524	-2.5125	(18:2/20:2), (18:1/20:3) and (18:3/20:1)	C43H79O8NP
PE(38:5)	766.5387	766.5359	-3.6293	*	C43H77NO8P
PE(38:6)	764.5230	764.5201	-3.8351	*	C43H75O8NP
PE(40:5)	794.5700	794.5675	-3.1237	*	C45H81O8NP
PE(40:6)	792.5543	792.5517	-3.3196	*	C45H79O8NP
PE identified as $[M-H]^-$					
LPE(15:0)	438.2621	438.2632	-2.5852	15:0	C20H41NO7P
PE(28:0)	634.4448	634.4460	-1.9198	*	C33H65NO8P
PE(33:2)	700.4917	700.4948	-4.3798	(16:0/17:2) and (15:0/18:2)	C38H71NO8P
PE(35:2)	728.5230	728.5247	-2.2896	(17:0/18:2) and (17:1/18:1)	C40H75NO8P
PE(36:6)	734.4761	734.4789	-3.8367	(18:3/18:3) and (18:3O)	C41H69NO8P
PE (37:2)	756.5543	756.5534	1.2306	(18:1/19:1)	C42H79NO8P
PE (37:3)	754.5387	754.5375	1.5665	(18:2/19:1)	C42H77NO8P
SM identified as $[M+H]^+$					

SM(d34:1)	703.5754	703.5750	0.5699	**	C39H80N2O6P
SM(d35:1)	717.5911	717.5904	0.9072	*	C36H76N2O7P
PA identified as [M-H]$^-$					
LPA(18:2)	433.2355	433.2358	-0.6532	18:2	C21H38O7P
PA(34:1)	673.4808	673.4818	-1.4358	*	C37H70O8P
PA(34:2)	671.4652	671.4669	-2.5571	(16:0/18:2)	C37H68O8P
PA(34:3)	669.4495	669.4514	-2.7889	(16:0/18:3) and (16:1/18:2)	C37H66O8P
PA(36:1)	701.5121	701.5101	2.8980	(18:0/18:1)	C39H74O8P
PA(36:2)	699.4965	699.4981	-2.3117	(18:1/18:1) and (18:0/18:2)	C39H72O8P
PA(36:3)	697.4808	697.4822	-1.9599	**	C39H70O8P
PA(36:4)	695.4652	695.4668	-2.3251	(18:2/18:2) and (18:1/18:3)	C39H68O8P
PA(36:5)	693.4495	693.4512	-2.4039	(18:2/18:3)	C39H66O8P
PA(36:6)	691.4339	691.4359	-2.9171	(18:3/18:3)	C39H64O8P
PA(35:2)	685.4808	685.4819	-1.5566	(17:0/18:2) and (17:1/18:1)	C38H70O8P
PA(35:3)	683.4652	683.4667	-2.2196	(17:1/18:2)	C38H68O8P
PA(38:2)	727.5278	727.5272	0.8013	*	C41H76O8P
PA(38:3)	725.5121	725.5145	-3.2625	*	C41H74O8P
CL identified as [M-H]$^-$					
CL(54:6)	1185.7347	1185.7350	-0.2184	*	C63H111O16P2
CL(66:0)	1379.9957	1379.9904	3.8449	*	C75H145O17P2
CL(70:2)	1432.0270	1432.0208	4.3337	*	C79H149O17P2
CL(70:3)	1430.0114	1430.0063	3.5356	*	C79H147O17P2
CL(70:4)	1427.9957	1427.9900	3.9958	*	C79H145O17P2
CL(70:5)	1425.9801	1425.9766	2.4229	(16:0/18:1/18:2/18:2), (16:0/18:0/18:2/18:3), (16:1/18:0/18:2/18:2) and (17:0/17:0/18:2/18:3)	C79H143O17P2
CL(70:6)	1423.9644	1423.9548	6.7460	(16:0/18:2/18:2/18:2), (16:1/18:1/18:2/18:2) and (16:0/18:1/18:2/18:3)	C79H141O17P2
CL(72:3)	1458.0427	1458.0359	4.6336	*	C81H151O17P2
CL(72:4)	1456.0270	1456.0214	3.8502	(18:0/18:0/18:1/18:3), (18:0/18:1/18:1/18:2) and (18:1/18:1/18:1/18:1)	C81H149O17P2
CL(72:5)	1454.0114	1454.0123	-0.6492	(18:1/18:1/18:1/18:2)	C81H147O17P2
CL(72:6)	1451.9957	1451.9946	0.7617	*	C81H145O17P2

CL(72:7)	1449.9801	1449.9834	2.3069	(18:0/18:2/18:2/18:3) and (18:1/18:1/18:2/18:3)	C81H143O17P2
CL(72:8)	1447.9644	1447.9646	-0.1340	(18:1/18:1/18:2/18:3)	C81H141O17P2
CL(72:9)	1445.9488	1445.9451	2.5284	(18:2/18:2/18:2/18:3)	C81H139O17P2
CL(74:10)	1471.9644	1471.9594	3.4009	*	C83H141O17P2
CL(74:11)	1469.9488	1469.9456	2.1470	*	C83H139O17P2
CL(74:7)	1478.0114	1478.0049	4.3680	*	C83H147O17P2
CL(74:9)	1473.9801	1473.9757	2.9546	*	C83H143O17P2
PI identified as [M-H]$^-$					
PI(34:1)	835.5337	835.5349	-1.4865	*	C43H80O13P
PI(34:2)	833.5180	833.5192	-1.4301	(16:0/18:2) and (16:1/18:1)	C43H78O13P
PI(34:3)	831.5024	831.5031	-0.8924	(16:0/18:3) and (16:1/18:2)	C43H76O13P
PI(36:0)	865.5806	865.5803	0.3558	*	C45H86O13P
PI(36:1)	863.5650	863.5674	-2.8290	(18:0/18:1)	C45H84O13P
PI(36:2)	861.5493	861.5513	-2.3121	(18:1/18:1) and (18:0/18:2)	C45H82O13P
PI(36:3)	859.5337	859.5356	-2.2594	(18:1/18:2) and (18:0/18:3)	C45H80O13P
PI(36:4)	857.5180	857.5200	-2.3230	(18:2/18:2) and (18:1/18:3)	C45H78O13P
PI(35:1)	849.5493	849.5491	0.2448	(17:0/18:1) and (16:0/19:1)	C44H82O13P
PI(35:2)	847.5337	847.5348	-1.3474	(17:1/18:1) and (17:0/18:2)	C44H80O13P
PG identified as [M-H]$^-$					
PG(34:1)	747.5176	747.5179	-0.3839	*	C40H76O10P
PG(34:2)	745.5020	745.5031	-1.5265	(16:0/18:2) and (16:1/18:1)	C40H74O10P
PG(36:2)	773.5333	773.5329	0.4693	*	C42H78O10P
PG(36:3)	771.5176	771.5178	-0.2424	(18:1/18:2) and (18:0/18:3)	C42H76O10P
PG(36:4)	769.5020	769.5029	-1.2190	*	C42H74O10P
PG(36:5)	767.4863	767.4874	-1.4163	*	C42H72O10P
PS identified as [M-H]$^-$					
PS(34:2)	758.4972	758.4983	-1.4344	(16:0/18:2)	C40H73NO10P

SM 6 – Triacylglycerols identified by LC-MS and LC-MS/MS of neutral lipid extracts of *Lasiodiplodia theobromae*, in the positive ion mode. The complete list of TG molecular species

identified in positive mode, in MS and MS/MS spectra, are annotated. Data are presented as the respective sums of carbon atoms (C) and double bonds (N), followed by the calculated *m/z* values (ratios of mass to charge), plus the observed m/z values, followed by the error (< 5 ppm) and fatty acyl chains that compose the lipid, plus the respective formula.

Lipid species (C:N)	**Calculated *m/z***	**Observed *m/z***	**Error (ppm)**	**Fatty acyl chains (C:N)**	**Formula**
TAG identified as $[M+NH_4]^+$					
TG(47:4)	802.6925	802.6956	-3.9069	*	C50H92NO6
TG(47:1)	808.7394	808.7364	3.7268	*	C50H98NO6
TG(47:0)	810.7551	810.7514	4.5192	*	C50H100NO6
TG(48:4)	816.7081	816.7104	-2.7990	*	C51H94NO6
TG(48:2)	820.7394	820.7358	4.4033	*	C51H98NO6
TG(48:1)	822.7551	822.7512	4.6964	*	C51H100NO6
TG(48:0)	824.7707	824.7668	4.7456	*	C51H102NO6
TG(49:4)	830.7238	830.727	-3.8954	*	C52H96NO6
TG(49:2)	834.7551	834.7512	4.6289	*	C52H100NO6
TG(49:0)	838.7864	838.7823	4.8451	*	C52H104NO6
TG(50:6)	840.7081	840.7108	-3.1949	*	C53H94NO6
TG(50:5)	842.7238	842.7268	-3.6026	*	C53H96NO6
TG(50:4)	844.7394	844.7391	0.3717	*	C53H98NO6
TG(50:3)	846.7551	846.7508	5.0357	*	C53H100NO6
TG(50:2)	848.7707	848.7689	2.1372	(14:0/18:2/20:0), (16:0/16:1/18:1) and (16:0/16:0/18:2)	C53H102NO6
TG(50:1)	850.7864	850.7847	1.9558	(18:1/16:0/16:0) and (16:1/16:0/18:0)	C53H104NO6
TG(51:4)	858.7551	858.7579	-3.3025	*	C54H100NO6
TG(51:3)	860.7707	860.7671	4.1986	*	C54H102NO6
TG(51:2)	862.7864	862.7831	3.7831	*	C54H104NO6
TG(51:1)	864.8020	864.7981	4.5259	*	C54H106NO6
TG(52:7)	866.7238	866.7255	-2.0029	*	C55H96NO6
TG(52:6)	868.7394	868.7417	-2.6314	*	C55H98NO6
TG(52:5)	870.7551	870.755	0.0735	*	C55H100NO6
TG(52:4)	872.7707	872.7676	3.5679	(16:0/18:2/18:2), (16:0/18:1/18:3) and (16:1/18:1/18:2)	C55H102NO6
TG(52:3)	874.7864	874.7827	4.1885	(16:0/18:1/18:2) and (16:1/18:1/18:1)	C56H92NO6
TG(52:2)	876.8020	876.7983	4.2358	(16:0/18:0/18:2) and (16:1/18:0/18:1)	C55H106NO6
TG(53:8)	878.7238	878.7272	-3.9102	*	C56H96NO6

TG(52:1)	878.8177	878.8131	5.1933	(16:0/18:0/18:1)	C55H108NO6
TG(53:7)	880.7394	880.742	-2.9362	*	C56H98NO6
TG(53:6)	882.7551	882.7574	-2.6463	*	C56H100NO6
TG(53:5)	884.7707	884.7724	-1.9056	*	C56H102NO6
TG(53:4)	886.7864	886.7892	-3.1981	*	C56H104NO6
TG(53:3)	888.8020	888.7975	5.0787	*	C56H106NO6
TG(54:9)	890.7238	890.7234	0.4087	*	C57H96NO6
TG(53:2)	890.8177	890.8134	4.7866	(17:0/18:1/18:1), (17:1/18:1/18:0) and (17:0/18:2/18:0)	C56H108NO6
TG(54:8)	892.7394	892.7408	-1.5525	*	C57H98NO6
TG(53:1)	892.8333	892.8308	2.8158	*	C56H110NO6
TG(54:7)	894.7551	894.7556	-0.5990	*	C57H100NO6
TG(54:6)	896.7707	896.7675	3.5840	*	C57H102NO6
TG(54:5)	898.7864	898.7823	4.5217	*	C57H104NO6
TG(54:4)	900.8020	900.7974	5.1221	(18:1/18:1/18:2) and (18:0/18:2/18:2)	C57H106NO6
TG(55:10)	902.7238	902.7249	-1.2584	*	C58H96NO6
TG(54:3)	902.8177	902.813	5.1660	(18:1/18:0/18:2) and (18:1/18:1/18:1)	C57H108NO6
TG(55:9)	904.7394	904.7412	-1.9740	*	C58H98NO6
TG(54:2)	904.8333	904.8286	5.2098	(18:0/18:1/18:1), (18:0/18:0/18:2), (16:0/20:0/18:2) and (16:0/18:1/20:1)	C57H110NO6
TG(55:8)	906.7551	906.7572	-2.3557	*	C58H100NO6
TG(54:1)	906.8490	906.8444	5.0328	(18:0/18:0/18:1), (16:0/20:0/18:1)	C57H112NO6
TG(55:7)	908.7707	908.7728	-2.2954	*	C58H102NO6
TG(55:6)	910.7864	910.7882	-2.0158	*	C58H104NO6
TG(55:5)	912.8020	912.8037	-1.8471	*	C58H106NO6
TG(55:4)	914.8177	914.8195	-2.0070	*	C58H108NO6
TG(56:5)	926.8177	926.8138	4.1691	*	C59H108NO6
TG(56:2)	932.8646	932.8603	4.6245	*	C59H114NO6
TG(56:1)	934.8803	934.8756	4.9889	*	C59H116NO6
TG(57:7)	936.8020	936.8054	-3.6144	*	C60H106NO6
TG(57:1)	948.8959	948.8927	3.3871	*	C60H118NO6
TG(58:6)	952.8333	952.8304	3.0582	*	C61H110NO6
TG(58:5)	954.8490	954.8493	-0.3519	*	C61H112NO6
TG(58:4)	956.8646	956.8611	3.6724	*	C61H114NO6
TG(58:2)	960.8959	960.8916	4.4896	*	C61H118NO6
TG(58:1)	962.9116	962.9069	4.8436	*	C61H120NO6

TG(59:7)	964.8333	964.8357	-2.4730	*	C62H110NO6
TG(59:6)	966.8490	966.8508	-1.8990	*	C62H112NO6
TG(59:5)	968.8646	968.8661	-1.5338	*	C62H114NO6
TG(59:4)	970.8803	970.8801	0.1689	*	C62H116NO6
TG(59:3)	972.8959	972.8909	5.1537	*	C62H118NO6
TG(59:2)	974.9116	974.9061	5.6046	*	C62H120NO6
TG(59:1)	976.9272	976.9225	4.8253	*	C62H122NO6
TG(60:5)	982.8803	982.88	0.2686	*	C63H116NO6
TG(60:4)	984.8959	984.8923	3.6694	*	C63H118NO6
TG(60:3)	986.9116	986.9068	4.8272	*	C63H120NO6
TG(60:2)	988.9272	988.9224	4.8679	*	C63H122NO6
TG(60:1)	990.9429	990.9378	5.1103	*	C63H124NO6
TG(61:7)	992.8646	992.8673	-2.7053	*	C64H114NO6
TG(61:6)	994.8803	994.8821	-1.8454	*	C64H116NO6
TG(61:5)	996.8959	996.8972	-1.2900	*	C64H118NO6
TG(61:4)	998.9116	998.9078	3.7681	*	C64H120NO6
TG(61:3)	1000.9272	1000.9222	5.0094	*	C64H122NO6

SM 7 – Triacylglycerols identified by LC-MS and LC-MS/MS of neutral lipid extracts of *Lasiodiplodia hormozganensis*, in the positive ion mode. The complete list of TG molecular species identified in positive mode, in MS and MS/MS spectra, are annotated. Data are presented as the respective sums of carbon atoms (C) and double bonds (N), followed by the calculated *m/z* values (ratios of mass to charge), plus the observed m/z values, followed by the error (< 5 ppm) and fatty acyl chains that compose the lipid, plus the respective formula.

Lipid species (C:N)	**Calculated *m/z***	**Observed *m/z***	**Error (ppm)**	**Fatty acyl chains (C:N)**	**Formula**
TAG identified as $[M+NH_4]^+$					
TG(47:1)	808.7394	808.7375	2.3666	*	C50H98NO6
TG(47:0)	810.7551	810.7535	1.9291	*	C50H100NO6
TG(48:1)	822.7551	822.7516	4.2102	*	C51H100NO6
TG(48:0)	824.7707	824.7674	4.0181	*	C51H102NO6
TG(49:2)	834.7551	834.7523	3.3112	*	C52H100NO6
TG(49:1)	836.7707	836.7678	3.4824	*	C52H102NO6
TG(50:4)	844.7394	844.737	2.8577	*	C53H98NO6
TG(50:3)	846.7551	846.7521	3.5004	*	C53H100NO6
TG(50:2)	848.7707	848.7683	2.8441	*	C53H102NO6

TG(50:1)	850.7864	850.78385	2.9549	(16:0/16:0/18:1), (18:0/18:1/14:0), (16:0/16:1/18:0), (15:0/15:0/20:0), (15:0/17:0/18:1) and (16:1/17:0/17:0)	C53H104NO6
TG(51:6)	854.7238	854.7279	-4.8390	*	C54H96NO6
TG(51:5)	856.7394	856.7406	-1.3843	*	C54H98NO6
TG(51:4)	858.7551	858.7538	1.4719	*	C54H100NO6
TG(51:3)	860.7707	860.7678	3.3853	*	C54H102NO6
TG(51:2)	862.7864	862.7836	3.2036	*	C54H104NO6
TG(51:1)	864.8020	864.7987	3.8321	*	C54H106NO6
TG(52:6)	868.7394	868.7382	1.3974	*	C55H98NO6
TG(52:5)	870.7551	870.7522	3.2891	*	C55H100NO6
TG(52:4)	872.7707	872.7679	3.2242	*	C55H102NO6
TG(52:3)	874.7864	874.7835	3.2739	(18:1/18:2/16:0), (18:1/18:1/16:1) and (18:0/18:2/16:1)	C55H104NO6
TG(52:2)	876.8020	876.7983	4.2358	*	C55H106NO6
TG(52:1)	878.8177	878.8139	4.2830	*	C55H108NO6
TG(53:7)	880.7394	880.743	-4.0716	*	C56H98NO6
TG(53:6)	882.7551	882.7564	-1.5134	*	C56H100NO6
TG(53:5)	884.7707	884.7742	-3.9400	(17:0/18:2/18:3)	C56H102NO6
TG(53:4)	886.7864	886.7842	2.4403	*	C56H104NO6
TG(53:3)	888.8020	888.7989	3.5036	*	C56H106NO6
TG(53:2)	890.8177	890.8144	3.6640	*	C56H108NO6
TG(53:1)	892.8333	892.8308	2.8158	*	C56H110NO6
TG(54:8)	892.7394	892.7391	0.3517	*	C57H98NO6
TG(54:7)	894.7551	894.7525	2.8656	*	C57H100NO6
TG(54:6)	896.7707	896.7678	3.2494	*	C57H102NO6
TG(54:5)	898.7864	898.7829	3.8541	(18:2/18:2/18:1), (18:1/18:1/18:3) and (18:0/18:2/18:3)	C57H104NO6
TG(54:4)	900.8020	900.7982	4.2340	(18:1/18:1/18:2)	C57H106NO6
TG(55:10)	902.7238	902.7282	-4.9140	*	C58H96NO6
TG(54:3)	902.8177	902.8136	4.5015	(18:0/18:1/18:2), (18:0/18:1/18:2), (18:0/18:0/18:3), (16:0/20:0/18:3), (16:1/20:1/18:1), (16:0/20:1/18:2) and (16:1/20:0/18:2)	C57H108NO6
TG(55:9)	904.7394	904.7428	-3.7425	*	C58H98NO6

TG(54:2)	904.8333	904.8292	4.5467	(18:0/18:1/18:1) and (20:0/18:2/16:0)	C57H110NO6
TG(55:8)	906.7551	906.7589	-4.2305	*	C58H100NO6
TG(54:1)	906.8490	906.8454	3.9301	(18:0/18:0/18:1) and (16:0/18:1/20:0)	C57H112NO6
TG(55:7)	908.7707	908.774	-3.6159	(17:1/18:1/20:5), (17:0/18:2/20:5), (17:2/18:3/20:2) and (17:1/18:3/20:2)	C58H102NO6
TG(55:6)	910.7864	910.7905	-4.5411	*	C58H104NO6
TG(56:3)	930.8490	930.8449	4.3659	*	C59H112NO6
TG(56:2)	932.8646	932.8613	3.5525	*	C59H114NO6
TG(56:1)	934.8803	934.8772	3.2774	*	C59H116NO6
TG(57:1)	948.8959	948.8929	3.1763	*	C60H118NO6
TG(58:5)	954.8490	954.8466	2.4758	*	C61H112NO6
TG(58:3)	958.8803	958.8760	4.4469	*	C61H116NO6
TG(58:2)	960.8959	960.8930	3.0326	*	C61H118NO6
TG(58:1)	962.9116	962.9084	3.2859	*	C61H120NO6
TG(59:4)	970.8803	970.8783	2.0229	*	C62H116NO6
TG(59:2)	974.9116	974.9076	4.0660	*	C62H120NO6
TG(59:1)	976.9272	976.9238	3.4946	*	C62H122NO6
TG(60:5)	982.8803	982.8777	2.6087	*	C63H116NO6
TG(60:4)	984.8959	984.8932	2.7556	*	C63H118NO6
TG(60:3)	986.9116	986.9084	3.2060	*	C63H120NO6
TG(60:2)	988.9272	988.9249	2.3399	*	C63H122NO6
TG(60:1)	990.9429	990.9392	3.6975	*	C63H124NO6

SM 8 – Fatty acids identified by GC-MS of total lipid extracts of *Lasiodiplodia theobromae*. The complete list of FA molecular species identified in GC-MS, are annotated. Data are presented as the fatty acid and common name, followed by the respective sums of carbon atoms (C) and double bonds (N), plus the observed *m/z* values (ratios of mass to charge), followed the respective formula.

Fatty acid	Common name	Lipid species (C:N)	Observed *m/z*	Formula
FA identified as FAMEs				
Isotridecanoate	Isomyristic acid	FA(14:0)	242.21	C14H2802
Isotetradecanoate	Isopentadecylic acid	FA(15:0)	256.21	C15H30O2
9-methyltetradecanoate	-	FA(15:0)	256.21	C15H30O2
Hexadecanoate	Palmitic acid	FA(16:0)	270.24	C16H32O2
9-hexadecenoate	Palmitoleic acid	FA(9-16:1)	268.18	C16H30O2

11-hexadecenoate	Lycopodic acid	FA(11-16:1)	268.18	C16H30O2
Isoheptadecanoate	Isomargaric acid	FA(17:0)	284.24	C17H34O2
Heptadecanoate	Margaric acid	FA(17:0)	284.25	C17H34O2
9-heptadecenoate	Margaroleic acid	FA(9-17:1)	282.24	C17H32O2
8-heptadecenoate	Civetic acid	FA(8-17:1)	282.21	C17H32O2
Octadecanoate	Stearic acid	FA(18:0)	298.27	C18H36O2
13-octadecenoate	-	FA(13-18:1)	296.26	C18H34O2
7,12-octadecadienoate	Rumenic acid	FA(7,12-18:2)	294.24	C18H32O2
Nonadecanoate	Nonadecylic acid	FA(19:0)	312.28	C19H38O2
9,12,15-octadecatrienoate	α-Linolenic acid	FA((18:3)*n-3*)	292.21	C18H30O2
Eicosanoate	Arachidic acid	FA(20:0)	326.29	C20H40O2
9-eicosanoate	Gadoleic acid	FA(9-20:1)	324.26	C20H38O2
11,14-eicosadienoate	-	FA((20:2)*n-6*)	322.23	C20H36O2
Isoheneicosanoate	Isobehenic acid	FA(22:0)	354.32	C22H44O2
Docosanoate	Behenic acid	FA(22:0)	354.32	C22H44O2
21-methyldocosanoate	Isotricosanoic acid	FA(23:0)	368.34	C23H46O2
Tricosanoate	Tricosylic acid	FA(23:0)	368.34	C23H46O2
Tetracosanoate	Lignoceric acid	FA(24:0)	382.36	C24H48O2

SM 9 – Fatty acids identified by GC-MS of total lipid extracts of *Lasiodiplodia hormozganensis*. The complete list of FA molecular species identified in GC-MS, are annotated. Data are presented as the fatty acid and common name, followed by the respective sums of carbon atoms (C) and double bonds (N), plus the observed *m/z* values (ratios of mass to charge), followed the respective formula.

Fatty acid	Common name	Lipid species (C:N)	Observed *m/z*	Formula
FA identified as FAMEs				
Isotridecanoate	Isomyristic acid	FA(14:0)	242.21	C14H2802
9-methyltetradecanoate	-	FA(15:0)	256.21	C15H30O2
Isotetradecanoate	Isopentadecylic acid	FA(15:0)	256.21	C15H30O2
Hexadecanoate	Palmitic acid	FA(16:0)	270.24	C16H32O2
11-hexadecenoate	Lycopodic acid	FA(11-16:1)	268.15	C16H30O2
9-hexadecenoate	Palmitoleic acid	FA(9-16:1)	268.20	C16H30O2
Isoheptadecanoate	Isomargaric acid	FA(17:0)	284.25	C17H34O2
Heptadecanoate	Margaric acid	FA(17:0)	284.26	C17H34O2
9-heptadecenoate	Margaroleic acid	FA(9-17:1)	282.14	C17H32O2
8-heptadecenoate	Civetic acid	FA(8-17:1)	282.24	C17H32O2
Octadecanoate	Stearic acid	FA(18:0)	298.27	C18H36O2
13-octadecenoate	-	FA(13-18:1)	296.23	C18H34O2

7,12-octadecadienoate	Rumenic acid	FA(7,12-18:2)	294.24	C18H32O2
Nonadecanoate	Nonadecylic acid	FA(19:0)	312.29	C19H38O2
9,12,15-octadecatrienoate	α-Linolenic acid	FA((18:3)n-3)	292.21	C18H30O2
Eicosanoate	Arachidic acid	FA(20:0)	326.29	C20H40O2
9-eicosanoate	Gadoleic acid	FA(9-20:1)	324.26	C20H38O2
11,14-eicosadienoate	-	FA((20:2)n-6)	322.21	C20H36O2
Isoheneicosanoate	Isobehenic acid	FA(22:0)	354.32	C22H44O2
Tricosanoate	Tricosylic acid	FA(23:0)	368.33	C23H46O2
Tetracosanoate	Lignoceric acid	FA(24:0)	382.36	C24H48O2